T H E U N I V E R S I T Y O F M I C H I G A N

COLLEGE OF ENGINEERING
Department of Mechanical Engineering

Student Project Reports

INVESTIGATION OF DESIGN MEANS FOR HOME LAUNDRY APPLIANCES

Timothy E. Hickox
Douglas H. Lane
James G. Morgan
John Robinson
Ishwar Lal Thakur

ORA Project 07494

under contract with:

WHIRLPOOL CORPORATION
BENTON HARBOR, MICHIGAN

administered through:

OFFICE OF RESEARCH ADMINISTRATION ANN ARBOR

December 1967

TABLE OF CONTENTS

TABLE OF CONTENTS (Continued)

Computer Simulation of
Velocity Extraction Drying Equipment

TABLE OF CONTENTS (Concluded)

AN EXPERIMENTAL INVESTIGATION OF THE COMPUTER MODEL FOR PREDICTING PERFORMANCE OF DIRECT CONTACT CONDENSERS

Timothy E. Hickcox

PROJECT DEFINITION

The purpose of this project is the evaluation of a computer tool designed to predict performance of direct contacting, or spray, condensers. This computer model of a direct contacting condenser was developed last year in the Whirlpool program by Vern Wedeven. The evaluation will be accomplished by comparing experimental results with those predicted by the computer tool. The input data for the computer will be the measured inputs of the experimental work. The compared outputs will be the computer-predicted condenser outlet results, and those outlet values measured in the experimental work.

Additional investigation was undertaken in the area of total cycle simulation for the velocity extraction dryer system. A feasibility study was made of the use of analog computer simulation of the system. The reason for such investigation was the attractive "man in the computing loop" flexibility and the continuous time unsteady solution capability of the analog computer. These are two advantages the digital computer does not have.

COMPUTER TOOL DEFINITION

The computer model of the direct contacting condenser presents definite problems in formulation. These problems led to the model created by Vern Wedeven.

The primary problem concerns the simultaneous heat and mass transfer processes. At present there is no analytical tool to predict these internal processes, since their physics is not known in detail. There is work being done in this field to predict heat transfer characteristics from a heated plate into an air-fine water-fog mixture. Although the heat transference in the condenser occurs in the opposite direction, this work might give the first method of predicting this type of heat transfer.

The alternative to predicting the internal processes is looking at the system from a macroscopic point of view. On the assumption that only a small amount of heat would be lost through transfer to the ambient, we can disregard such loss. Then the First Law of Thermodynamics may be written for the spray condenser control volume, resulting in a thermodynamic balance which gives implicit relations for the outlet temperature. This is a steady-state approach, and assumes thermodynamic equilibrium of the system. The approach assumes that all rate processes (internal heat and mass transfer, in this case) have been completed internally. It assumes that there is no remaining driving force for the process, i.e., temperature difference, vapor pressure difference, etc. Thus the outlet liquid water, made up of cooling water and condensed vapor, is assumed to be at the same temperature as the air-water vapor mixture, and the exit air-water vapor mixture is assumed to be at 100% relative humidity. Since these conditions are expressed by an equilibrium equation with no heat transfer, the result is that enthalpy flow into the control volume equals enthalpy flow out of the control volume. The equation is:

$$MCW(T2-TW1) = MA\{-.241(T_2-T_1)-W_{T2}[.407(T2+460)+877.6]+W_{T1}[.407(T_1+460)$$

$$+877.6] - (W_{T1}-W_{T2})[T_2+460)-492.53]\}$$

Note: This is Equation (14) in Vern Wedeven's report; 07494-2-P.

The computer model involves an iterative trial and error solution of the above equation. The outlet temperature is assumed; the cooling water flow rate is obtained and compuared to the actual value. Based on the error found, a new outlet temperature is selected. This iteration procedure continues until the error between the actual and calculated cooling water flow rates is less than a predetermined value. The outlet temperature for this case is the predicted outlet temperature.

This governing equation involves the humidity ratio, which must be calculated for each value of temperature. To make the calculation manageable, the air was assumed to at 100% humidity. Since this was already the case for the outlet mixture, this simply meant assuming that the inlet air was also at 100% relative humidity. Because this would also be the maximum water vapor entry to the condenser, it might be a limiting factor in the use and flexibility of the tool.

The computer model requires inlet air flow rate and temperature and cooling water flow rate and temperature as input data. It will predict outlet temperature and liquid outflow.

The experimental investigation compared experimental values obtained

from an actual direct contact condenser with those of the computer model. The inlet air flow rate and temperature, and cooling water flow rate and temperature were measured in the experimental apparatus and used as input data for the computer model. The outlet air-water vapor mixture temperature, outlet water temperature, and outlet water flow rate were measured for comparison with the computer predicted values. Also the inlet air wet and dry bulb temperatures were measured to determine actual inlet air relative humidity.

After inlet requirements were met, a variable range of air flow rates and temperatures, and cooling water flow rates and temperatures were chosen.

The air supply was a centrifugal blower with a valve on the outlet to allow varying air flow rates and temperatures. The air flow rate was measured by use of a standard thin plate orifice and manometer. The heating and water vapor saturation of the air presented a problem since no stream was readily available in the area. Heating and saturation of the air was achieved by using calrod heaters in a large flow tube following the air flow measurements. The calrod heaters could be turned on and off individually and could be used with either 120 v or 240 v to allow input power variation, and thus air-water vapor temperature variation.

Hot water was sprayed directly on one of the heaters for vaporization. At the exit of this chamber was a separator to remove liquid water. At the air-vapor exit of the separator, wet and dry bulb temperatures were measured to check the 100% relative humidity requirement. This outlet flow was the inlet air to the condenser.

The cooling water flow rate was measured with a nonstandard, precalibrated thin plate orifice and manometer while its temperatures were measured with a thermometer well. The cooling water was introduced through the duct wall at a right angle to the air flow. It simply entered through a 1/4 in. pipe as a stream with no spray. The air and water then travelled through a close return trap that required a vertical upward flow at its exit. Following the trap was another brass cyclone separator for removing the liquid water. Thus, the separator itself had to be considered part of the condenser. The outlet air-water vapor dry bulb temperature was measured and an occasional wet bulb temperature measurement was made. The temperature of the outlet water was measured, and the flow rate of the outlet water was measured by the beaker and stopwatch method. See Fig. 1 for a schematic of the apparatus.

Some problems were encountered with this system. A relatively long stabilization time was required when temperatures or flow rates were changed, and several water leaks developed around the heaters. The greatest problem, however, was that 100% relative humidity at the inlet to the spray condenser could never be achieved. Generally, the actual conditions were about 75% to 90% relative humidity. Also the air supply was limited to about 2 lb mass/min.

The error values were defined as:

$$\% \text{ error } T = \frac{T_{predicted} - T_{actual}}{T_{predicted}} \times 100$$

$$\% \text{ error } \dot{m}_{water\ out} = \frac{\dot{m}_{predicted} - \dot{m}_{actual}}{\dot{m}_{predicted}} \times 100 \quad .$$

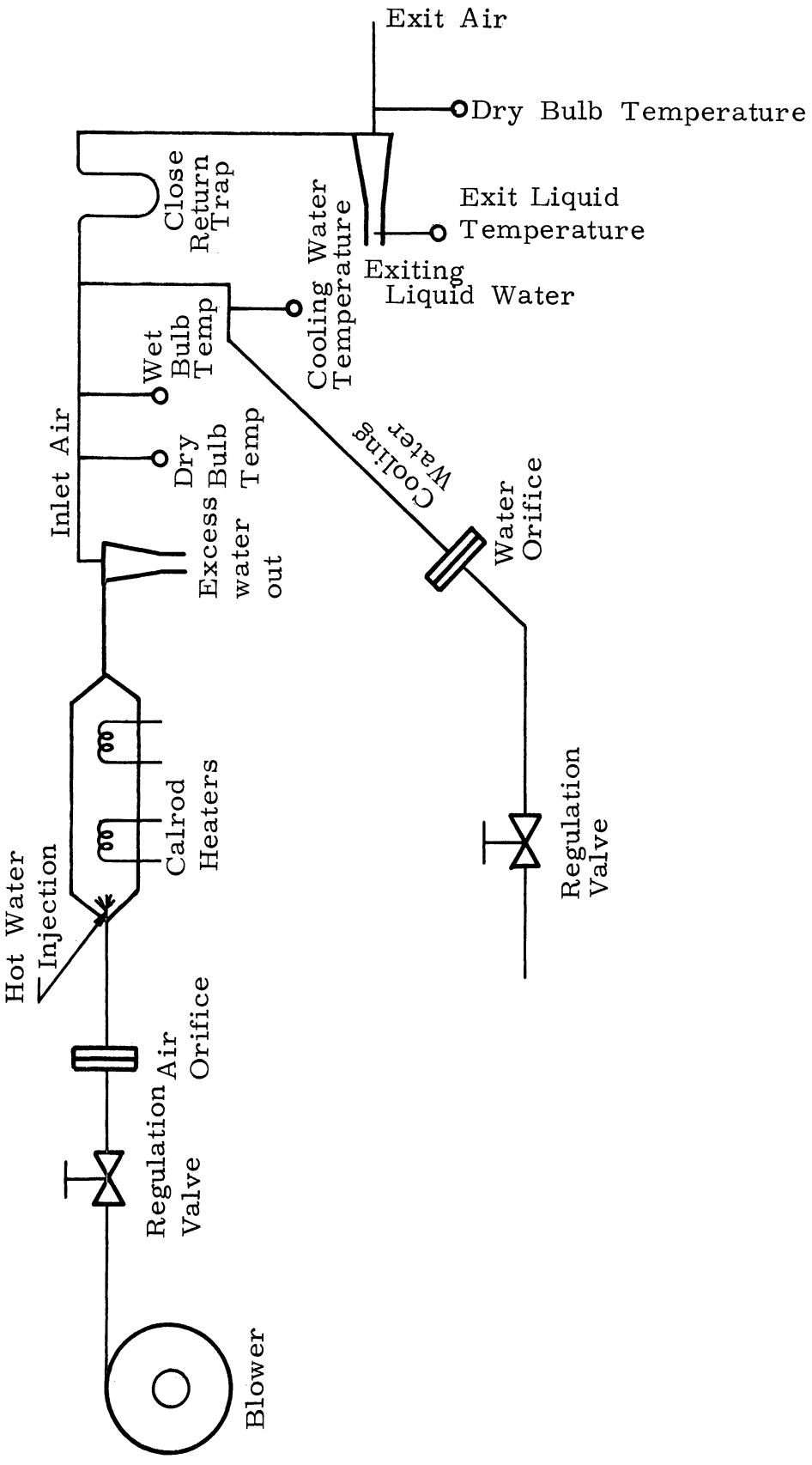

Fig. 1. Schematic of experimental apparatus.

The inlet air temperature varied from 120°F to 167°F, the inlet air flow rate from 0.75 to 2.0 lb mass/min, the cooling water flow from 1.15 to 3.08 lb mass/min.

RESULTS AND DISCUSSION

When the dry bulb temperature of the inlet air-water vapor mixture was used, the predicted outlet temperatures and water flow rates were very much in error, from 7% to 17.8% predicted. This was probably due to our being unable to achieve 100% relative humidity in the inlet air. A number of combinations of wet and dry bulb temperatures were then tried to see if repeatable accuracy could be achieved. Very good agreement between experimental results and computer predictions was achieved over a wide range of data, when the inlet air wet bulb temperature was used instead of the dry bulb temperature. Therefore, the computer tool can be extremely flexible and accurate over a wide range of operating conditions if the inlet relative humidity is relatively high and the wet bulb inlet temperature is used. This is advantageous as 100% relative humidity would probably not always be achieved in the velocity extraction system.

The predicted outlet temperature error varied from 0.08% to 2.7%, while the outlet liquid water flow rate error varied from 9.4% to -3.2%. These results are in extremely close agreement (Figs. 2,3, and 4) (while error figures are subject to experimental error, this was minimized by repeated measurements at each operating condition.)

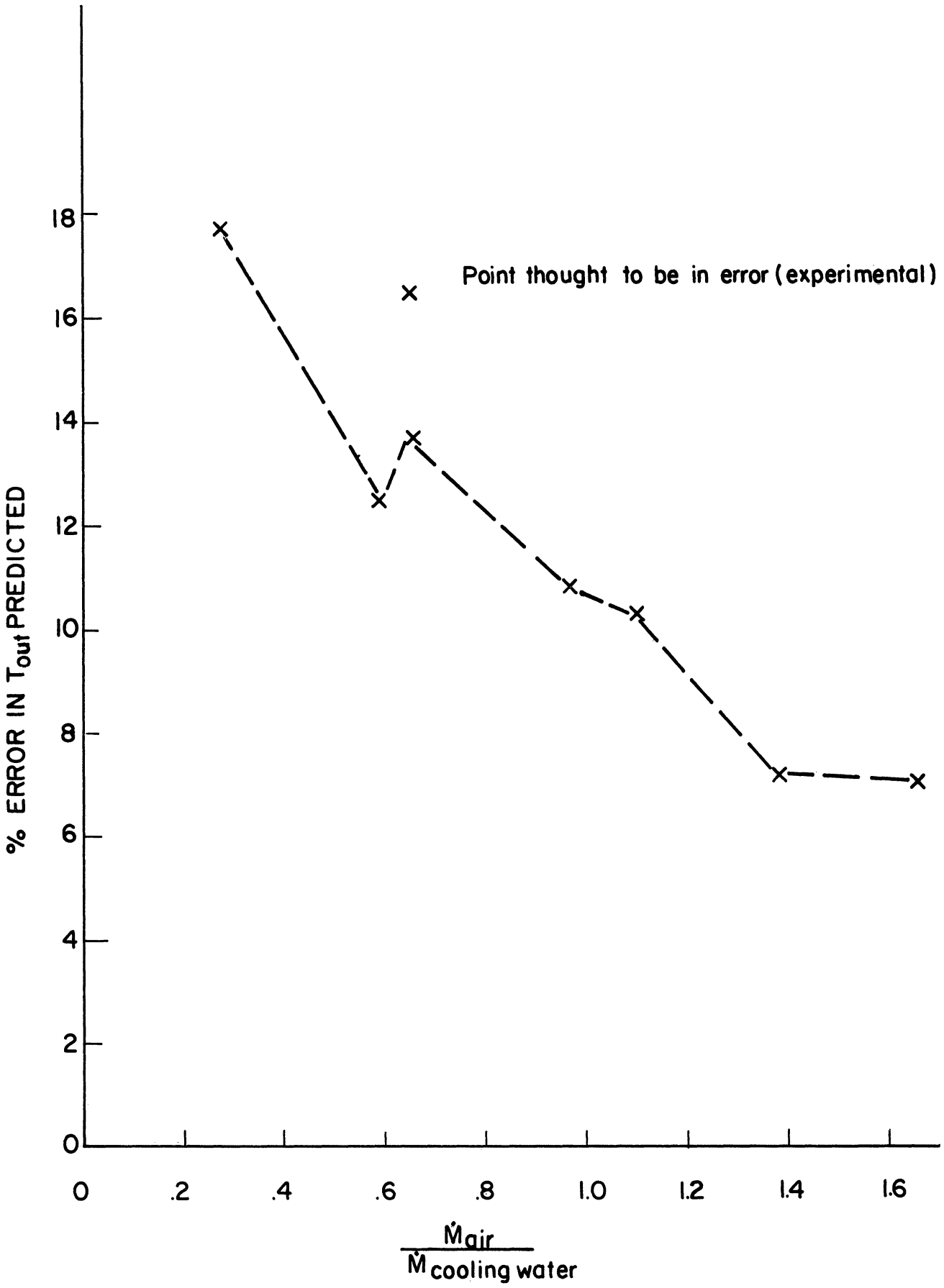

Fig. 2. Error in predicted outlet temperature based on inlet dry bulb temperature vs. inlet mass flow ratio.

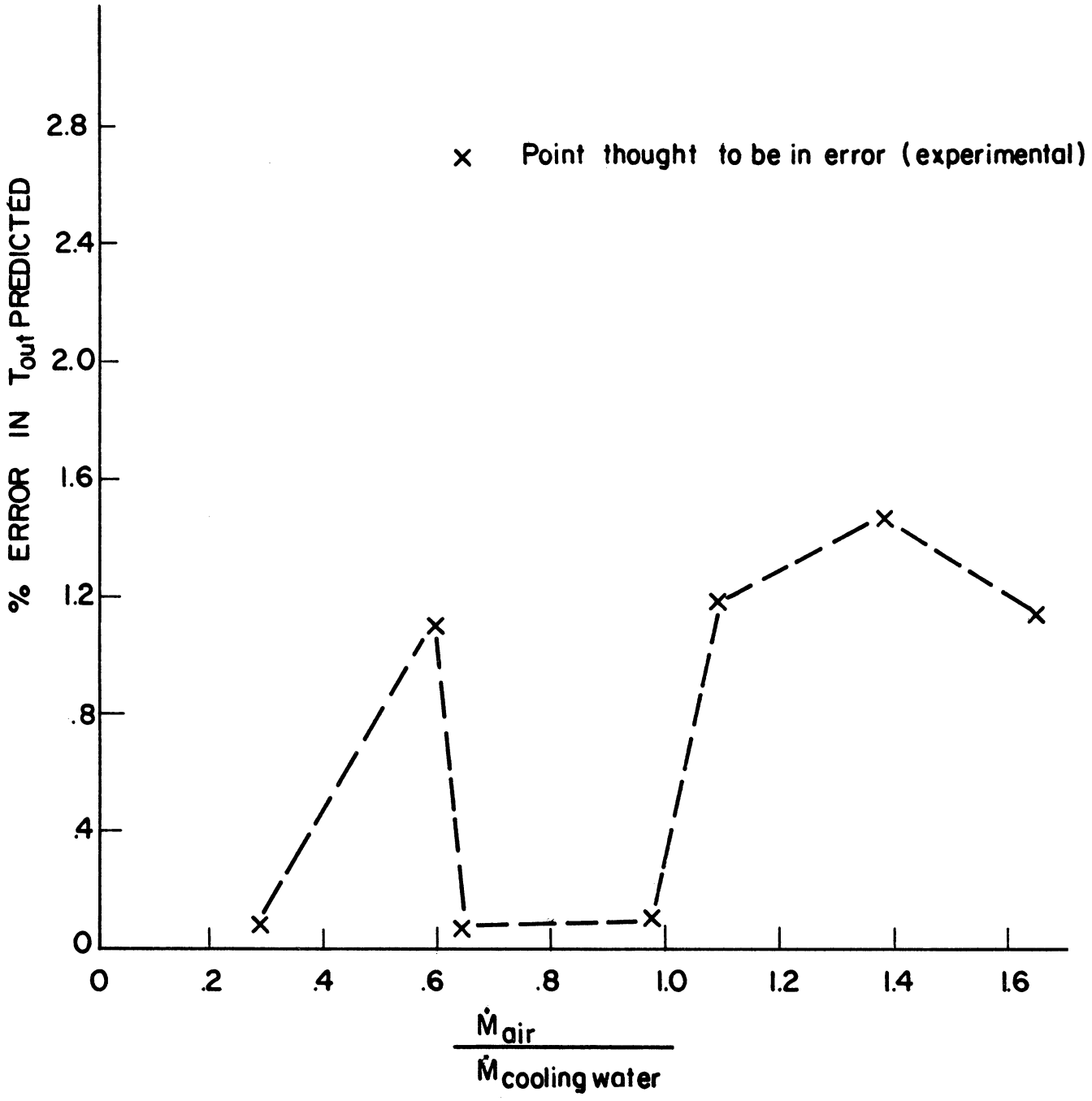

Fig. 3. Error in predicted outlet temperature based on inlet wet bulb temperature vs. inlet mass flow ratio.

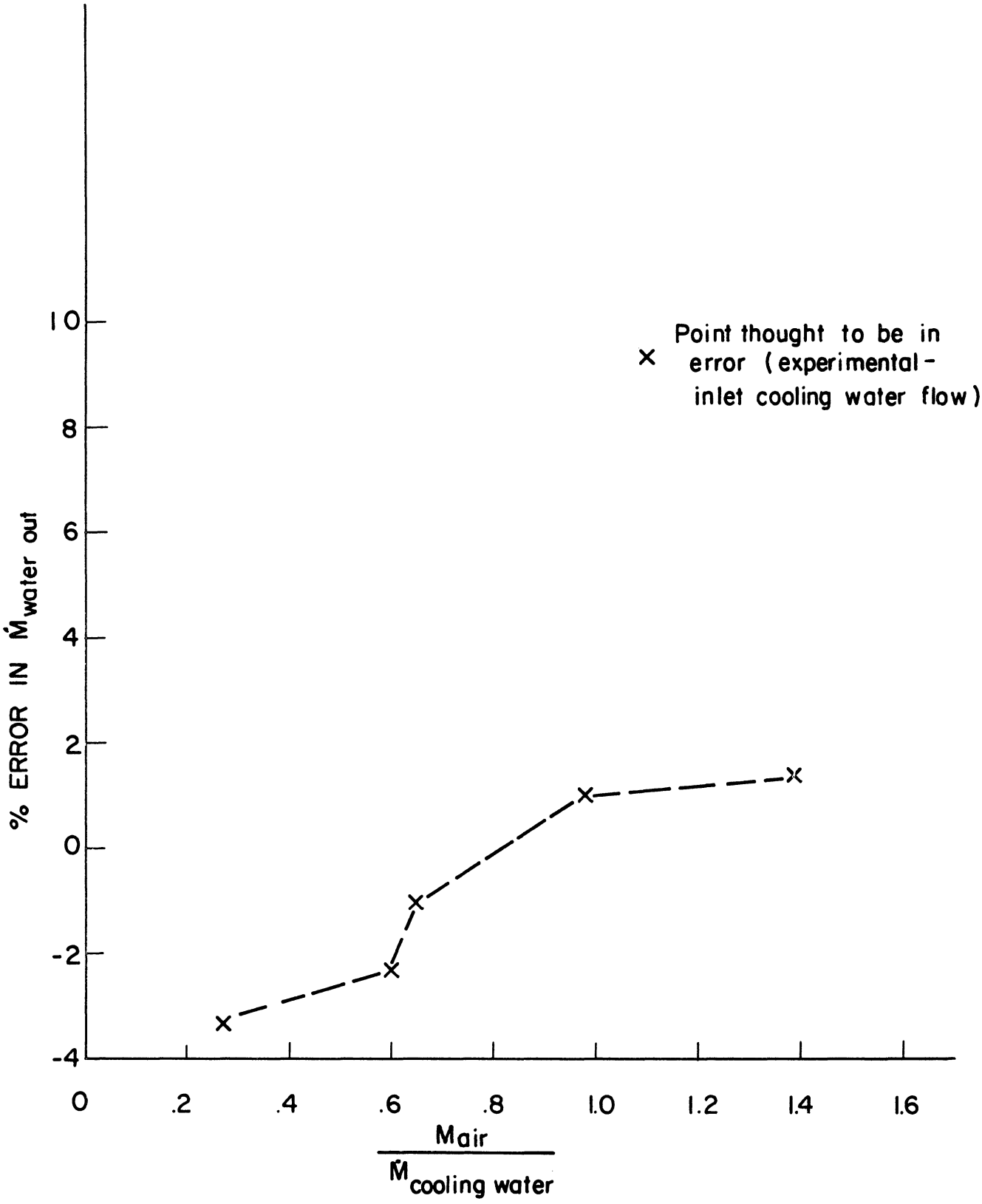

Fig. 4. Error in predicted mass outflow vs. inlet mass flow ratio based on inlet wet bulb temperature.

However, the use of this computer tool should be restricted to relatively high humidity. If low humidity inlet air is used, the cooling before condensation might take so long that the rate processes would not have time to go to completion. Further experimental investigation is needed for low inlet relative humidity conditions.

The assumptions implicit in the model, those of saturated exit air, and exit air, and exit water being at the same temperature, were also checked. Since wet and dry bulb temperatures were the same for a variety of conditions, the exit air was at 100% relative humidity as assumed. A small temperature difference, which varied between 1°F and 4°F with the air always hotter, was noted between the exit air and exit water temperatures. This temperature difference was not a direct function of air flow rate, water flow rate, or inlet temperature but was due to heat transfer across the brass separator. The water was in intimate contact with the wall of the brass separator as it swirled down the cone, while the air had only limited intimate contact with the brass separator as it exited out the top. Thus, both the implicit assumptions of the model were valid.

To determine optimum stream break up, the cooling water inlet spray was studied. However, whether the incoming stream simply ran in a small stream down the duct, or intruded into the air stream and broke up, had no measurable effect on condenser performance. Thus, at least in this configuration, it is more correct to call the condenser a direct contact contact condenser than a spray condenser.

There are two primary reasons for the computer equilibrium model predicting so closely the condenser performance. The extremely high heat

transfer coefficient for condensing vapor means that heat transfer, and in this case mass transfer, proceeds at a high rate and will go to completion before the flow exits from the condenser. Also in this close return trap, the primary mixing of air and water occurs in the upward duct out of the bottom of the trap. The water is moved up only by the action of viscous shear with the air, and extremely good break up with very high contact areas occurs here. The combination of high heat transfer coefficient and large contact area lead to equilibrium conditions.

ANALOG COMPUTER INVESTIGATION

The eventual goal of the total project is a digital computer simulation of the velocity extraction drying cycle. Basically, it will involve the grouping of modelled components, such as the direct contact condenser, in a closed loop. All the component modelling is essentially steady-state with the resulting governing equations being algebraic, requiring trial and error solution. Any unsteady state use of the cycle program will involve step by step short time interval approximation.

Thus, the possible use of the analog computer for simulation was investigated, for in many ways it is an extremely interesting and advantageous method. With the analog computer, the operator may change parameters and immediately observe the results of such changes. Further, the operation and output are continuous and unsteady approximations are unnecessary. Exact solutions may be obtained to unsteady problems.

There are some disadvantages, however. Each component would have to be remodelled. The modelling for the digital computer is basically steady-state with algebraic equations requiring trial and error solution. The analog is extremely good for trial and error solutions, but requires integration. With the present modelling there is no integration. Also present modelling is for steady-state and does not include unsteady state terms. Thus, the components would have to be remodelled using the unsteady forms of the First Law of Thermodynamics, Continuity Equation, and Momentum Equation, with appropriate limiting assumptions and boundary conditions.

Equipment requirements might be a problem. For reasonable trial and error solution times, patchable logic control of the analog computer would probably be necessary, and perhaps a true analog-digital hybrid computer would be required. There would probably also be relatively high requirements for the number of amplifiers and nonlinear elements.

Thus the use of the analog computer would involve much work and probably a good deal of equipment which might not be available. It has the advantage of flexibility and time unsteady solution, but might not be economical.

INVESTIGATION OF PRESSURE DROP IN CENTRIFUGAL SEPARATORS FOR WHIRLPOOL CORPORATION

Douglas H. Lane

FOREWORD

The work which was done during the Fall Semester was experimental only. Tests were conducted on two different separators to determine their pressure drop under steady-state operating conditions and to compare the test results with an analytical prediction. The reader is referred to the previous report 07494-2-P, on centrifugal separation by this writer for the previous analytical and experimental work, as well as the theoretical background study. The separators were designed to give inlet air velocities of 88 ft/sec at 50 cfm and 120 ft/sec at 67 cfm. These velocities are withir the recommended limits for water separation.

TEST SETUP

The test setup for the experiments is shown in Fig. 1. The air was taken from the air supply of the Fluid Mechanics Laboratory and fed through a Fischer regulator before being fed through the flowmeter. A rotometer was used to measure the air flow from 0-25 cfm, and the orifice was added in parallel with the rotometer to measure air flow rates from 25-67 cfm. Water was added to the air flow, and the air-water mixture was fed to the centrifugal separator being tested. After the water had been separated, it was fed to a drain by gravity while the air left the separator out the top. The pressure drop across the separator was measured with a manometer with pressure taps 15 in. before and 18 in. after the separator. Straight duct

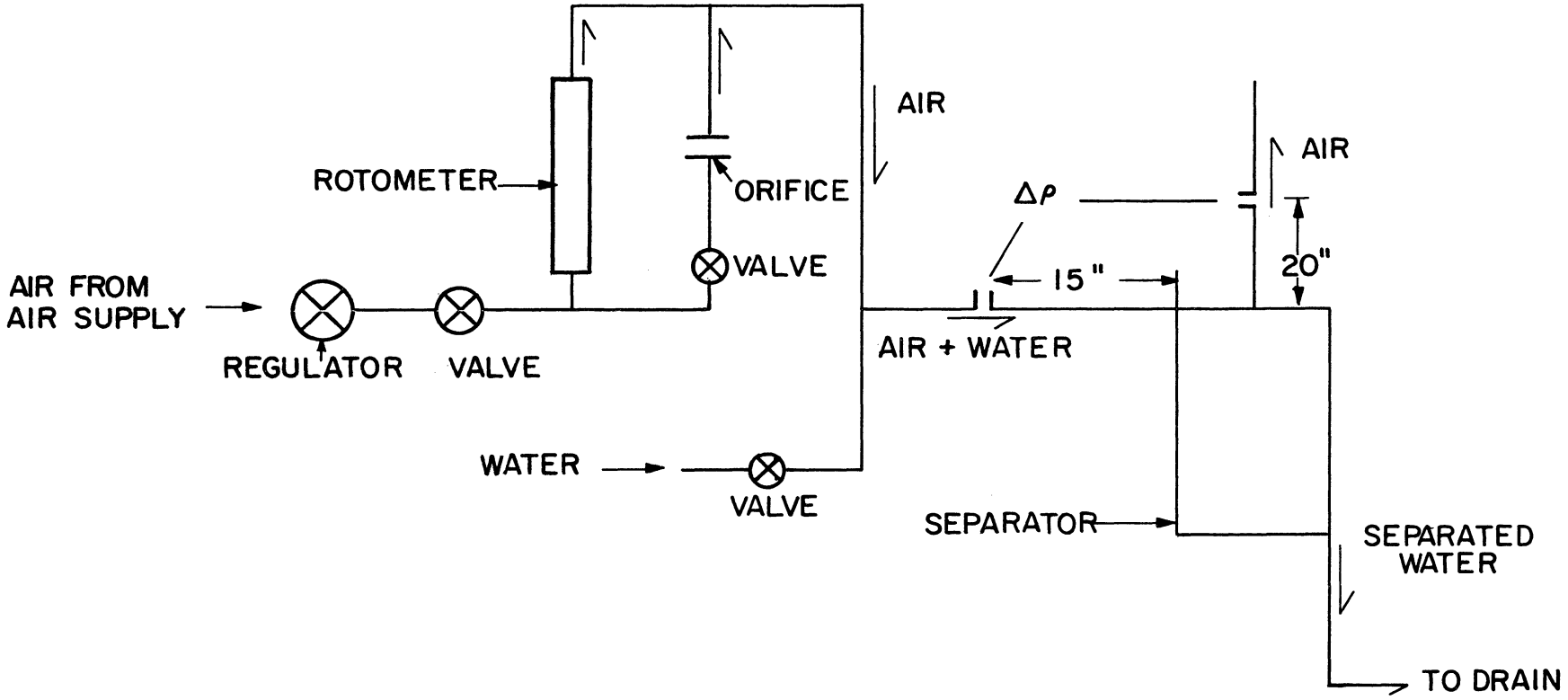
AIR
ROTOMETER
ORIFICE
AIR
Δρ
VALVE
20"
15"
AIR FROM
AIR SUPPLY
REGULATOR
VALVE
AIR + WATER
WATER
VALVE
SEPARATOR
SEPARATED
WATER
TO DRAIN

Fig. 1.

was added before and after the separator to eliminate external effects. The water flow rate was measured by determining the time to fill 500 ml.

TEST NO. 1

The first series of tests were conducted on the separator whose dimensions are illustrated in Fig. 2a. The separator was initially tested with no reentrainment shield installed. Appreciable reentrainment was present with this geometric configuration for most operating conditions. This performance would be unsatisfactory in an actual extraction cycle. The distance the exit duct extends into the separator was varied. No difference in pressure drop occurred.

A small diameter reentrainment shield (Fig. 2b) was added in the next test of the large separator. Reentrainment was still present but had been reduced. The results of this test are illustrated in Fig. 3. Reentrainment occurred because the diameter of the reentrainment shield was almost as small as the diameter of the exit duct. The water was picked up by the air before the air flowed into the bottom of the exit duct.

The next test of the large separator was conducted with a larger reentrainment shield (Fig. 2c). No reentrainment was present under all operating conditions. The results of this test are illustrated in Fig. 4. The length of the previous reentrainment shield was decreased 1 in. and tested. No difference in performance was noted.

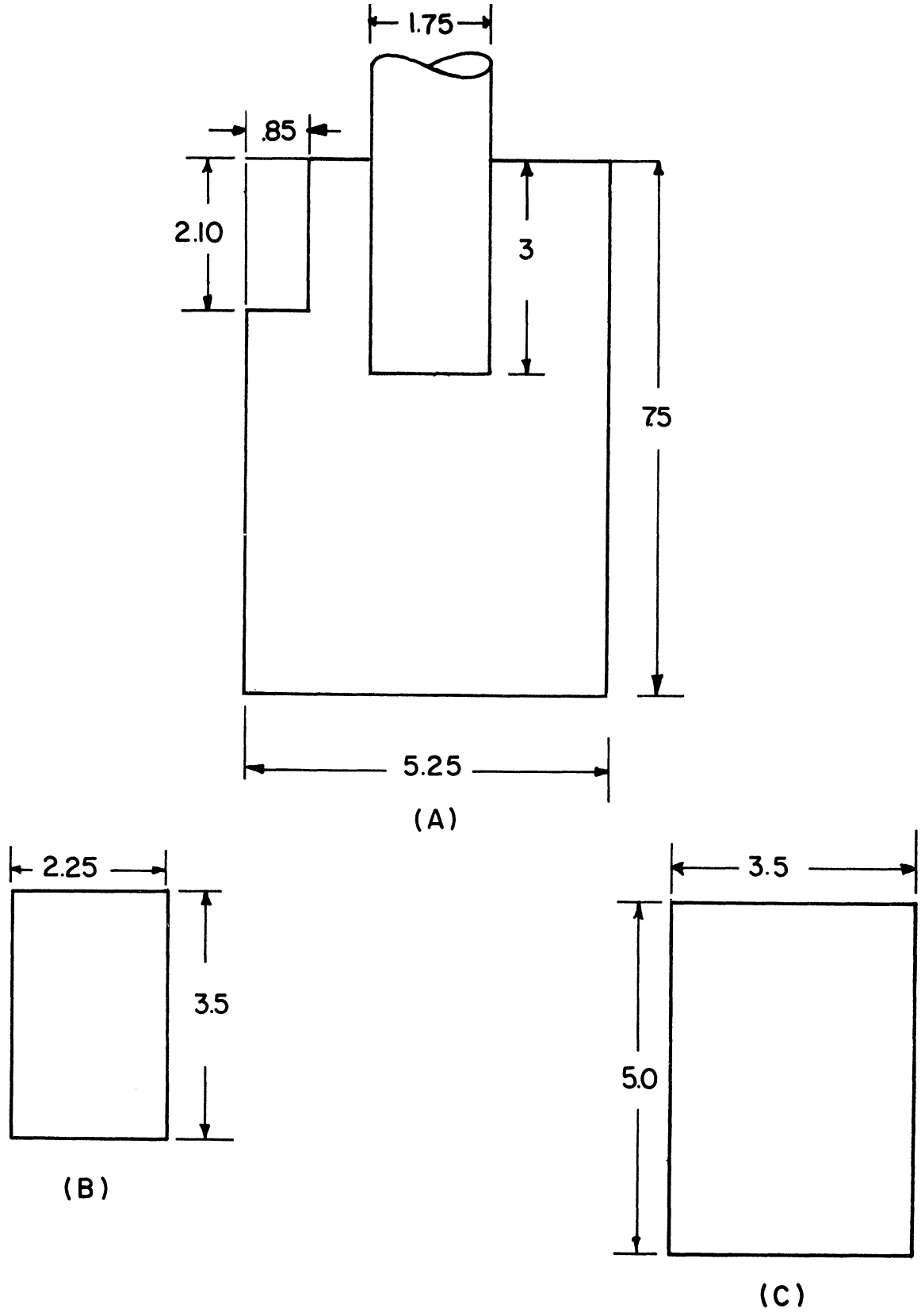

Fig. 2. Large separator.

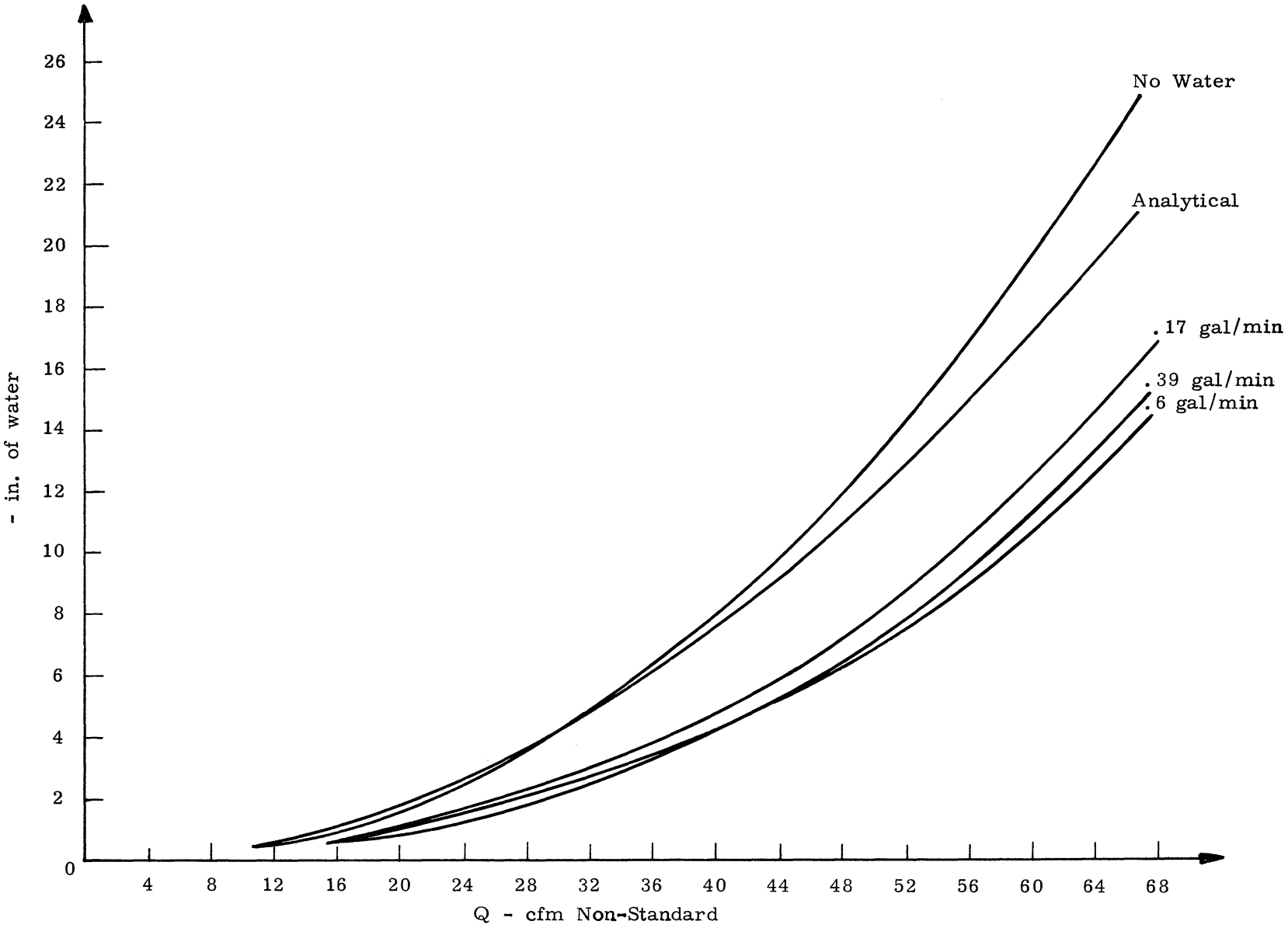

Fig. 3. Large separator, small shield.

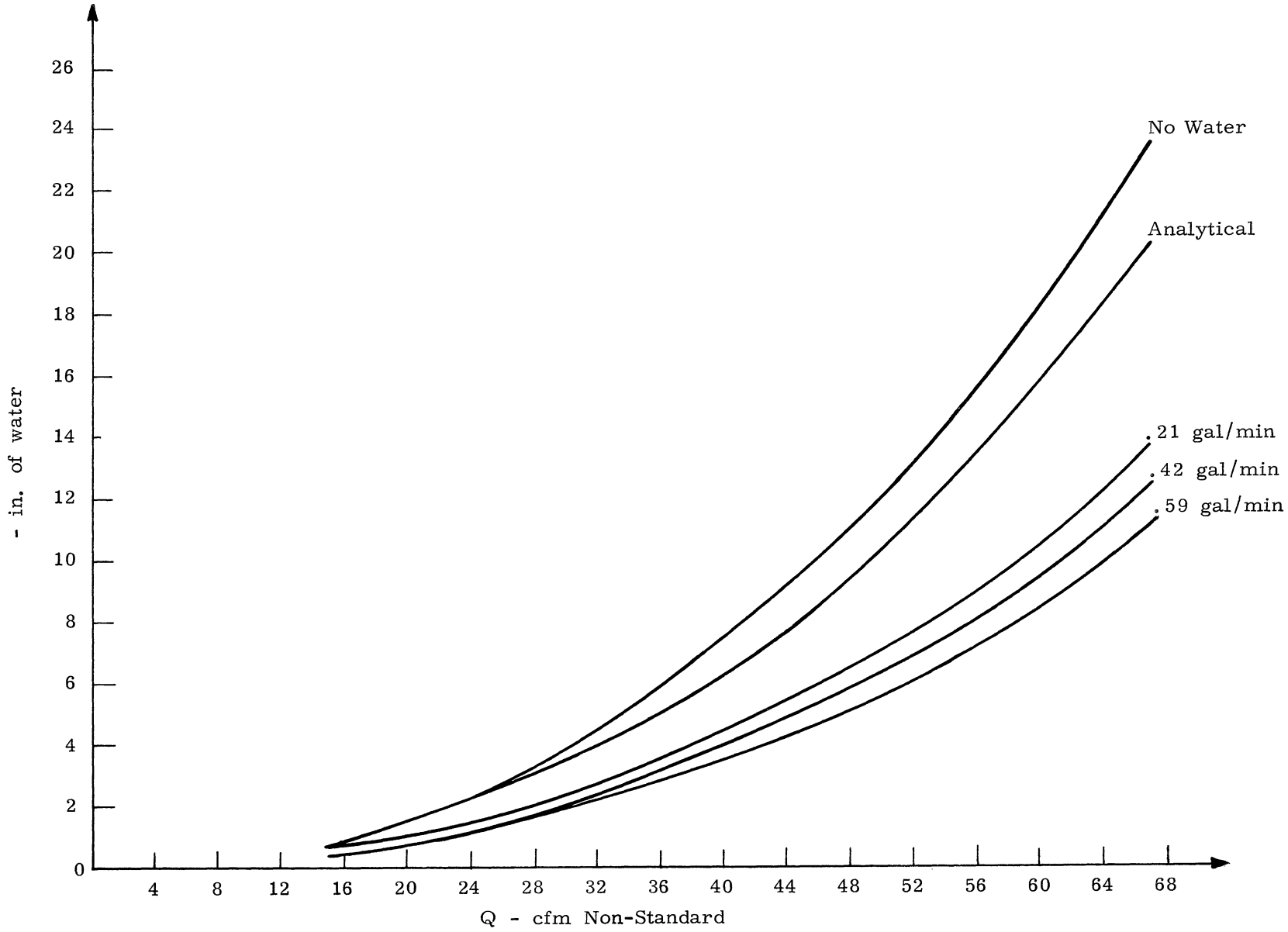

Fig. 4. Large separator, large shield.

TEST NO. 2

The second series of tests were conducted on the separator whose dimensions are illustrated in Fig. 5. The separator was tested with no reentrainment shield present. Appreciable reentrainment resulted for most operating conditions (Fig. 6). The separator was then tested with a small reentrainment shield (Fig. 2b). Reentrainment was reduced, but the separation efficiency was still in adequate. No data was recorded for this test. A slightly larger reentrainment shield (Fig. 3b) reduced reentrainment even more, but the separation efficiency was not satisfactory (Fig. 7).

ANALYTICAL RESULTS

The computer program, as programmed in the previous report, was not used because the pressure drop equation was programmed for circular inlets, and the area of the reentrainment shield was not considered. The pressure drop equation could be programmed to consider a rectangular inlet and the area of the reentrainment shield.

The analytical pressure drop has been calculated by assuming the inlet to be rectangular and considering the area of the inside and outside of the reentrainment shield (see Appendix).

ANALYSIS AND CONCLUSIONS OF TESTS

In both separators the presence of the reentrainment shield reduced the pressure drop under all operating conditions. The analytical results

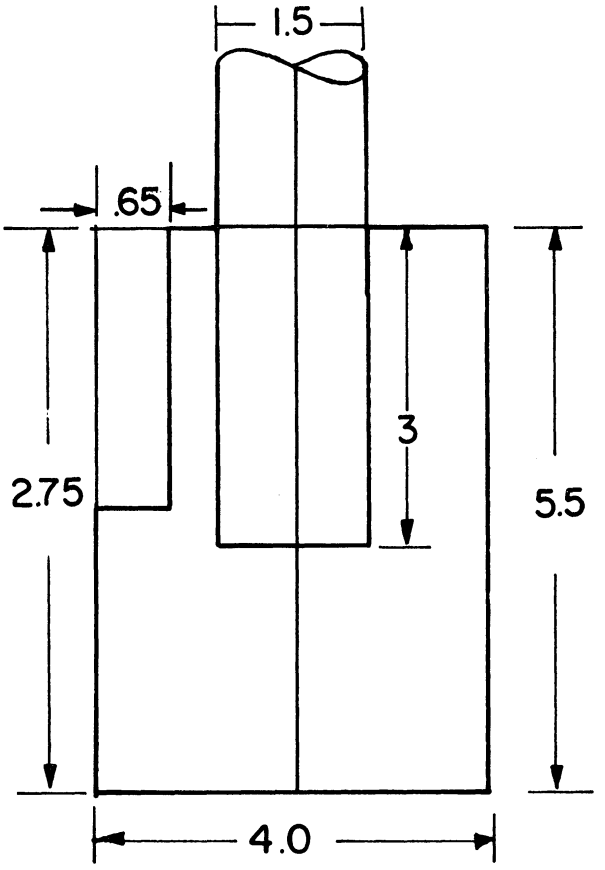

Fig. 5. Small separator.

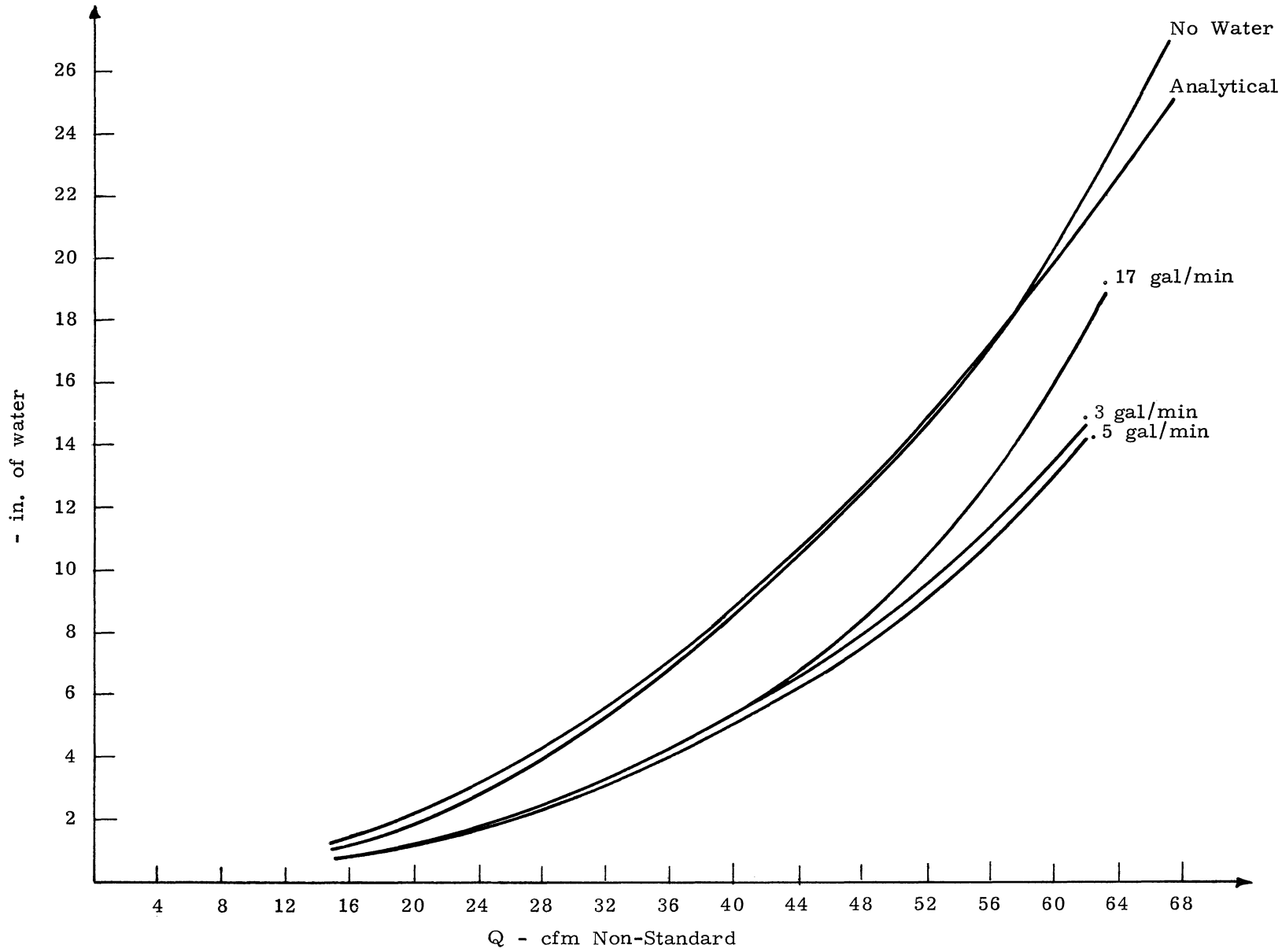

Fig. 6. Small separator, no shield.

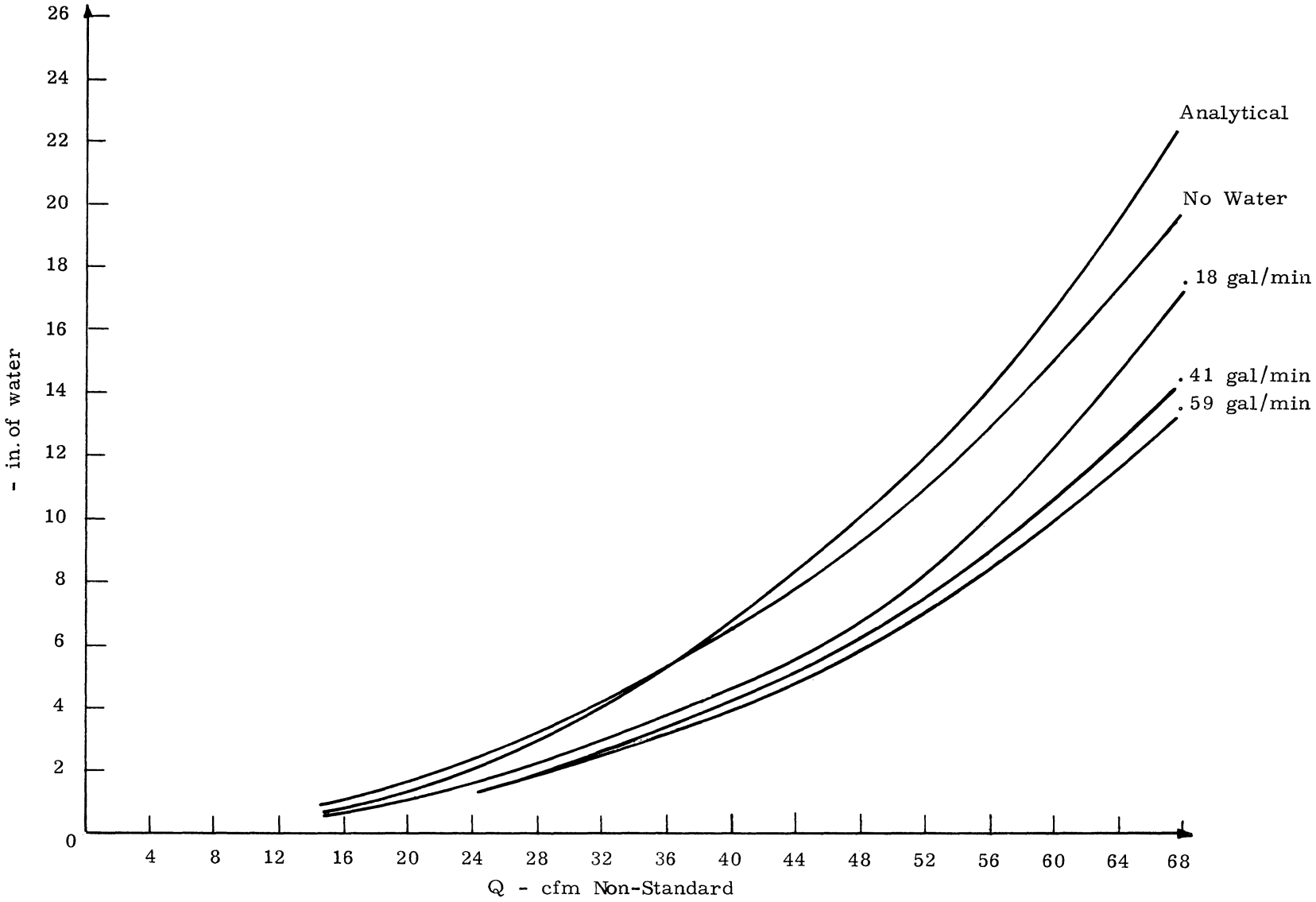

Fig. 7. Small separator, large shield.

of the large separator for both cases illustrated (Figs. 3 and 4) were less than the experimental results with no water present. These results compare favorably. The analytical results of the small separator agree favorably with the experimental results for the case of no water present. In the larger separator the analytical results were less than the experimental (Fig. 6), while in the smaller separator the analytical results were greater than the experimental results (Fig. 7). It was true in all cases that the greater the water flow rate, the lower the pressure drop. Water reduced the pressure drop in all cases.

The tests were conducted with positive pressure rather than with a vacuum as is the actual operating condition in the extraction and dry cycle. The pressure drop across the separator is independent of whether positive pressure or a vacuum is used to produce the flow. In the tests water tended to accumulate in the bottom of the separator. It appeared that this separated water was being picked up by the air leaving the separator and not the incoming, unseparated water. That is to say, reentrainment rather than true separation was the cause of separator inefficiency in the test conditions. A water pump, as is used in the actual extraction and dry cycle, may remove the separated water fast enough to prevent water buildup in the bottom of the separator and thus eliminate reentrainment. It is recommended that future tests be run under a vacuum and with a water pump.

The tests were conducted under steady-state operating conditions although these conditions rarely exist in the actual extraction and dry cycle. It was observed that reentrainment increased under transient operat-

ing conditions. A separator which performs well under steady-state conditions may have unsatisfactory performance under transient conditions. Therefore, tests under transient conditions should be conducted and a larger separator may then give better performance than a smaller one.

APPENDIX

Large Separator—Fig. 2a

Reentrainment Shield—Fig. 2c

$$A = \pi(2(D_C^2/4) + L_C D_C + L_E D_E + 2L_S D_S)$$

$$= \pi(2(5.25^2/4) + (7.5)(5.25) + (2)(1.75) + 2(5)(3.625)) = 93\pi$$

$$a = L_I W_I = (2.10)(.85)$$

$$K_3 = GA/a = 93\pi/(200)(2.1)(.85) = .8185$$

$$K_3^2 = .671$$

$$K_4 = D_E/2(D_C - W_I) = 1.75/2(5.25-.85) = .1703$$

$$K_4^2 = 0.0290$$

$$B = .1703+(2)(.8185)-\sqrt{.0290+(4)(.8185)(.1703)}/.671 = 1.552$$

$$[1 + B(\frac{1}{K_4} - 1) + 2K_1^4]$$

$$[1 + (1.552)(\frac{1}{.1703} - 1)+(2)(.551)] = 9.65$$

$$aV_I = Q$$

$$V_I^2 = \frac{Q^2}{a^2} = \frac{Q^2(ft^3/min)^2}{(2.1)^2(.85)^2 in.^4} \frac{(144)^2 \frac{in^4}{ft^4}}{3600(sec/min)^2}$$

$$CP = 15.5 \text{ psi} \quad t = 76F$$

$$\Delta P = \frac{(.00808)(15.5)(9.65)(Q^2)}{(536)} \frac{144^2}{2.1^2 .85^2 3600} = 4.06 \times 10^{-3} Q^2$$

COMPUTER-AIDED CENTRIFUGAL PUMP DESIGN FOR HOME LAUNDRY APPLIANCES

James G. Morgan

LIST OF SYMBOLS

Symbol	Description	Units
U	linear velocity	fps
V_{in}	volute eye velocity	fps
V_e	volute exit velocity	fps
V	absolute velocity	fps
V_r	relative velocity	fps
anvel	impeller inlet passage velocity	fps
W	angular velocity	rad/sec
SN	impeller speed	rpm
BH	impeller blade height at outlet	in.
B5	impeller blade height at inlet	in.
h	impeller blade height in general	in.
R	coordinate in polar coordinates	in.
Beta	coordinate in polar coordinates	deg
D	diameter in general	in.
D3	diameter at cut water area	in.
S	head coefficient	none
Fl-CO	capacity coefficient	none
PNS	specific speed	none
T	impeller blade taper angle	deg
A	impeller angle	deg
z	angle defined in Figure 4	deg
Y	angle defined in Figure 11 and Eq. (45)	deg

LIST OF SYMBOLS (Continued)

Symbol	Description	Units
H	pump head	ft
Q	pump flow rate	gpm
F	force	lb
P^a & P^b	pressure	psi
N	number of impeller blades	none
NHY	hydraulic efficiency	percent
NOA	overall efficiency	percent
SR; WR	scaling ratios	none
i,Sw,SHg	specific weight	none
d	density or differential depending on use	lb/ft^3
K	constant	none
C	constant	none
g	gravitional constant	fps^2
Δ	incremental quantity	units of term
x	distance along a streamline	in.
HPin	horsepower input	horsepower
HPout	horsepower output	horsepower
HPmech	horsepower mechanical	horsepower
WK	work rate	ft-lb/sec
L;L1;L2	dynamometer scale loads	gm
Hact	head produced at some R	ft

LIST OF SYMBOLS (Continued)

Symbol	Description	Units
area 1	area at impeller inlet passage	ft^2
area 2	area at impeller outlet passage	ft^2
$\bar{R}$	centroidal radius	in.
Den Bun F1 - F13 G4 - G7 C1 F, I B1 - B4 . . . etc.	defined in computer program in the Appendix	
Wid	volute width	in.
y	vertical Cartesian coordinate	in.
Subscript 1	inlet condition	
Subscript 2	outlet condition	
Hg	mercury	
w	water	
H1	flow rate data reading	in.
H2	dynamometer scale reading	units
H3	head manometer data reading	in.
N1	pump shaft speed reading	rpm
DEF	dynamometer scale reading (dry)	units
do	orifice plate diameter	in.
d1	outlet pipe diameter coupled to orifice	in.

LIST OF SYMBOLS (Concluded)

Symbol	Description	Units
*;·	Multiplication symbols	none
F	temperature Fahrenheit	deg

ABSTRACT

The objective of this project was to develop a procedure for designing a centrifugal pump. The ultimate purpose of this procedure was to define pump geometry for a pump that would operate at a given head, flow rate, and shaft speed. Operating conditions were in the low head (10-20 ft of water) and low flow (10-20 gpm) range. The report is written in two separate sections, a major detailed report and a brief design procedure supplement.

A detailed study of analytical and experimental design methods was made. A method combining the analytical and experimental modes was then formulated into a design procedure to produce "first trial" pump geometry dimensions.

The procedure was programmed in computer language and employed to design three prototype impellers. In addition, another prototype was fabricated based on scaling principles.

These prototypes were tested, and experimental conclusions are given and discussed. The major design requirement is impeller flow channel design. The percent deviation between the characteristics predicted and that measured experimentally was approximately 5% for one prototype.

This procedure should be of considerable value in designing centrifugal pumps for a given head flow rate operation.

I. SUMMARY

A. General Introduction

A program was initiated in September, 1965, at The University of Michigan to formulate a computer procedure for designing small centrifugal pumps. The procedure has two basic requirements: (1) it should require persons unskilled in pump design to specify only a small number of operating parameters; and (2) it should permit the computer, with the operating parameters as input, to define the pump geometry for the necessary operating conditions.

This investigation is considered essential because current procedures for designing centrifugal pumps are inadequate. Adequate information exists regarding pump operation, installation, maintenance, and selection. However, because of extreme competition between pump manufacturers, little information regarding analytical design has been published. Furthermore, the few analytical-empirical techniques available are intended essentially for pumps operating at large heads (30-100 ft) and extremely high-flow rates (200-2000 gpm) relative to the normal range of operation for appliances (approx. 10 ft and 10 gpm).

Moreover, most of the literature about pump design deals essentially with pumps for ordinary water, not those for washing machines, which must be able to pump water full of dirt, soap suds, long strings of clothes lint, and, upon occasion, even a ball-point pen.

Basically, the computer program will require the designer to supply the desired operational data (i.e., flow rate, head, shaft speed, outlet blade angle, etc.). The computer output will specify all the geometrical parameters (i.e., impeller diameter, vane height, inlet blade angle, housing dimensions, etc.) and additional information required to manufacture a pump that will oerate near the specified operating conditions.

The use of this technique should result in substantial cost and time savings in engineering, drafting, and model work.

The main report is divided into the following areas:

I. Summary

II. Analytical Study

III. Experimental Study

IV. Design Calculations

V. Bibliography

VI. Appendix

VII. Supplement

Four pump prototpyes that had been fabricated by Whirlpool in St. Joseph, Michigan, were tested. In addition, the present production pump used in the Whirlpool combination washer and dryer (combo) was tested. The results and conclusions from these tests are given later in this report.

1. PRIMARY PROBLEMS

a. Present design methods are expensive.

b. Theoretical fluid mechanics do not adequately predict pump performance.

c. Little information has been published concerning small centrifugal pumps.

d. The pumping medium is unique.

2. PUMP DESCRIPTION

Discussed in this report are centrifugal pumps having horizontal shafts, single entries along the shaft (eye), tangential outlets, open-faced curved blades with variable height and designed to operate between 10-20 ft of head, delivering 20 gpm, and operating at constant shaft speeds of 1350, 1750, 2100, and 2400 rpm. Figure 1B shows the major geometry of the prototype pump; Fig. 1A shows the prototype and the combo pump. Figure 1C shows the four prototype impellers.

3. WORK PLAN

II. Analytical Study
- A. Literature Search
- B. Impeller Design
- C. Volute Design

III. Experimental Study
- B. Program Objectives
  1. Four prototype impellers (Fig. 1D) and one prototype volute were designed and built based on the analytical study. They are:
     Impeller 1—design by a scaling procedure.
     Impeller 2—designed by method 1, A2 = 15°.
     Impeller 3—designed by method 1, A2 = 30°.
     Impeller 4—designed by method 1, A2 = 55°.
     Volute 1—designed by volute method 1.
     The important physical characteristics of these components are listed in Table I. The volute is described by the equation r = R2*e^n*theta. It has a circular cross-section and tapered sides. The combo pump has a circular casing.

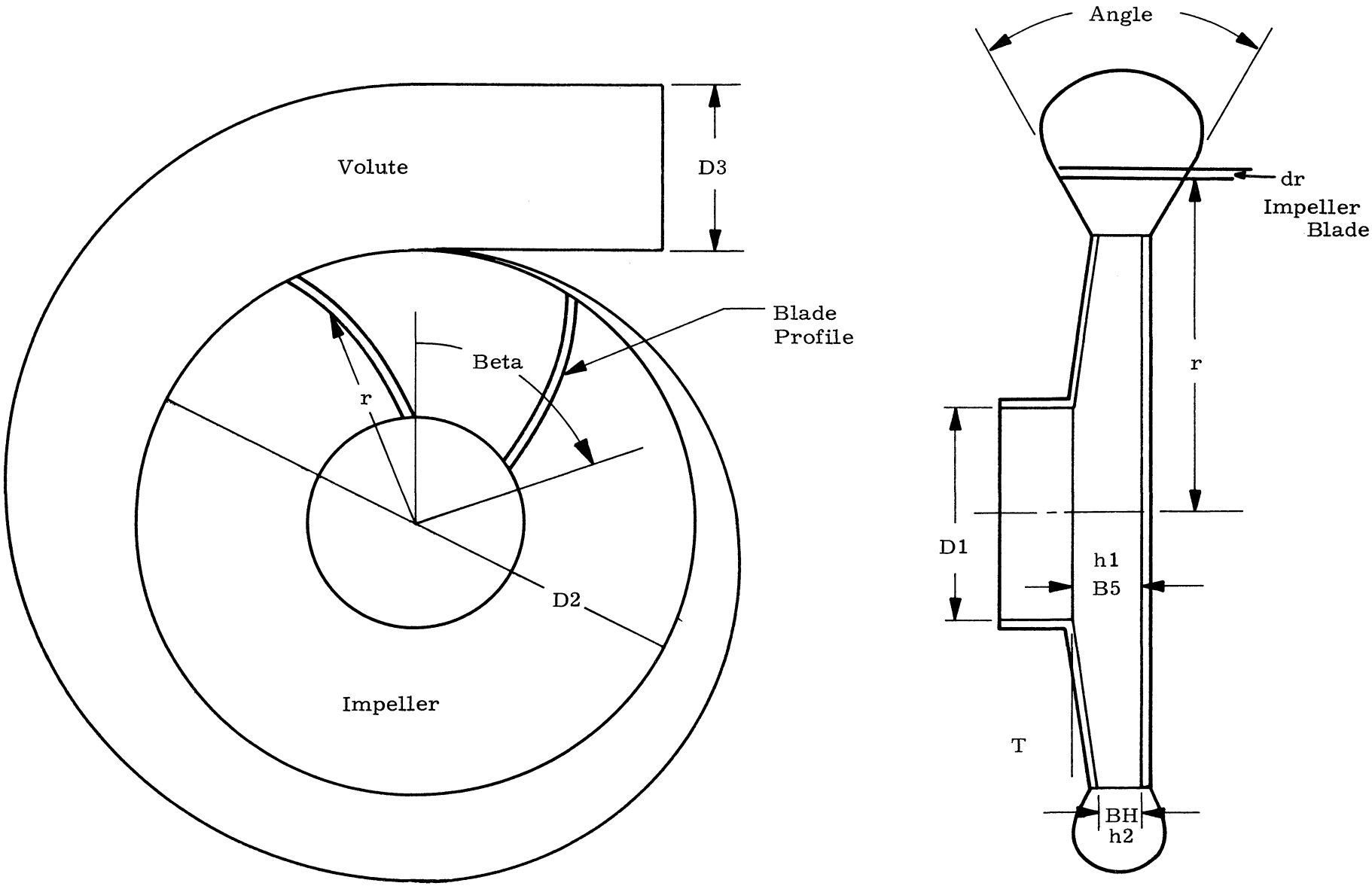

Fig. 1. Schematic layout of a centrifugal pump.

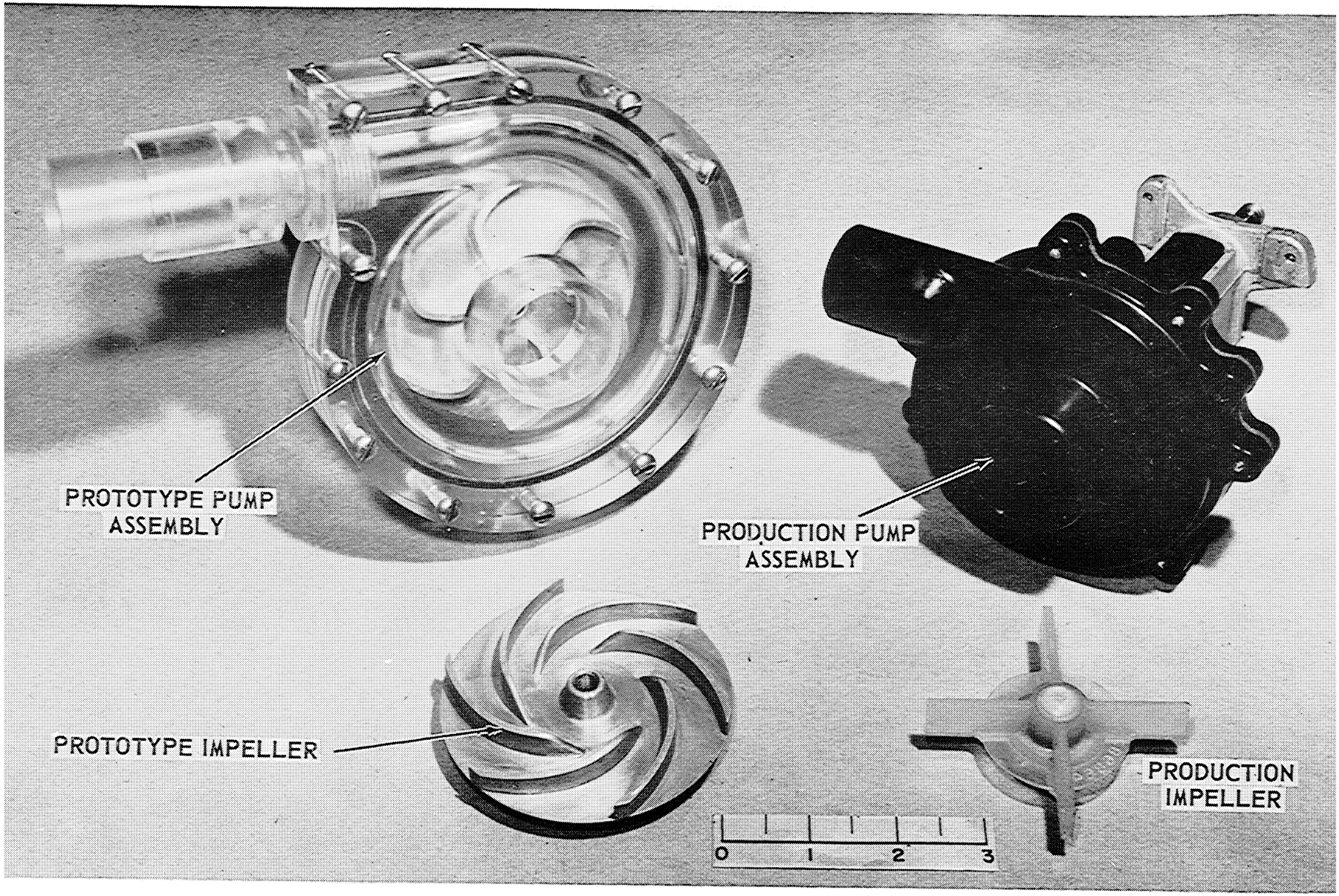

Fig. 1A. Comparison of prototype and production pump assemblies and impellers.

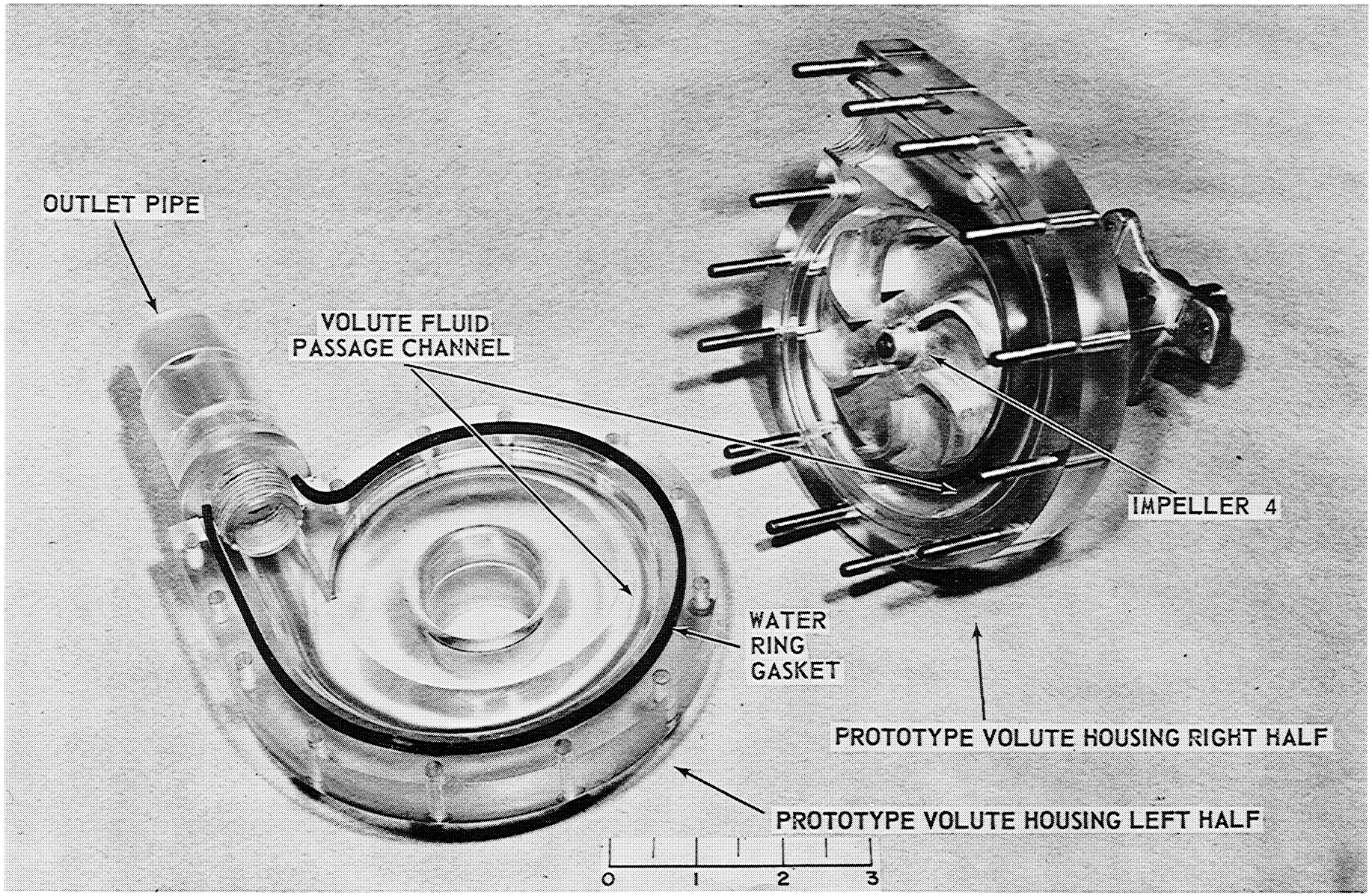

Fig. 1B. Prototype housing, impeller, and assembly.

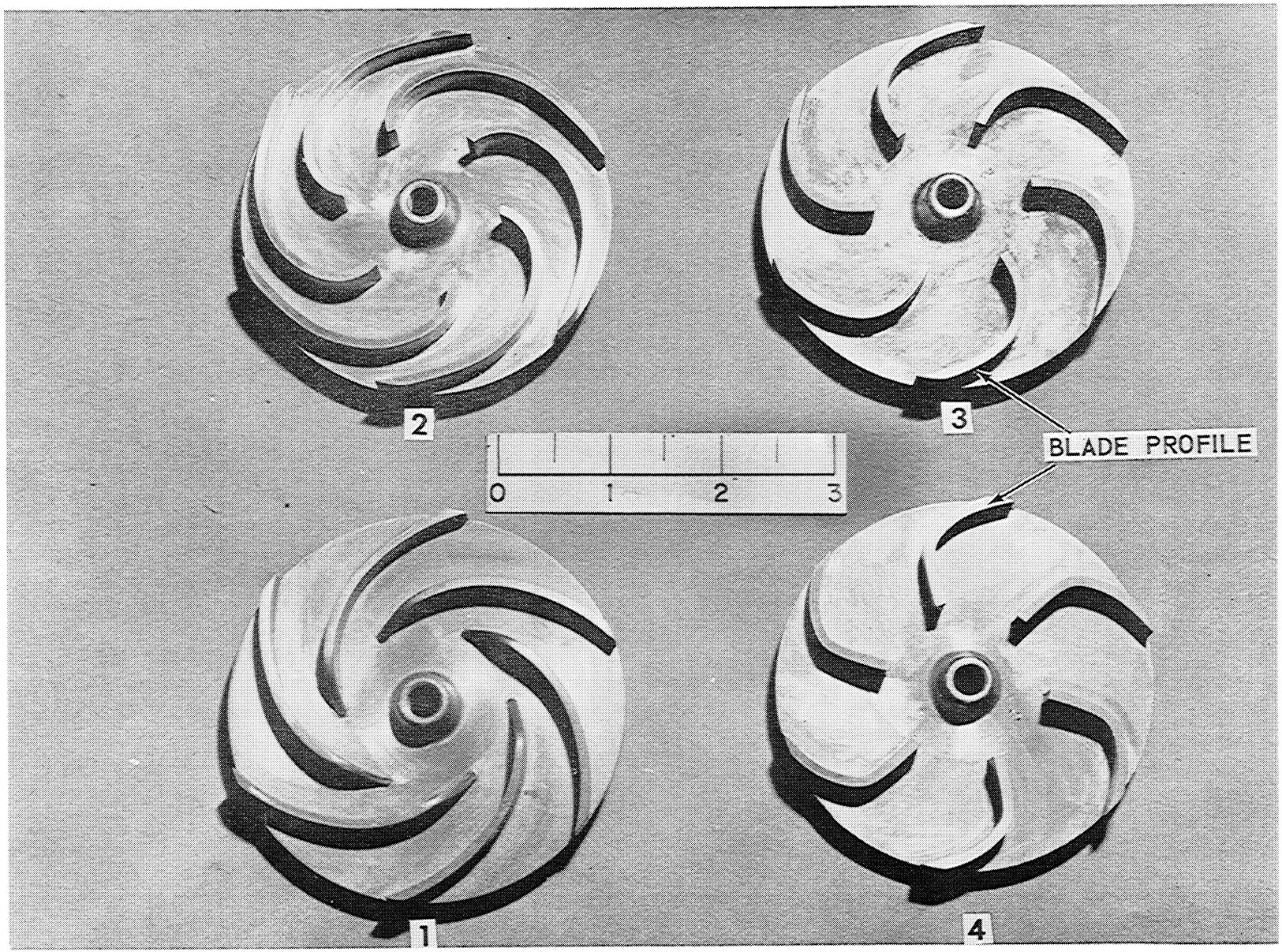

Fig. 1C. Prototype impellers 1, 2, 3, and 4.

TABLE I

PROTOTYPE DIMENSIONS

Impeller	D1	D2	A1	A2	B5	BH
1	1.37	3.44	18°	33°	.412	.279
2	1.37	3.22	12°	55°	.412	.279
3	1.37	3.22	12°	30°	.412	.279
4	1.37	3.22	12°	15°	.412	.279
combo	1.50	3.00	radial	radial	9/16	9/16

2. Testing apparatus with instrumentation to make required measurements was built.

3. Four impellers and a combo pump were tested.

B. Experimental Results and Conclusions

1. GENERAL CONCLUSIONS

a. A computer-aided centrifugal pump design procedure was formulated and used to determine "first trial" pump geometry values. Prototype 4, designed with the analytical procedure, generated a head and flow rate within approximately 5% of required performance at a reasonable efficiency (Fig. 1D). The results are shown below in Table II.

TABLE II

COMPARISON OF ACTUAL VS. PREDICTED HEAD-FLOW CHARACTERISTICS, PROTOTYPE 4

Speed, rpm	Flow Rate, gpm	Head (H)		Deviation, %
		Predicted	Measured	
1350	7.610	5.95	5.6	5
1750	10.05	10.003	9.60	5
2100	12.00	14.405	13.80	5
2400	13.75	18.814	17.90	5

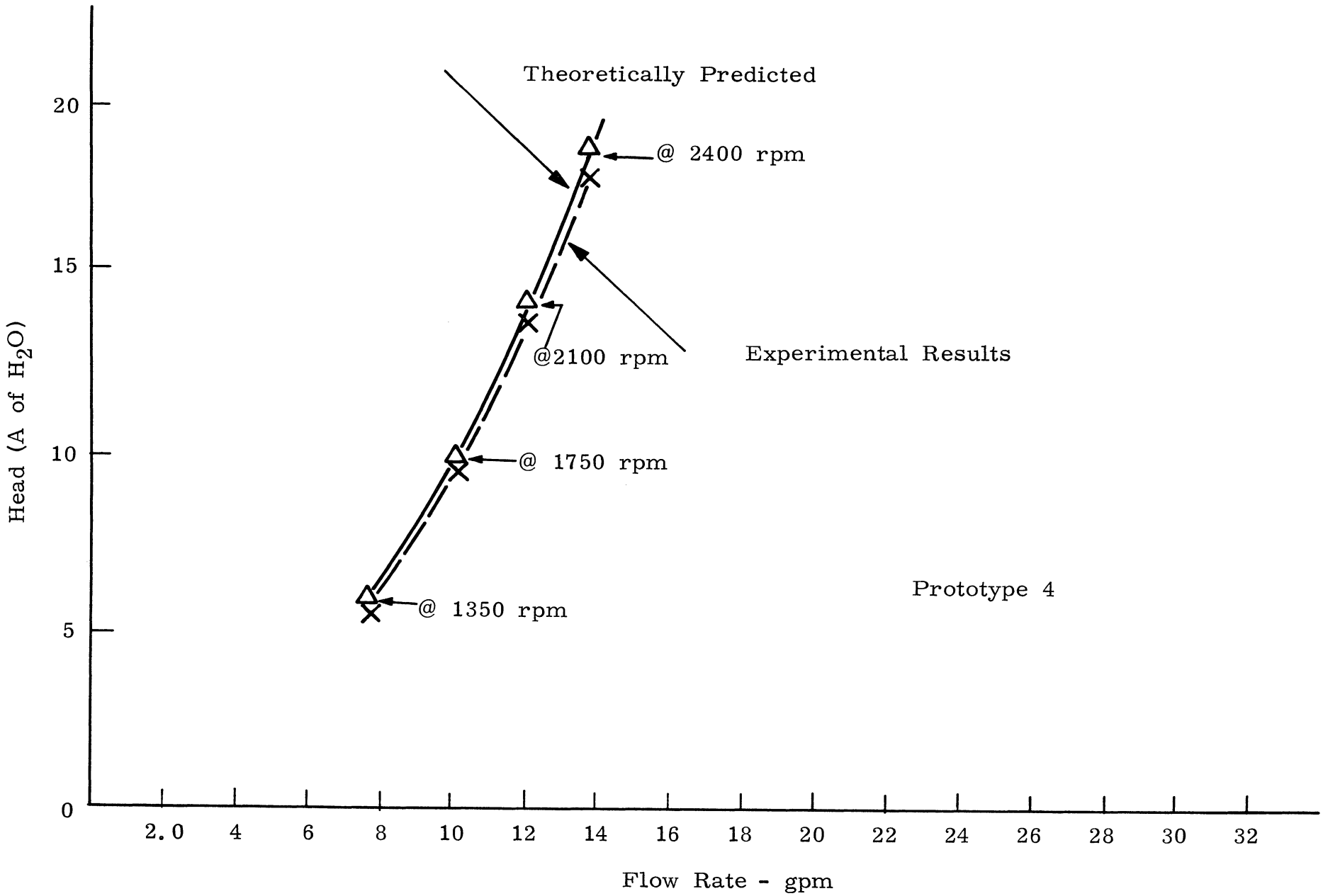

Fig. 1D. Comparison of theoretical vs. experimental.

b. Lint-contaminated water was observed to have negligible effect on pump performance.

c. A 15° outlet angle, A2, appears reasonable.

2. HEAD VS. FLOW RATE CONCLUSIONS

a. The head capacity curves show a gradual decrease in head for corresponding increase in flow rate for each of the four prototypes tested (Figs. 22-25). The resultant head and capacity at maximum efficiency (determined by drawing a smooth curve through the test points) is summarized in Table III.

TABLE III

SUMMARY OF PROTOTYPE PERFORMANCE AT MAXIMUM EFFICIENCY

Prototype	1350 rpm			1750 rpm			2100 rpm			2400 rpm		
	H	Q	N_{HY}	H	Q	N_{HY}	H	Q	N_{HY}	H	Q	N_{HY}
1	6.5	8.6	68.5	9.35	15.5	74.2	12.1	21.0	64.5	16.1	23.2	57.0
2	5.15	6.0	66.0	6.7	11.5	65.8	8.9	15.2	63.8	14.3	13.0	62.5
3	5.35	8.8	60.0	9.0	13.3	65.5	11.7	16.6	70.0	15.5	18.6	64.5
4	5.36	10.8	62.0	8.8	14.0	67.4	12.6	16.7	67.0	16.2	20.0	57.0

H = head (ft of water); Q = flow rate (gpm); N_{HY} = hydraulic efficiency (%).

b. The prototypes show considerable consistency at the constant speeds tested (1350, 1750, 2100, and 2400 rpm). At each speed it was observed that prototype 1 produced a substantially larger head for the same flow rate than did 4, 3, and 2. The relative head generating capabilities of the three latter impellers ranked in descending order of largest head produced, were 4,3, and 2 (Fig. 23).

c. For a given speed and at shutoff conditions, 1 produced a considerably larger head than 4. This difference gradually decreased as flow rate was augmented until a relatively small difference in head existed at maximum flow rate.

d. At medium to large flow rates, impellers 1 and 3 were noted to have approximately the same decrease in head increment for the same increment increase in flow rate (slope). Impeller 4 was observed to have a smaller head increment decrease than 3 and 1 while 2 was measured to decrease head at a substantially greater rate than 3 and 1.

e. Prototype 1 was noted to have superior performance characteristics compared to the present Whirlpool combination pump performance at 1750 rpm (Fig. 26). It developed considerable more head for corresponding flow rates (see Table IV).

TABLE IV

COMPARISON OF PROTOTYPE 1 VS. COMBO AT CONSTAND SPEED

Prototype 1			Whirlpol Combo			Percent Increase	
Q	H	NHY	Q	H	NHY	NHY	H
12.0	10.3	70.0	12.0	7.5	45.5	55.5	37.0

3. EFFICIENCY VS. FLOW RATE CONCLUSIONS

a. The hydraulic efficiency was noted to increase gradually from zero at Q = 0 to a maximum and then drop off for corresponding further increase in flow rate.

b. The hydraulic efficiency curves in general show a considerably flat characteristic at high efficiency values over a substantial flow rate range.

c. The maximum hydraulic efficiency for the impellers were relatively close in magnitude.

d. The mechanical energy losses were very large (Fig. 28).

4. DISCUSSION

a. General Conclusions

The computer-aided centrifugal pump design procedure generated a head and flow rate within approximately 5% of required performance at reasonable efficiency for prototype 4 (Fig. 1). Lint did occasionally "hang up" on the volute tongue momentarily before continuing downstream, but it had negligible effect on pump performance.

b. Head vs. Capacity Conclusions

The fact that the head capcity curve shows a moderate decrease in head for corresponding increase in flow rates can be explained by subtracting the major losses encountered throughout the complete flow range from what is predicted. Theoretically, the head capacity should exhibit a constant slope of decreasing head for increasing rate of flow (predicted from simple two-dimensional analysis, Ref. 5). From a macroscopic viewpoint, the major losses encountered, which cause adjusted performance in practice, are circulatory flow (Fig. 10), turbulence, blade length size, and surface viscous losses.

Some circulatory flow is present throughout the complete flow range. These losses are relatively constant, and their major effect is to give a lower head (see p. 79).

Because of fixed inlet blade angle, fixed outlet blade angle, and other fixed geometry, the actual pump conditions can approach this theoretical head-capacity curve at only one point. Furthermore, due to the impeller's short blade length, inlet and outlet disturbances affect a large percentage of the blade surface. Consequently, a substantial amount of loss is generated in the form of eddies and separation.

Surface viscous losses and turbulent losses are present at both high and low flow rates. However, viscous losses predominate at higher flow rates, turbulence at the lower flow rates and shut-off. At high or maxium flow rates, irreversible surface viscous losses are directly proportional to the velocity squared. Hence, viscous losses are significant at high flow rates, tubulent losses at low.

Impeller flow channel design (IFCD) and outlet diameter caused impeller 1 to generate substantially more head than impellers 4,3, and 2. Blade surface area is of secondary importance. While it is not physically or technically correct to discuss these quantities as completely separate entities (see p. 62), some qualitative and quantitative feel for these parameters is possible based on the test data.

Study of the data yielded the subsequent empirical design hypothesis applicable to impeller flow channel design, hereafter referred to as IFCD hypothesis. Two adjacent blades should diverge in a uniform continuous fashion and, in order to maintain an approximately constant velocity from inlet and outlet, the cross-sectional area must be constant. This was done in our design by a tapered blade height. Diverging flow passages allow excellent

fluid passage and give superior fluid guidance by reducing the amount of separation.

In contrast, the performance penalty for employing converging adjacent blades is demonstrated by impellers 3 and 4 that had identical dimensions except for outlet blade angle and resultant blade profile. Impeller 4 shows a much larger head for the same flow rate than 3. Furthermore, its head increment gradually increased over impeller 3 for correspondingly larger flow rates because of partial flow blockage, turbulence, and velocity variation from inlet to outlet.

Since, theoretically, head is a function of $U2^2$, the outlet diameter is another primary parameter with respect to head generation. Knowing that U2 = W*D2/2, the outlet diameter has an approximate squared influence on head. Because prototype 1 has a D2 of 3.44 while D2 of 4, 3, and 2 is 3.28, this is important when prototype 1 is compared to 2, 3, and 4.

In addition, a small amount of decrease in head can be explained qualitatively by differences in blade surface area. We noted earlier that viscous loss increased with increased flow velocities and surface area. However, it can be concluded that blade surface area (function of blade wrap angle) is quite subordinate to flow channel design and outlet diameter. This observation is based on comparison of impellers 1 and 2, which had essentially the same amount of blade wrap. Although velocity was somewhat different at various values of R, each was subjected to the same surface viscous losses. Comparison of performance curves for 1 and 2 (Fig. 23), indicates a large difference in performance. Consequently, the major difference can not be at-

tributed to blade surface wrap but to impeller flow channel design (IFCD), with the prototype impellers showing that the greater the deviation from smoothly diverging blades, the greater the performance penalty.

Based on the observation that impellers 1 and 2 had approximately the same value of A2 (outlet angle), yet differing performance, one might conclude that A2 has little affect. However, this is not a valid conclusion because the blade profile for these two cases is quite different. In addition to the formal program, Whirlpool combination pump was tested. The results (Fig. 26) show the prototype's vast improvement both in head-flow rate and efficiency for the same size pump. The combo has a constant rectangular cross-section with a constant radius volute profile and a four-bladed radial impeller blade (Fig. 1B). This design should be compared to the previously described geometry for the prototypes.

These results substantiate the improved performance by employing method 1 impller and volute design techniques. Although it is difficult to generalize from the observation, one design factor has been articulated. The clearance between the impeller and the volute casing should be kept to a minimum to prevent cross channel flow. Although we are dealing with a complex multifactor system, an understanding of some of these factors allows us to apply them to the design of centrifugal pumps. Furthermore, with the use of the computer program, design time is reduced and results are very likely to be more nearly accurate.

c. Efficiency Conclusions

The fact that hydraulic efficiency was noted to increase gradually from

zero at Q = 0 to a maximum for increasing flow rate and then drop off slightly for corresponding further increases in flow rate can be accounted for by examining the relationship for efficiency, i.e., NHY = K*Q*H/HP_{in}. When Q = 0, NHY is zero. As flow rate is augmented, the head decreases with corresponding increase in input power. However, the overall effect is increased efficiency because the flow rate head product increases at a greater rate than the consequences of decrease head and augmented power input. As the flow rate is increased by opening the valve, the flow conditions approach the optimum operating condition where real fluid velocities and fixed inlet and outlet blade angles correspond. After this point is reached, higher flow rates cause higher fluid velocities until a point is reached where resultant surface viscous losses reverse the slope of the curve and efficiency declines.

The peak efficiencies for the four prototypes were determined to be within a narrow magnitude band, even though they occurred at different flow rates. This means that although some of the prototypes generated lower quantities of head and maximum flow rates, they also consumed less input power. This seems to be contradictory to that expected(namely, that when IFCD are converging in nature, flow restrictions, adverse velocity variations, and turbulences would increase losses), but mechanical losses were very large and consumed a considerable portion of the input energy because of the shaft bearings and water seal friction.

C. Recommendations for Future Work

1. Do conceptual study to ascertain the feasibility of designing a centrifugal pump, general in nature.

   a. Formulate a single volute design which would be sized large enough to test the largest diameter impeller expected. Then smaller diameter impellers could be tested by incorporating volute defining internal inserts in the larger housing.

   b. Design generalized impeller which would permit a large number of interchangeable profiles to be attached to the same impeller disk with minimum adjustment. Further impeller flow channel design relationships could then be ascertained quantitatively.

2. Reduce the articulating dynamometer arm to increase the amount of deflection recorded by the spring scale for the same load by relocating the arm's scale-rest point.

3. Alter the two low performance prototypes by removing appropriate blade profile segments at sections where converging occurs and retest to determine the effects.

4. Investigate the effect of a smaller number of blades by removing every other one on the present prototype impellers.

5. Employ clay to ascertain geometry changes on blade outlet angle, blade shape, etc.

6. Investigate different shaft bearings to ascertain ones that substantially reduce mechanical losses.

7. Program a computer external function to print out rad, beta calculations in graphical form, e.g., Michigan Cal-Comp.

TABLE V

RECOMMENDATION EVALUATION

Recommendation	Cost	Knowledge Gained	Time	Significance
1	high	high	long	very high
2	low	low	short	low
3	low	medium	short	medium
4	low	medium	short	medium
5	low	medium	short	medium
6	medium	medium	medium	high
7	low	--	short	medium

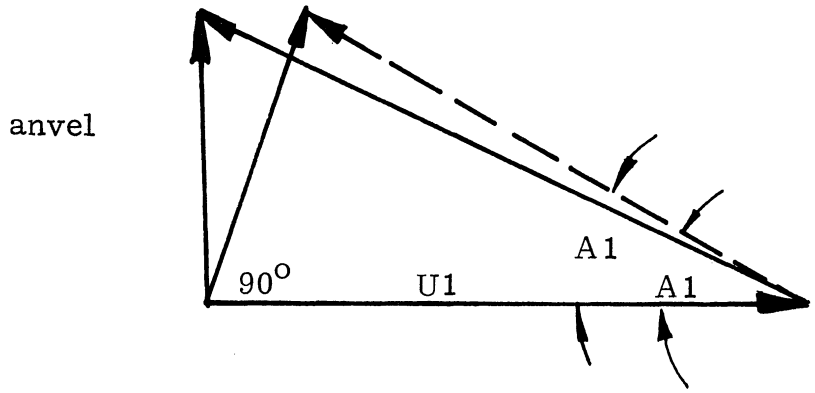

Fig. 2. Effect of prerotation on the inlet diagram.

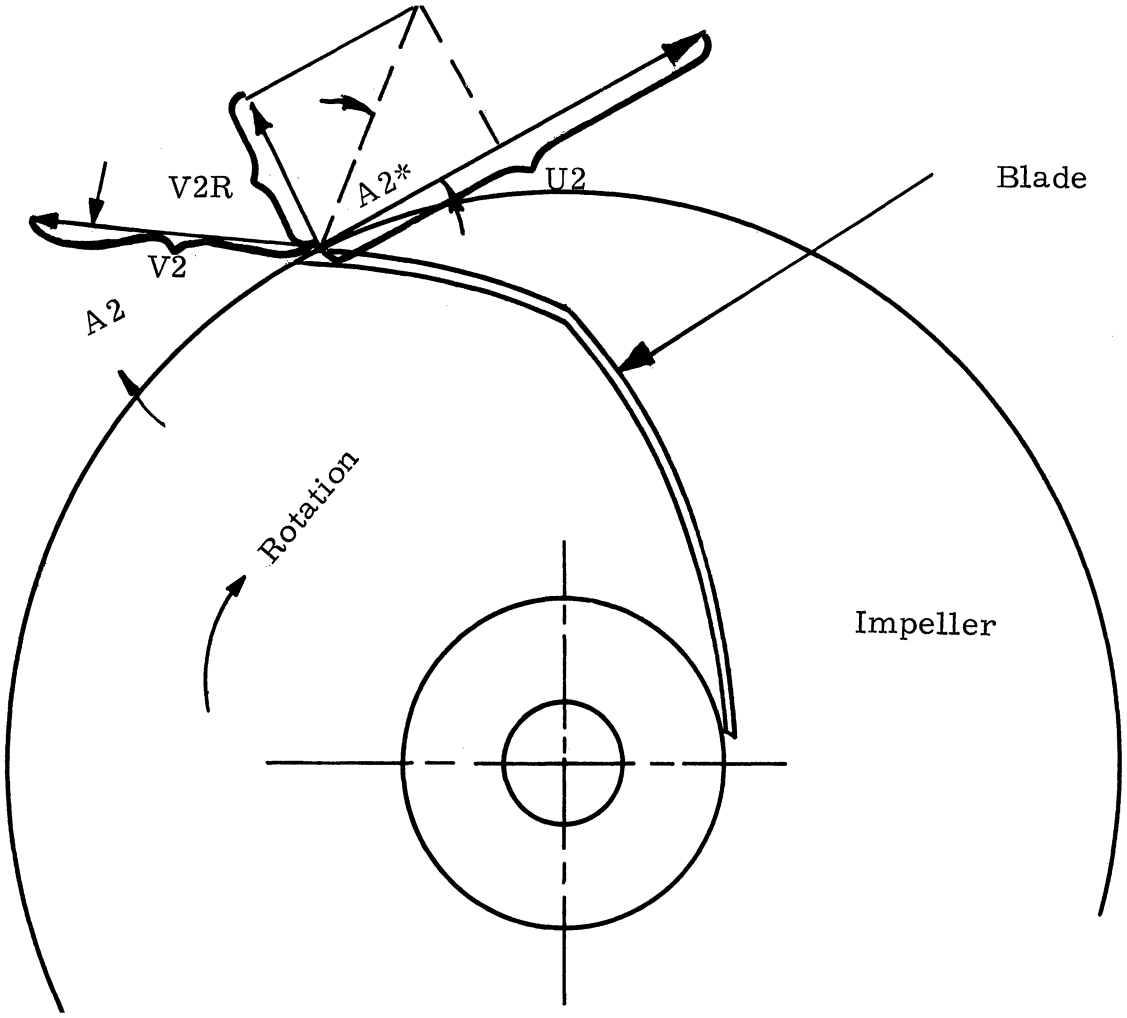

Fig. 3. Ideal outlet velocity diagram.

II. ANALYTICAL STUDY

A. Literature Search

Methods of centrifugal pump design have not been standardized. Centrifugal pump practice is usually based on the historical, one-dimensional flow hypothesis governed by Bernoulli's equation, even though it has been shown experimentally to be three-dimensional. Some assumptions are necessary to obtain Bernoulli's equation from the general energy equation.

$$H/d + y = V^2/2g = \text{constant} \quad \text{Bernoulli's Equation} \qquad (1)$$

Assumptions:

(1) Frictionless fluid
(2) Steady flow
(3) No mechanical loss (reversible)
(4) Flow along a streamline
(5) Impeller with infinite number of blades

It is apparent that the expressions derived from this one-dimensional theory cannot accurately describe normal pump operation where the actual number of blades is small, where friction is a relevant phenomena, and where a very turbulent flow condition with vortices, reversed flow, and eddy currents sometimes exists. Therefore, investigators have introduced a theory based on more orthodox fluid mechanics. Some investigations have employed a three-dimensional approach to describe the flow for imcompressible and inviscid flow through mixed-flow turbomachines while others have been associated with analysis employing the basic assumptions of potential flow. The Japanese have been quite

active in this field. Additional highly sophisticated work (boundary layer theory) has been proposed to aid the designer. While literature describing these investigations provides added insight into the physics of the problem, it is seldom of value to the designer because of the complexity of the formulation, the idealized concept of known velocity profiles, and the fact that even with this mathematical sophistication these analyses must assume a frictionless, nonturbulent medium in order to obtain solutions to the differential equations.

Consequently, the standard practice is to use a general, classical, one-dimensional approximation as a guide, based on the general laws of centrifugal pump operations, with the realization that the analysis will have to be corrected by factors determined from actual experience and tests.

This report attempts to combine these two approaches. Mathematical analysis will be employed where it describes the physical case and supplies answers that normally are found through a costly trial and error process. This gives a workable procedure based on fluid mechanic fundamentals that will satisfactorily predict operating conditions.

A literature search investigating possible methods of centrifugal pump design has brought to light the following possible techniques in formulating a centrifugal pump design procedure:

(1) Impeller and volute design with given loading distribution.

(2) NASA turbine pump design procedure.

(3) Potential flow theory design.

(4) Conventional procedures based on one-dimensional flow and experience.
(Future reference to these techniques will be by method 1, method 2, etc.)

Method 1 employs basic fluid mechanics rather than "years-of-experience techniques" as a criteria for centrifugal pump design. According to this method, the impeller blade loading is described analytically as a function of pressure, radius, and area. Assuming the pressure differential across the blade is constant, the complete design is specified by incorporating empirical approximations that supplement the blade loadings and analytically express relationships in terms of geometric parameters. In addition, a compatible method of centrifugal pump volute design has been formulated by M. V. Duong. Since pump design involves a system, the integral environment of impeller and volute should be considered in the design of each component.

NASA turbine pump design (method 2) is a highly sophisticated mathematical analysis which employs the momentum and continuity equations in differential form to formulate the following expressions:

(1) Equations for the derivation of the relative velocity in a direction normal to a streamline.

(2) Equation for blade surface velocity and head rise.

A numerical procedure has been outlined which could produce a pump design based on fundamental fluid mechanics. In addition, mathematical analysis is necessary before NASA's method can be applied to centrifugal pumps. This method assumes a non-viscous media and streamline flow.

The potential flow approach (method 3), based on a series of Japanese papers, defines a frictionless, idealized, potential flow function which is substituted into the governing equations of fluid mechanics to obtain expressions involving flow characteristics. This theoretical analysis employs the theory

of straight cascades of thin wings, thin wing lattice theory, etc., to derive the expressions in terms of pump geometry.

The conventional design procedure (method 4) is the experience-art form of pump design and has traditionally involved the scaling of parameters from operating pumps which closely resemble the operating characteristics of the one being built.

Each of the above methods lacks experimental evidence to substantiate the assumptions and approximations employed to simplify the analysis. This is especially true in the case of the first three methods. Moreover, information regarding previous results and performance curves of actual pumps designed according to these methods is almost nonexistent. Consequently, I have chosen to concentrate on method 1. While the other approaches might prove useful, their complexity seems to rule out their immediate effectiveness.

B. Impeller Design

1. INTRODUCTION

Our impeller is a three-dimensional, unshrouded design with radial backward curved blades that are mounted open-faced on a flat disc (Fig. 1A). The blade profile is best pictured in a polar coordinate plane with constant tapered blade cross section.

The other component of the system is the volute (casing) (Fig. 1B). The casing has a circular diverging annular channel purposely for directional flow control and for optimum head generation with minimum losses. The remainder of

the unit essentially follows the cross sectional profile of the impeller blade cross section. In addition, clearances between impeller and casing are kept to a minimum to prevent flow stagnation pockets and cross channel flow.

2. LITERATURE RESEARCH SUMMARY

Popular pump texts[2,5,6,13] rely heavily on "experience" in designing impeller shapes. Church[5] states, "There is no published information concerning the effect of the vane curvature between the inlet and exit on the pump efficiency, although it must have a great influence." He then proceeds to outline a technique based on a plot of flow velocities versus impeller radius to obtain the angle A. He continues, "There are two satisfactory methods of constructing the vane shape from these curves. One is to construct a blade profile of tangent circular arcs, and the other is to calculate and to plot the shape by polar coordinates." In neither method does he explain in terms of mechanics why the use of these procedures produces satisfactory pumps.

Stepanoff[6] presents a very complex and time consuming impeller design method for determining blade profile based on error triangles analysis. He says, "The shroud curvature should be as gradual as possible to minimize uneven pressure and velocity distribution." (p.95) One must question the vagueness of "...gradual as possible..." for Stepanoff does not explain it.

He later states, "For best results, experience and skill are necessary to represent graphically the requirements for best efficiency." Although it is claimed that this technique has led to high efficiency pumps, the reasons are not evident. Furthermore, nowhere are the fluid mechanic considerations logically explained.

Addison's impeller design technique[2] is based on the statement: "An infinite number of blade shapes might be struck, each having the specified inlet and outlet angle. For ordinary purposes two of these are worth considering, a compound curve formed of two circular arcs, and a simple curve formed of a single circular arc." A study of Addison's explanation is even less satisfactory than Stepanoff's. He justifies the one and two circular arc techniques by saying:

> "Comparative tests have shown that blade forms embodying arcs of circles are likely to yield as high a pump efficiency as more complex shapes." (p.97)

He then adds the following qualification. "In particular instances it may be worthwhile examining other shapes fulfulling particular conditions such as" (Fig. 1)

(1) "The impeller passages may be so designed that there is a uniform rate of deceleration as the relative velocity falls from the value V_{r1} relative at entry to the value V_{r2} relative at exit.

(2) "The blade may have the form of a logarithmic spiral.

(3) "The shape may be such as to impose a tangential velocity component that increases linearly with the radial distance, from zero at impeller entry to maximum at exit."

Unfortunately, the hydrodynamic justification of any of these variations is not discussed, not is there any indication they were considered.

Shephard's[13] method of centrifugal impeller design concerns two observations:

> "When more is known about the actual channel flow, it may be possible to design a vane shape and hence a channel shape to obtain the optimum results. At present, however, the shape is largely dictated by the qualitative factors of designing to make a flow of assumed uniform velocity across the channel follow a smooth path with no sudden irregularities of flow.

"The second consideration is simplicity in design and manufacture. An incompressible fluid with radial and rotational motion will ideally follow a logarithmic spiral path in which the streamlines (theoretically) at any point have a constant inclination with the tangent to the radius at that point. As this has a certain rational basis and as a logarithmic spiral is geometrically simple, pump vanes are often designed on this basis. Sometimes the vanes are made by a simple circular arc, although it is known that this does not give the best results. The problem is to design the shape with inlet and outlet angles and velocities known or assumed, a problem which is not simple if the vanes are to have three-dimensional characteristics." (p. 248)

In summary, the approaches of the leading experts on pump impeller design have been based primarily on empirical observation tempered with imagination and engineering fortitude. Their approaches leave a substantial void in explaining the hydrodynamics of pump impeller design and in applying sound elementary fluid mechanics.

Engineering journals and other technical publications can be divided into two broad parts. The first part, similar to the above discussion, involves an empirical approach to obtain engineering factors that have been used in past designs. Information in this area is limited. The second area is based on physical and mathematical formulations that essentially neglect the real properties and action of the pumping fluid. Here the emphasis is on the formulation and solution of the Navier-Stokes' equations for special cases with little regard to correlation between theoretical solutions and experimental results.

Since each of these approaches is inadequate, it was decided to combine them into a procedure for predicting figures for pump design. This has resulted in one skeleton impeller design method that seems to be based on sound fluid mechanic principles and tempered by experience. This technique is enclosed and explained in detail.

3. METHOD OF DESIGN

A simple method for designing centrifugal pumps with prescribed blade loading and variable passage height, resulting from the literature search and author's formulation, involves designing pump impeller blades with constant tapered blades and constant blade loading. Included is a method of volute design based largely on the research of Mr. Minh Duong and References 2 through 5. Both methods, combined, give a relatively simple and direct method for the complete design of centrifugal pump hydraulic components.

In addition, an initial check is made of the influence of tapered blades on pump performance. It will be shown that a direct correlation between passage length, blade curvature, and the amount of blade taper exists for a given blade loading.

The report will discuss both the impeller design and the volute design.

Although methods of impeller design have not been standardized, the design texts usually base impeller design on geometrical rather than fluid mechanics considerations. When attempts are made to consider fluid mechanics, the resulting analysis is usually quite involved.[7] As a compromise between these two extremes, a simplified method of impeller design is presented here, based on the manner in which the impeller adds energy to the flow to obtain head.

While conventional methods are simple in concept. they give no indication of what constitutes a "desirable" manner of adding energy to a fluid, one that does not result in large fluid flow losses. Separation of the main flow from blade surfaces and the formation of eddies in blade passages causes some loss. Flow separation which occurs when the flow no longer follows channel passeges,

is dependent upon pressure variations within the impeller passages. Basing an impeller design upon this principle promised a method which could minimize impeller losses, if desirable loading characteristics were known. The influence of various loading distributions has been studied and the results compared with actual impeller designs. Impellers with constant blade loading were usually found in high efficiency pumps. It was therefore decided to pay particular attention to the design of blades with constant loading.

However, an impeller design by itself does not constitute a pump, which is a "system" in which various parts must be matched for optimum performance. A good impeller will not ensure a good pump, unless the volute is properly matched to the impeller characteristics.

4. DEVELOPMENT OF BLADE PROFILE

Consider a section of a backward curved pump impeller blade (Fig. 4). (See also Fig. 1). The force on an area element of the blade is given by

$$dF = \Delta P^a \cdot h \cdot dx \quad (\Delta P^a = \text{pressure difference}) \tag{1-a}$$

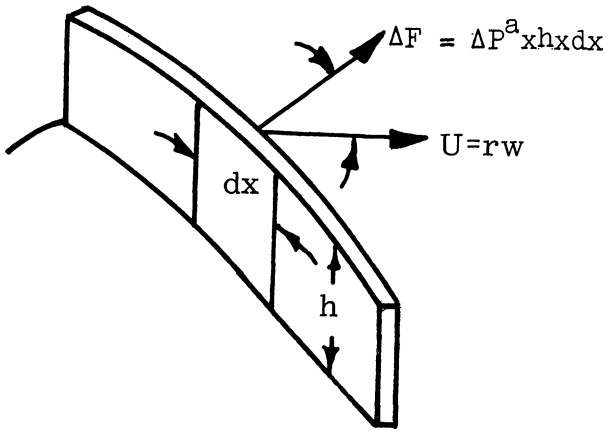

Fig. 4. Impeller blade.

The rate of work done on this blade element is $dF \cdot \cos z \cdot U = \Delta P \cdot h \cdot U \cdot (\cos z\ dx)$ where z is the angle between dF and the peripheral blade velocity $U = rw$.

In polar coordinates by definition

$$\cos z\ dx = dr \tag{1-b}$$

Therefore,

$$\text{Rate of work done on element} = \Delta P^a \cdot h \cdot U\ dr \tag{2}$$

In the foregoing ΔP^a is an average pressure difference for the area element dx. As such, ΔP^a will be considered to be a function of r alone.

The net rate of work done by the blade on the fluid will be

$$WK = \int_{r_1}^{r_2} U \cdot N \cdot \Delta P^a \cdot h(r)\ dr \tag{3}$$

where N = number of blades

r_1, r_2 inlet and exit radii

and $h = h(r)$ is the variation of h with r.

Not all of the work done by the blade goes into producing head. Some of it raises the fluid temperature and heat transfer. The rate at which head is produced, up to a certain radius r divided by the power input, defines a local hydraulic efficiency: (NHY)

$$NHY = \frac{\text{OUT PUT}}{} = \frac{i \cdot H_{act} \cdot Q}{\int_{r_1}^{r} N\ \Delta P^a U h dr} \tag{4}$$

where Q = capicity

i = specific weight

H_{act} = actual head produced up to point r

Thus

$$H = \frac{NHY}{iQ} \int_{r_1}^{r} N \cdot \Delta P^{a} \cdot U \cdot h \cdot dr \tag{5}$$

It follows that if NHY is constant with r, then the rate of change of H with r is given by

$$\frac{dH}{dr} = \frac{NHY}{rQ} \Delta P^{a} \cdot N \cdot h \cdot U \tag{6}$$

We next assume that the flow enters the blade passage without pre-whirl (at design) and, that at any given position, the local head is related to the Duler head by the ratio which is derived from the theoretical Euler velocity triangles. (Equation 3:27, Ref. 5, Church)

$$S = \frac{H \cdot g}{UVu} = \frac{H \cdot s}{U^2 - \frac{U \tan AQ}{6.283 \cdot rn}} \tag{7}$$

where V_u = absolute circumferential flow velocity.

Therefore

$$g \cdot H = S\left(U^2 - \frac{U \tan AQ}{6.283 \cdot r \cdot h}\right) \tag{8}$$

$$g \cdot H = S\left(w^2 r^2 - \frac{wr \tan A \cdot Q}{6.283 \cdot r \cdot h}\right) \tag{8-A}$$

It follows that if S is assumed constant, differentiating Eq. (8) yields

$$\frac{d(gH)}{dr} = S\left[2w^2 r - \frac{WQ}{6.283}\left\{-\frac{\tan A \cdot dh}{h^2 \cdot dr} + \frac{1}{h}\frac{d \tan A}{dr}\right\}\right] \tag{9}$$

From (6) and (9)

$$\frac{NHY}{\rho Q}\Delta P^a \cdot N \cdot h \cdot U = S\left[2w\, r + WQ\left\{\frac{\tan A}{h^2}\frac{dh}{dr} \quad \frac{1}{h}\frac{d \tan A}{dr}\right\}\right] \tag{10}$$

Let us define

$$\frac{NHY \cdot N - \Delta P^a}{S} = \Delta P^b \tag{11}$$

where we assume that

$$\frac{NHY \cdot N}{S} = \text{Constant} \tag{12}$$

Secondly, define the nondimensional pressure ratio

$$\Delta P = \frac{\Delta P^b}{\dfrac{\rho \cdot Q^2 \cdot W^2}{6.283 \cdot U1^2 \cdot (B5)^2}} \tag{13}$$

where B5 = inlet blade height.

It can then be shown quite readily that combining Eqs. (10), (11), and (13) gives

$$\Delta P = \frac{4 \cdot 3.1416 \cdot U_1^2 \cdot (B5)^2}{W\, Q\, \bar{H}} - \frac{1}{\bar{H}^2 R}\frac{d \tan A}{dR} + \frac{1}{\bar{H}^2 R}\frac{d\bar{H}}{dR} \tag{14}$$

where

$$\bar{H} = \frac{h}{B5} \tag{14-a}$$

$$R = \frac{r}{h}$$

Solving for $\frac{d \tan A}{dR}$ we have,

$$\frac{d \tan A}{dR} = \frac{4 \cdot 3.1416 \cdot U_1^2 \cdot B5}{Q \cdot W} \cdot \bar{H} \cdot R + \frac{dH}{dR} - \bar{H}^2 \cdot R \cdot \Delta P \qquad (15)$$

Integrating Eq. (15) from A to A_1 we obtain,

$$\tan A - \tan A1 = \frac{4 \cdot 3.1416 \cdot U_1^2 h_1}{WQ} \int_1^R \bar{H} R dR - \int_1^R \Delta P \cdot R \cdot \bar{H}^2 dr + (\bar{H}-1) \qquad (16)$$

Equation (16) is the general equation relating the angle A to blade loading (through Δp) and blade height h.

We now assume that Δp is constant and that the blade has a constant taper (Fig. 5).

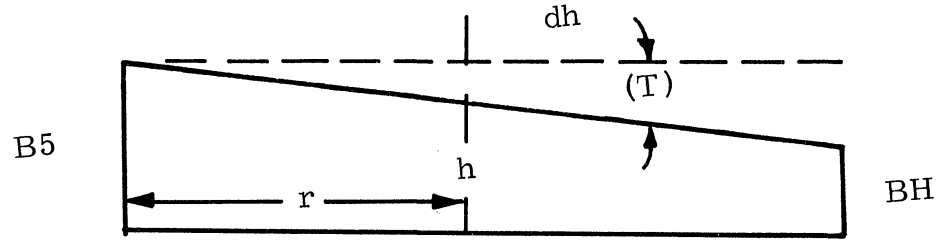

Fig. 5. Constant taper blade.

The slope of the blade can be defined in terms of the angle T as

$$\tan T = - \frac{d\bar{H}}{dR} \qquad (17)$$

$$d\bar{H} = - \tan T \, dR \qquad (17\text{-a})$$

$$\bar{H} - \bar{H} = - \tan T \, (R-1) \qquad (17\text{-b})$$

or

$$\bar{H} = 1 - \tan T \, (R-1) \qquad (18)$$

Using Eq. (18) and setting $\Delta p = C1$ in Eq. (16) and noting that $\tan A = \frac{Rd\ Beta}{dR}$ in polar coordinates, we may write

$$\tan A - \tan A1 = \frac{Rd\ beta}{dR} - \tan A1 = \frac{4*3.14*U_1^2\ B5}{WQ}\left\{\frac{(R^2-1)}{2} - \tan(T)\left(\frac{R^3-1}{3} \quad \frac{R^2-1}{2}\right)\right\} - C1\left\{\frac{R^2-1}{2} - 2\tan(T)\left(\frac{R^3-1}{3} \quad \frac{R^2-1}{2}\right) + \tan^2(T)\left[\left(\frac{R^4-1}{4} - \frac{2}{3}(R-1) + \frac{R^2-1}{2}\right)\right]\right\} - \tan(T)\ (R-1) \tag{19}$$

or

$$R\frac{d\ beta}{dR} = B1\ R^4 + B2\ R^3 + B3\ R^2 + B4\ R - (B1 + B2 + B3 + B4) + \tan A1 \tag{20}$$

where

$$B1 = \frac{C1\ \tan(T)}{4} \tag{21}$$

$$B2 = -\frac{4*3.1416*U_1^2(B5)\ \tan(T)}{W*Q} \quad \frac{2C1\ \tan T}{3} \quad \frac{2\ C1\ \tan^2(T)}{3} \tag{22}$$

$$B3 = \frac{4*3.1416\ U_1^2 B5}{2*W*Q}(\tan T + 1) - \frac{C1}{2}(1 + 2\tan(T)) + \frac{C1\ \tan^2 T}{2} \tag{23}$$

$$B4 = -\tan T \tag{24}$$

The polar equation of the impeller is now obtained by integrating Eq. (20):

$$beta = B1\frac{R^4-1}{4} + B2\frac{R^3-1}{3} + B3\frac{R^2-1}{2} + B4(R-1) + \left[\tan A1 - (B1 + B2 + B3 + B4)\right] L \cap R \tag{25}$$

In B1, B2, B3, and B4 the constant C1 appears. The constant C1 can be evaluated either for a specified H and Q or for a specified exit blade angle.

Let us consider this latter case. From Eq. (25) and A = A2 at R = R2

$$C1 = \frac{\frac{4 \cdot 3.1416\ U_1^2\ B5}{WQ}\left[\frac{R_2^2-1}{2} - \tan T\left(\frac{R_2^3-1}{3} - \frac{R_2^2-1}{2}\right)\right] - \left[\tan A2 - \tan A1 + \tan T\,(R_2-1)\right]}{\frac{R_2^2-1}{2} - 2\cdot\tan T\left(\frac{R_2^3-1}{3} - \frac{R_2^2-1}{2}\right) + \tan^2 T\left(\frac{R_2^4-1}{4} - \frac{2}{3}(R_2^3-1) + \frac{R_2^2-1}{2}\right)} \qquad (26)$$

For the special case of constant height blades, T = 0, and using Eq. (26), Eq. (25) becomes:

$$\text{beta} = \left(\frac{4 \cdot 3.1416\ U_1^2 B5}{2 \cdot W \cdot Q} - \frac{C1}{2}\right)\left(\frac{R^2-1}{2}\right) + \left[\tan A1 - \left(\frac{4\pi U_1^2 B5}{2 \cdot W \cdot Q} - \frac{C1}{2}\right)\right] \times \text{Ln } R \qquad (27)$$

where

$$\frac{C1}{2} = \frac{\frac{1}{2}(\tan A1 - \tan A2) + \frac{4 \cdot 3.1416\ U_1^2 B5}{2 \cdot W \cdot Q}\left(\frac{R_2^2-1}{2}\right)}{\left(R_2^2-1\right)/2} \qquad (28)$$

Substituting (28) into (27) yields

$$\text{beta} = \frac{\tan A2 - \tan A1}{(R_2^2-1)}\left[\frac{R^2-1}{2}\right] + \left(\tan A1 - \frac{\tan A - \tan A1}{(R_2^2-1)}\right)\cdot \text{Ln } R \qquad (29)$$

We now have a meaningful relationship (25) for blade profile, i.e., beta as a function of radius in polar coordinates, provided A1, A2, T, and the blade height at inlet and outlet are known.

These quantities (A1, A2, T, and blade heights) cannot always be determined analytically with sufficient engineering accuracy to be used. Consequently a number of approximations based on empirical results are made. One will see that A1 can be calculated frequently within usual engineering accuracy. However, A2 is more difficult to determine because important knowledge about flow

separation from the blade and other flow phenomena must be taken into account. Hence, Church[5] states, "Overall coefficients based on test results of previous built pumps are usually used to evaluate these discrepancies in actual design."

Blade taper may also be difficult to ascertain. The major aspects of this quantity and the selection of B5 and BH will be considered in a later section.

Now that a designed formulation for determining blade profile based on elementary fluid mechanics is available, it must be tempered by what engineering experience in pump design and empirical data has proven to be satisfactory.

5. PARAMETER DETAILS

a. Introduction

Suppose that head (H), capacity (Q), and speed (SN) of a pump are specified. (The method of calculating these quantities is found in most pump engineering tests.[5]) The principal design parameters can be calculated from a method based upon selecting values from empirical results. However, the analytical work involving these parameters indicates poor correlation with actual experimental results and the analytical attempts are based upon questionable assumptions. Determination of specific speed, head coefficient, angular velocity, inlet and outlet diameter, inlet and outlet angle, blade height, number of blades, and blade taper are now considered.

b. Specific Speed (PNS)

Specific speed classifies impellers on the basis of their performance and proportions regardless of their actual size and/or speed. Because specific speed is a function of the impeller proportions, it is constant for a series

of homologous (similar geometry) impellers or for one particular impeller operating at any speed.

Specific speed is the speed in revolutions per minute at which an impeller would operate if reduced proportionately in size so that the pump delivers a rated capacity of 1 gpm against a total head of 1 ft.

Mathematically,

$$PNS = \frac{SN_s(Q)^{1/2}}{H^{3/4}} \qquad (29\text{-a})$$

c. Angular Speed (W)

Angular velocity is determined by converting the units of speed from rpm to radians per minute.

$$W = \frac{SN_s 3.1416}{30.} \qquad (29\text{-b})$$

d. Head Coefficient (S)

Head coefficient is a nondimentional ratio of input energy per unit mass with an impeller of 1-ft diameter. It is usable because it is a dimensionless quantity that remains constant for all similar (geometrically) impellers.

The head coefficient[5] expresses the head in feet as a fraction of the maximum theoretical head at zero capacity. It can be defined mathematically by the relationship

$$S = \frac{Hg}{U_2^2/2} \qquad (30)$$

References mention that the value of S for pumps with flows less than 100 gpm usually varies between .9 and 1.25 (Fig. 6). Church[5] notes that low specific

speed (1000) pumps have an approximate average value of head coefficient around 1.05. This tends to be true, but the head coefficient may vary within a relatively large range (Fig. 8). The best values of S can be obtained from the experimental results of this report for low flow rate, low head pumps.

e. Outer Diameter (D2)

The empirical determination of the head coefficient magnitude provides the designer with a simple way of calculating a first approximation for D2. $U2 = \frac{W*D2}{2}$, by substituting this into Eq. (30) and rearranging, one obtains

$$D_2 = \frac{1840}{SN} \frac{H}{S} \qquad \begin{matrix} H \text{ in feet} \\ SN \text{ in rpm} \end{matrix} \qquad (31)$$

where the constant 1840 comes about when the dimension of D2 is required in inches.

f. Inlet Diameter (D1)

The size of D1 is determined by the continuity equation (area* V_{in} = Q). Since Q is known, the choice consists of either setting the magnitude of V_{in} and calculating D1, or selecting D1 by some other means and accepting the resulting velocity. Here the latter option is taken.

Existing pumps usually have an inlet diameter that allows the flow velocity through the inlet (eye) to be approximately 10 fps in large pumps. When the continuity equation is employed at the inlet, D1 can be written as

$$D1 = (4Q/3.14*V_{in})^{1/2} \qquad (32)$$

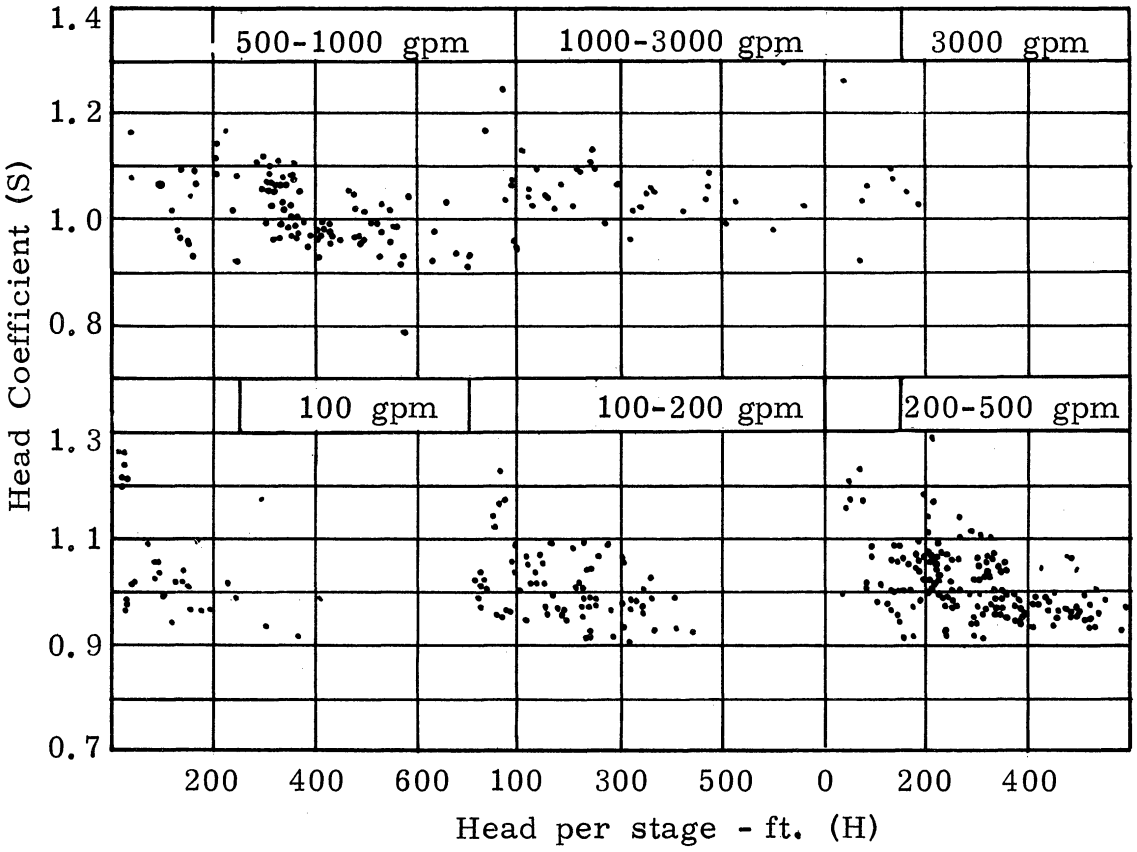

Fig. 6. Head coefficient vs. head in various flow rate ranges.

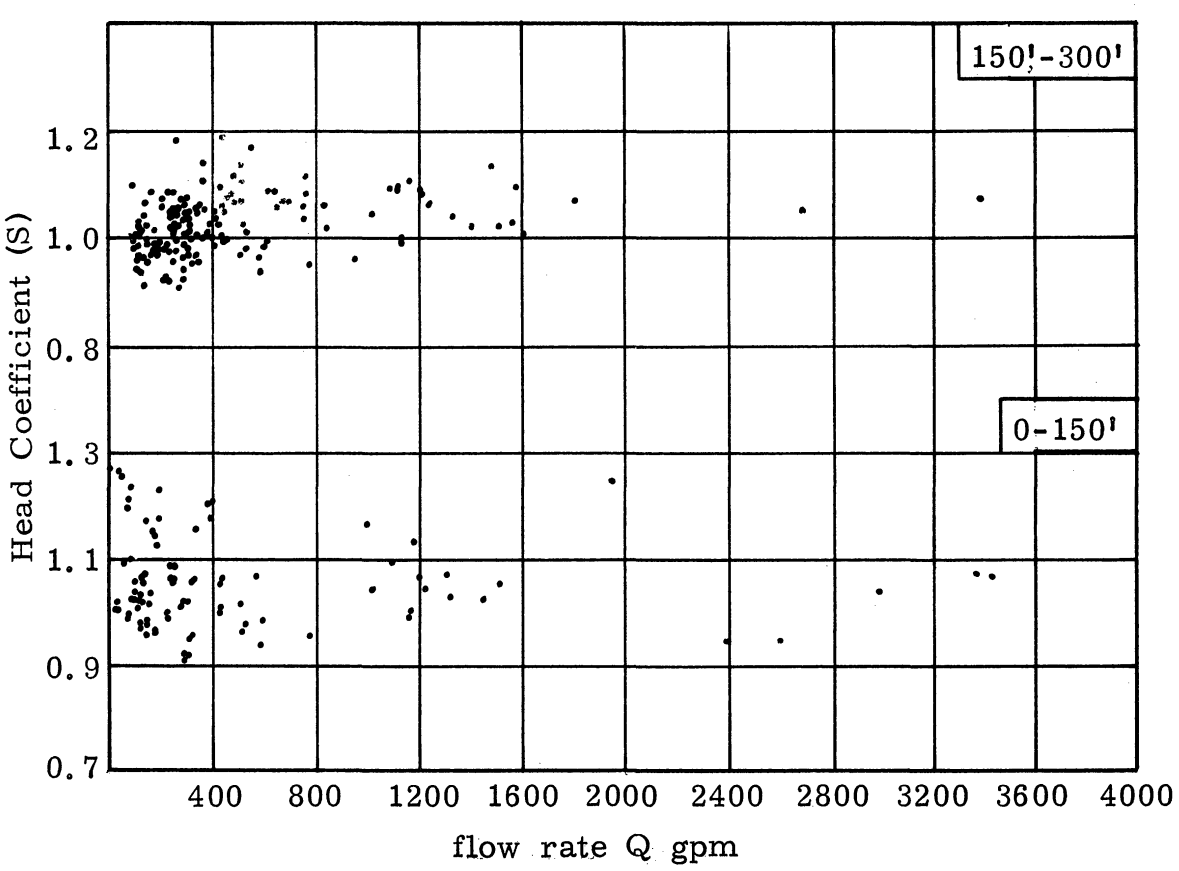

Fig. 7. Head coefficient vs. flow rate in various specific head ranges.

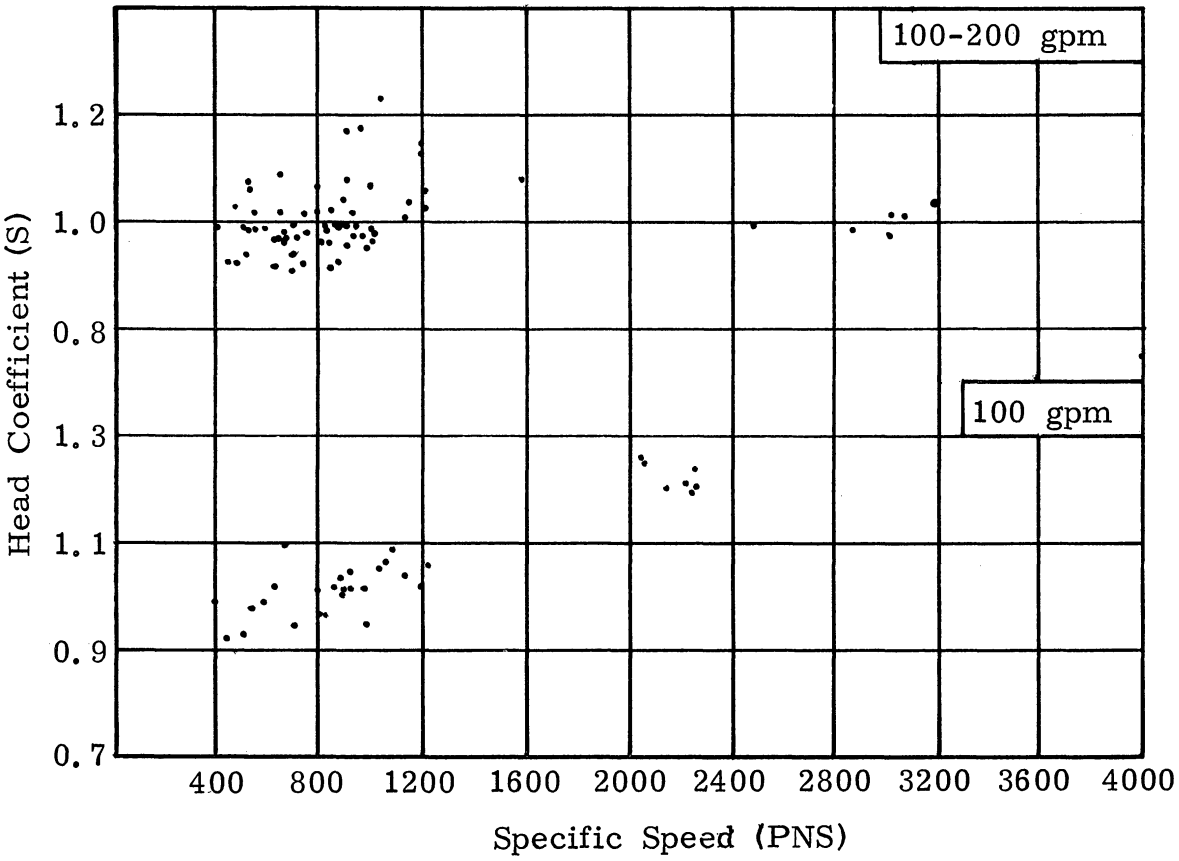

Fig. 8. Head coefficient vs. specific speed in various flow rate ranges.

However since our pump is quite small compared to those checked in obtaining the 10 fps figure, this value may be too large and might induce cavitation. If the pressure at some point inside a pump drops below the vapor pressure of the liquid, vapor pockets will form. These low pressure regions occur wherever the relative velocities are large. The vapor bubbles are carried along with the stream until a region of higher pressure is encountered where collapse occurs with attendant high pressure forces. This complex phenomenon is called cavitation. One important means of insuring that the inlet pressure is above the vapor pressure is to keep the relative inlet velocity V_{in} low.

Furthermore, experience indicates that the use of a scaling factor ratio (SR) to select D1 is reasonable. SR is defined as

$$SR = \frac{D2}{D1} = \text{const} \tag{33}$$

The value of SR, ascertained by studying pumps that have exceptional performance is 2.5. Consequently

$$D1 = D2/2.5 \tag{34}$$

In the range of pumps of interest, this value of SR will assure a low value of V_{in}.

g. Blade Height

The scaling method will also be applied to ascertain the blade inlet height. The blade inlet height was scaled from a pump that had a very successful operation and performance.

The formal mathematical expression is called the width ratio and is defined as

$$WR_2 = \frac{\text{blade height at outlet}}{\text{outlet diameter}} = \frac{BH}{D2} \tag{35}$$

$$WR_1 = \frac{\text{blade height at inlet}}{\text{inlet diameter}} = \frac{BS}{D1} \tag{35-a}$$

A survey of existing pumps shows $WR_1 = 0.08$ and $WR_2 = 0.30$ to be reasonable values.

$$BH = (.08)*D2 \tag{36}$$

$$B5 = 0.30*D1 \tag{36-a}$$

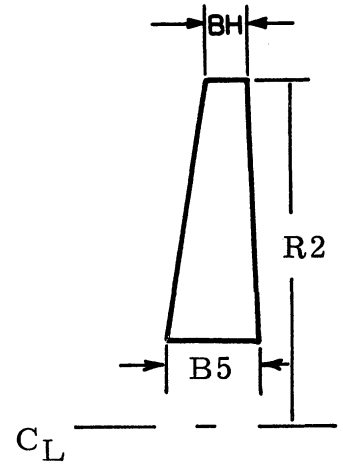

Fig. 9. Blade cross section.

h. Inlet Angle (A1)

Next, we calculated the blade inlet angle (A1). Once the inlet diameter, D1, and the blade width, B5 have been selected, the inlet radial velocity can be found from continuity.

$$\text{Area}_1 * \text{Anvel}_1 = Q \tag{37}$$

where 1 designates inlet condition.

$$\text{Since inlet area} = \frac{3.146*D1*B5*E1}{144} \tag{38}$$

where E1 is the impeller constriction factor.

Solving for anvel from Eq. (37) and assuming velocity is constant across the inlet cross-section yields

$$\text{Anvel}_1 = \frac{Q*0.1337}{\text{Area } 1*60.0} \tag{39}$$

The inlet angle (Fig. 2) can be defined as

$$A1 = A \tan\left(\frac{\text{Anvel}}{U1}\right) \tag{40}$$

U1 is known because it is simply the product of R1*W or the speed at a point on the inlet diameter circumference.

The above was based on an assumed fluid approach angle of 90° between the fluid velocity and the velocity of the impeller at the inlet (solid line Fig. 2). However, in design practice A1 is usually increased slightly to account for the contriction of the stream as it passes the inlet edges and for the rotating of the flow with the wheel as the fluid approaches the vane inlet and contacts the rotating impeller. Consequently a prerotation allowance of the inlet flow is usually used. It is accounted for by decreasing the ideal U1 by 5%, i.e.,

$$A1 = A \tan\left(\frac{\text{Anvel}}{.95U1}\right) \tag{41}$$

Therefore the net effect of these two separate effects is to make A1 larger (Fig. 2, dotted line).

It should be noted that the values of A1 are apt to be much higher than customary for high values of Q. It may not be wise to employ such large values of A1 since the impeller blades become excessivley long and have considerable wrap. This might be corrected to some extent by taper but only at the expense of increasing exit velocities and risking increased losses in the volute. A more reasonable solution would be to keep A1 somewhere between 10° and 18° and accept the mismatch of blades and flow angle. An alternate choice would be to decrease the inlet height, thereby increasing the inlet velocity. Ultimately, the inlet velocity might be large enough to cause either cavitation problems, loss problems, or both.

i. Outlet Angle (A2)

Theoretically, A2 can be determined by the relationship

$$A2 = A\tan\frac{0.15*D2*D2*W*3.1416*BH}{Q*4*2.228*1.2*1.2*1.2} \qquad (42)$$

where

$$BH = B5 - R2\tan(T) \qquad (42\text{-a})$$

With further mathematical manipulation which is not done here, A2 can be found as a function consisting of only H and PNS (specific speed).

At this point, it is helpful to consider the parameters and conditions that determine the real outlet angle. Before A2 can be ascertained, we must know

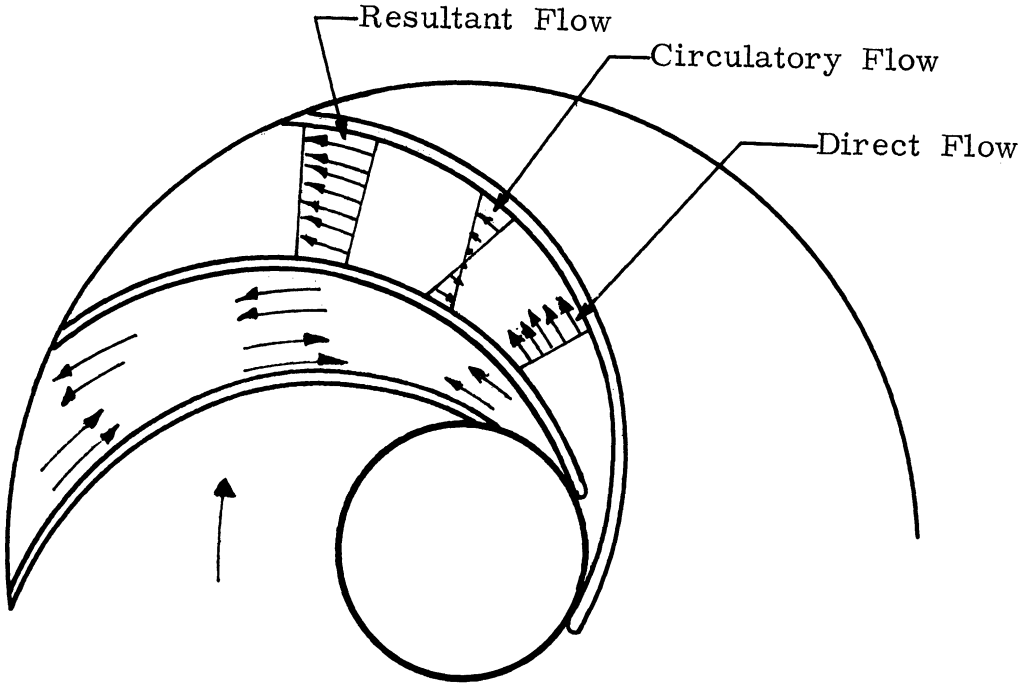

Fig. 10. Direct and circulatory flow through a pump.

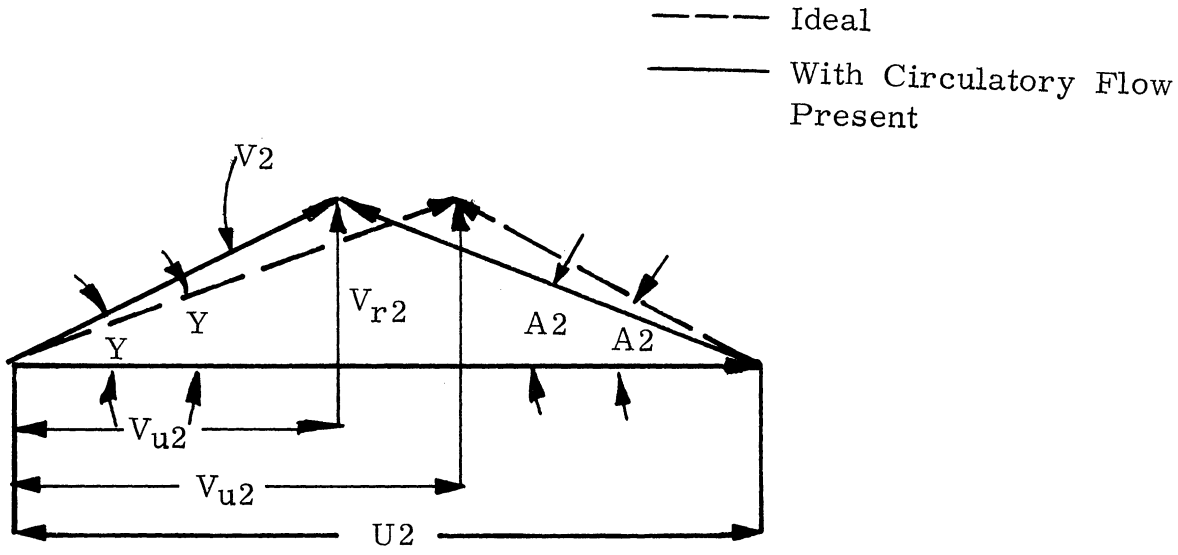

Fig. 11. Outlet velocity diagram, ideal and with circulatory flow.

what type of flow conditions exist in the fluid passage and at the impeller outlet. In a rotating impeller, two main flows take place simultaneously, the direct flow through the passage and a superimposed circulatory flow. Circulatory flow, which can be very significant, is the flow point where turbulence and vortices are observed and the flow pattern is very irregular. Turbulence causes the fluid to exit from the impeller at an angle less than the vane angle (i.e., decreased A2) and to increase the absolute angle (Y) at which the fluid leaves the wheel.

The exact quantity of turbulent flow depends upon the shape of the passage. For a given impeller, more blades (vanes) make the passage narrower, giving greater fuidance to the fluid and reducing the tendency of the flow to separate from the blade surface. However, as the number of blades increase surface viscous losses increase. Church[5] says, "Attempts have been made to set up formulas to calculate this (turbulent) phenomenon but they are rather unreliable. Consequently, the amount of circulatory flow is best determined from test results and experiments."

The results of Fisher and Thoma[11] are pertinent at this point. They found that the flow conditions, especially at low discharges, were completely different from the ideal assumptions. The water passages were never completely filled with active flow, and the fluid broke away from the vane surfaces. Dead water pockets formed in the passages on the low pressure side of the vanes. When off design operating conditions were present, the flow was unstable. The fluid in some instances even exited from one passage and entered into another adjacent passage. In addition, these observations have been substantiated by

Peck[1] and a number of other investigators. These conditions undoubtedly account for the discontinuities in the head-capacity curve obtained from extremely accurate laboratory tests. Consequently, it is very important in designing centrifugal pumps to avoid these turbulent flow conditions at the pump design point. This is another reason for employing a method designed to prevent separation of flow from the blades.

The importance of this turbulence problem is stressed by Stepanoff[6], who writes, "The vane discharge angle A2 is the most important single design element. It has been shown that the theoretical characteristics are determined by the vane angle alone. A2 is still the deciding factor in design. All the design constants depend on the value of A2. An average value of 22.5° can be called normal for all specific speeds. For forced output (high head) this may be raised to 27.5° without affecting the efficiency appreciably. The lower limit of A2, consistent with good design is about 17.5°."

In short, the designer has three options in selecting A2. He can obtain A2 from Eq. (42), determine A2 according to Ref. 6, or he can find the desired angle experimentally.

The literature research failed to give sufficient data to substantiate Stepanoff's[6] claims. Consequently an experimental program was initiated in order to ascertain the effect of outlet angle on operating performance. This could lead to greater understanding of the circulatory flow that is normally present in poorly designed centrifugal pumps. Three pump impellers were built that are identical in every respect except for outlet angle and the corresponding blade profile.

j. Number of Blades

The number of blades used in a pump is a compromise between two opposing factors. A sufficient number of blades are necessary to guide and direct the impending flow, but the number of vanes should be limited because a greater number of blades gives higher surface losses. In general, the decision to use a particular number of vanes is based largely upon experience and is fixed after the vane shape and outer diameter have been determined. Various formulas have been proposed, i.e., Pfleiderer in Die Kreiselpumpen has proposed the subsequent equation for the number of blades as

$$N = 6.5 \frac{D2 + D1}{D2 - D1} \sin BM \tag{43}$$

where

$$BM = \frac{A1 + A2}{2} \tag{43-a}$$

Hence large vane angles require more vanes to provide proper liquid guidance. Although this is a simple relationship for determining number of blades, the physical correlation between flow characteristics and optimum performance is dubious. Furthermore, little empirical evidence is available to substantiate the use of this equation in design.

k. Blade Taper

Blade taper should be employed as follows: As the taper angle is increased for a constant A1, A2, ..., etc., the amount of blade wrap increases (see computer program for changing T). Since little information exists on the absolute selection of this parameter, it was arbitrarly given a value of 8°. In general,

T should be selected to fulfill the requirements of IFCD Hypothesis.

6. SUMMARY PROCEDURE

The equations formulated here give only "first trial" values and may require modification.

a. Design Procedure

1. Determine the required head, capacity, and shaft speed.

2. Determine specific speed from Eq. (29-a).

3. Select a value for head coefficient (S) from PNS and Figs. 6, 7, and 8. This is usually from 1 to 1.3.

4. From these known quantities determine D2 from Eq. (31).

5. Find D1 from Eq. (34).

6. Select B5 and BH from Eqs. (36) and (36-a).

7. Calculate the inlet area and anvel from expressions (38) and (39), respectively. Then calculate the value of A1 from relationship (41).

8. Calculate the outlet angle A2 from (42) or assume this quantity (Probably 15°) on the report discussion.

9. Select the number of blades from report discussion.

10. Arbitrarily pick the blade taper as 8° or a value based on IFCD Hypothesis.

11. Find W from Eq. (29-B).

12. Determine value of U1 from U1 = R1*W/12.

13. Calculate R1 and R2 from the subsequent expression R = D/2.

14. Ascertain C1 from Eq. (26).

15. Find B1, B2, B3, and B4 from expressions (21) through (24), respectively.

16. Now with all necessary quantities known determine the blade profile from Eq. (25) by varying beta to obtain R.

The advantage of this procedure is that it lends itself readily to machine computation. Once the computer output is obtained, the information can be given to the designer.

C. Volute Design

1. INTRODUCTION

The volute design procedure discussed here will be a diverging spiral, nondiffuser type, with circular cross section and annual construction (Fig. 1 and 1B).

The objective of the volute (casing) is to convert a percentage of the kinetic energy of the fluid leaving the impeller into a pressure energy (head) as efficiently as possible. Unlike the numerous empirical methods that are used in impeller design, the volute design procedure for a given impeller design is more standardized though it too makes a number of ideal assumptions.[2,3,5,11,12] While this method is based on simple theory, it has had considerable success in producing good performance pumps. For those readers interested in the development and other details, the complete formulation is given in Ref. 12.

Considering the volute in pump design is necessary because experience has shown that often it is the main factor governing the exact operating condition (maximum efficiency point) of a pump.

2. FORMULATION OF PROBLEM

Duong's method[12] should be of considerable use since it is based on scientific principles with the emphasis on simple hydrodynamic theory. Furthermore, it has been applied successfully to some high performance built pumps.

The problem of volute casing formulation is three dimensional when a circular cross section annular channel is considered (Fig. 12).

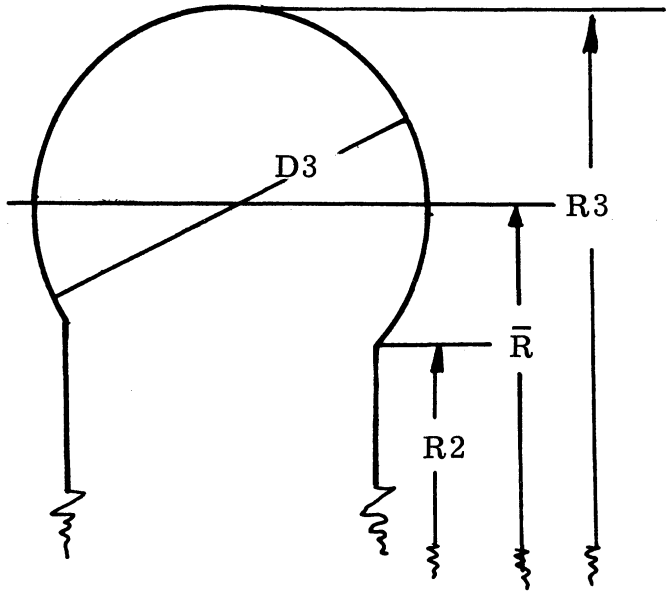

Fig. 12. Volute Cross Section.

From the Euler theoretical velocity triangles, based on the geometry of the impeller, the head and flow coefficient FL-CO can be defined

$$S = \frac{Hg}{U_2^2/2.} \tag{30}$$

$$FL - CO = \frac{Q}{\text{Area } 2*U_2} \tag{44}$$

The flow coefficient is a nondimensional ratio similar to S except that it reduces the flow rate to a common base for design comparisons. Assuming that

1. the flow in the volute is approximately spiral in nature

2. the summations of the torques exerted on the volute at the design point is essentially zero

3. flow from the impeller is uniform about its periphery

4. the flow is nonviscous

it can be shown that the relationship

$$\tan (Y) = \frac{NHY^* FL - CO}{S} \tag{45}$$

is valid. Combining assumptions 1, 2, and 3 and use of the momentum and continuity equations gives the relationship R*V = C where C is a constant determined at R = R2; V = V2.

From Fig. 14 we have

$$\frac{dR}{R^* d\,beta} = \tan Y \tag{46}$$

upon integrating we have

$$LN\ R = \tan Y * beta + LNC \tag{47}$$

Or

$$R = C\ e^{\tan Y * beta} \tag{48}$$

employing the boundary condition

$$beta = 0 \quad a \quad R = R2 \rightarrow C = R2$$

$$R = R2\ e^{\tan Y * beta} \tag{49}$$

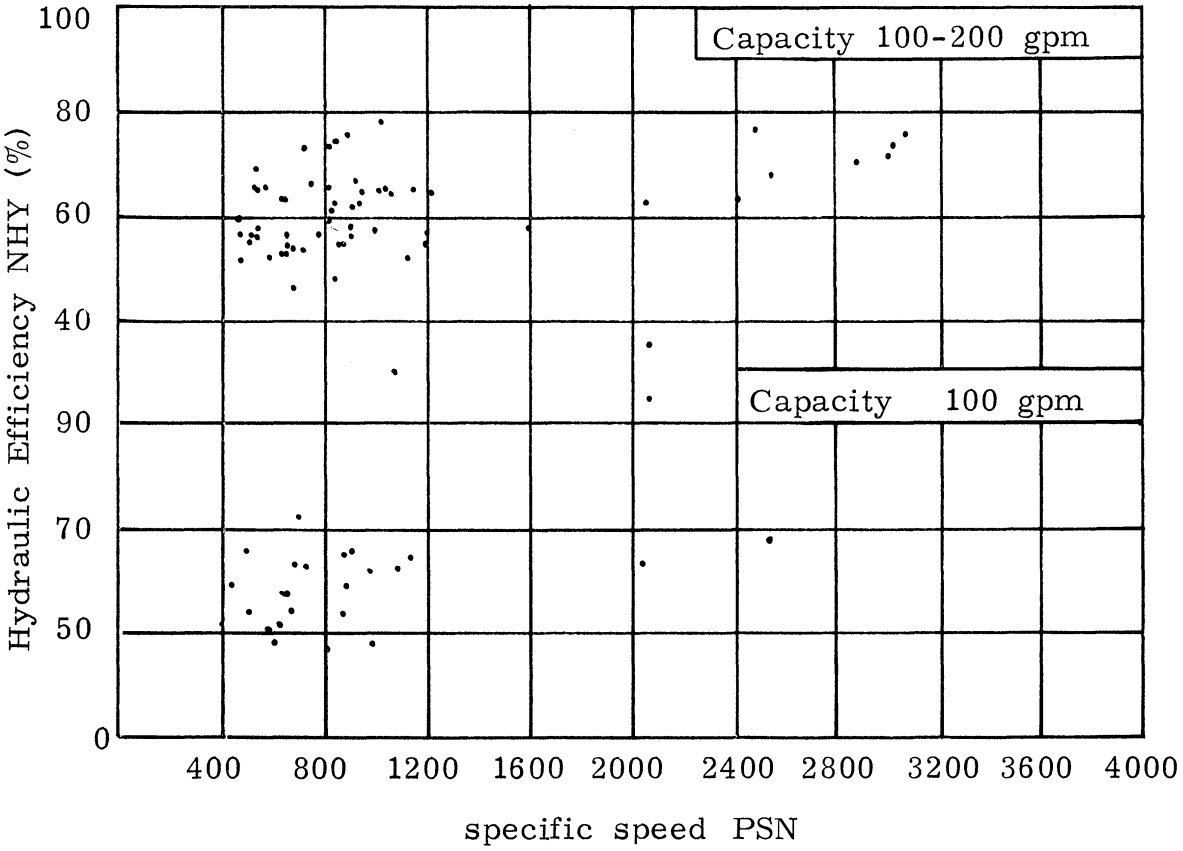

Fig. 13. Efficiency vs. specific speed in various flow rate ranges.

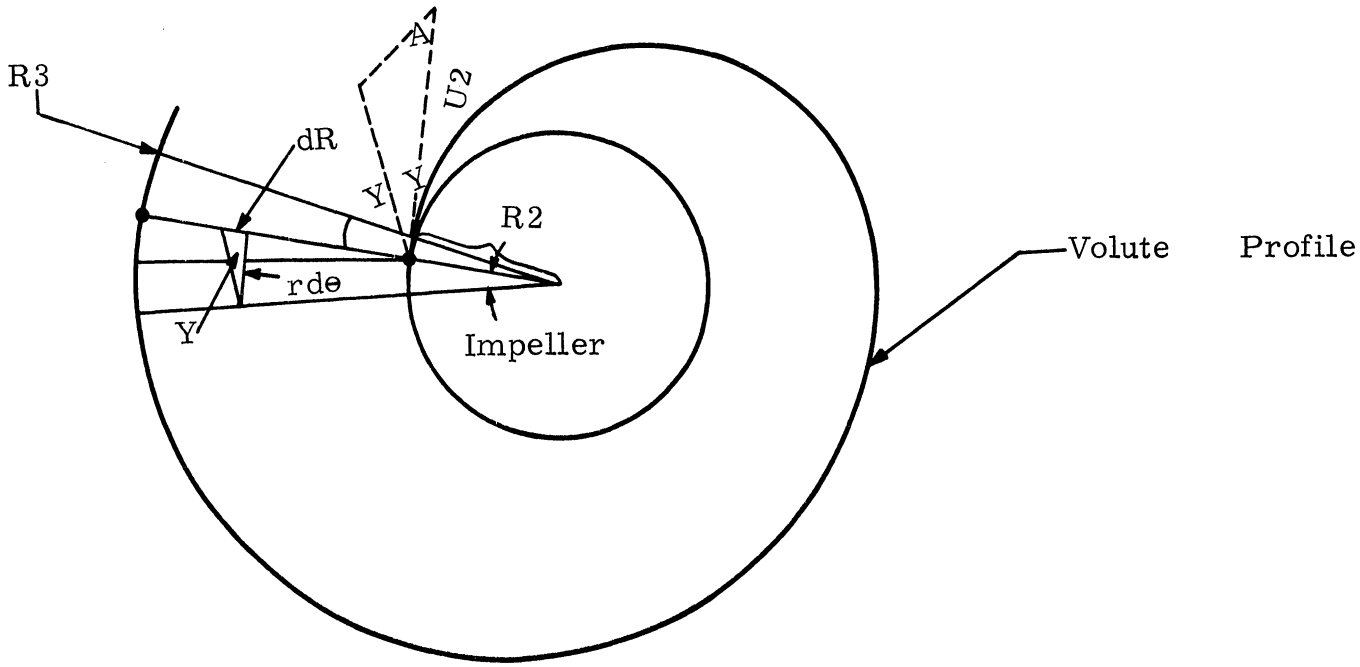

Fig. 14. Volute profile generation.

Substituting Eq. (45) into relationship (49)

$$R = R2\, e^{\frac{NHY \cdot FL - CO}{s} * beta} \tag{50}$$

or

$$R = f(beta)$$

The next portion of the development is to find the value of the crosssectional area, normally called the cut water area. This is defined as the area at beta equal to 2*3.1416 designated D3 (Fig.1).

Consequently

$$R3 = R2\, e^{NH*\frac{FL - CO}{s} *2*3.1416} \tag{51}$$

The difference of radii at the cut water point is

$$R3 - R2 = R2\left(e^{\frac{Nh*Fl - CO*6.283}{s}} - 1\right) \tag{52}$$

The actual cut water area in general is (Eq.(52) times the depth)

$$A3 = \left(R2\ e^{\frac{Nh*Fl - CO*6.283}{s}} - 1\right) \cdot \int db \tag{53}$$

Without further discussion, it can be shown that

$$\frac{A3}{\bar{R}} = 6.283 \cdot wid \cdot \sin Y = CONST. \tag{54}$$

where R is the centroid of the cross section measured from the impeller center of rotation and wid is the constant volute width (Fig. 15).

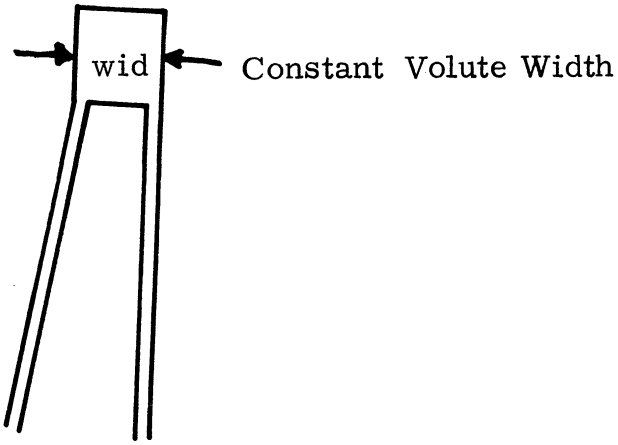

Fig. 15. Volute Cross Section with Constant Sides.

Since the volute cross section is circular in our particular design, another expression has to be formulated from expression (54). The conflicting opinions of the experts yielded nothing physically meaningful, therefore, the decision to employ a circular cross section was based on previously built pumps.

Using a circular cross section (Fig. 14), it can be obtained that

$$A3/\overline{R} = 6.283 \cdot wid \cdot e_c \cdot \tan y \qquad (55)$$

where

e_c = contraction factor

This analysis reaches essentially the same result as Kovats[3] and Church.[5] Duong's formulation[12] was presented because his is a more detailed explanation.

3. SUMMARY PROCEDURE

The procedure for determining the volute profile is given below. In addition, another method foreign to the discussion and based on empirical study

has been described.

a. Method 1

(1) Calculate the flow and head coefficient from Eqs. (30) and (40), respectively.

(2) Determine the quantity NHY from Figure 13.

(3) Obtain the quantity tan (Y) from expression (45).

(4) Using Eq. (50), substitute values of theta to find the radius for this particular value of theta. Ten values of theta equally divided into 360° will give sufficient points for volute layout.

b. Method 2

This method obtains the value of tan (Y) empirically by selecting a reasonable impeller exit velocity. The steps in applying the method are:

(1) Assume a reasonable value of exit velocity (V_e).

(2) Determine the area, A3, required to pass the discharge at this velocity from the continuity equation

$$A3 = \frac{Q}{V_e}$$

(3) Determine a pseudo-diameter D3 by assuming the cross sectional area of the volute calculated in 2 is circular, i.e.,

$$D3 = \sqrt{\frac{4\ A3}{\pi}}$$

(4) Then D3 is added to R2 to obtain the quantity R3.

(5) From Eq. (51) the value of tan (Y) is obtained

$$\tan (Y) = \frac{\ell n(R3/R2)}{6.283}$$

(6) Same as step 4 in method 1. Final equation to compute this step is:

$$R = R2\ e^{\tan(Y)\cdot beta}$$

III. EXPERIMENTAL STUDY

A. Introduction

The objective of the experimental phase was to obtain evidence and data that would ascertain the accuracy of the design procedure.

While it is true that substantial data exists on large centrifugal pumps, almost nothing is publically known about centrifugal pumpa designed for low flow rate (around 10 gpm and 10 to 20 ft H_2O).

B. Program Objectives

1. A closed circuit test apparatus was built to facilitate pump testing in a simple and accurate manner.

2. Four prototypes and one volute were designed, fabricated, and tested. These were based upon the design procedures presented in the formulation. Below is a listing of the pumps fabricated and tested:

   a. Whirlpool production combination washer and dryer pump.

   b. Prototype 1—designed by employing standard scaling procedures. The pump was scaled from a pump that has a reported efficiency of well over 70%.

   c. Prototypes 2, 3, and 4—these prototypes were designed from method 1 which is explained in detail in the discussion. The pump geometry was noted from computer output. The same volute was used to test these four prototype impellers.

3. Correlation and interpretation of experimental results (i.e., conclusions).

The production and prototype pumps are identical from the rear face of the pump backward (Fig. 16). Hence, the bearings, packing, etc., are the

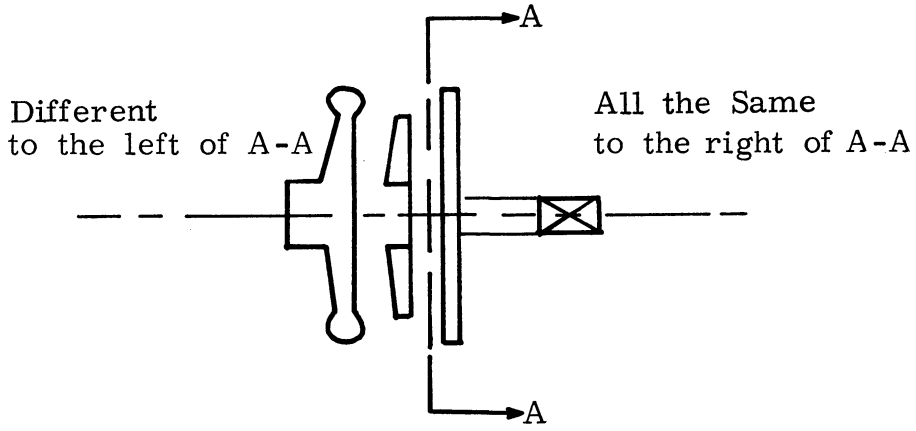

Fig. 16. Parts changed on pump prototypes.

same for both types of pumps. Only the impeller and the casing are different.

Whirlpool's present production combination washer and dryer pump was tested first (Part 2a). Since the testing apparatus was to be built from scratch, testing of the combo pump would permit early debugging of the test apparatus. Also, the operating performance of this pump would serve as a comparison for measuring the performance of the prototypes.

A pump based on scaling techniques described in most pumping tests was then designed (Part 2-b). This was done to obtain data for correlating the laws of scaling with small pump operation and to see if the efficiency reported in the scaled from unit would be realized in the model. The pump, prototype 1, was fabricated by Whirlpool's laundry division and tested.

Next the feasibility of impeller method 1 was investigated (Part 2-c).

The method's procedure was programmed on the computer and the actual output was used to build three phototypes.

The basis for selecting method 1 has been explained. The three impellers are identical in every respect except for outlet angle and blade profile. One of these can not be held constant while the other varies because blade profile is a function of outlet angle A2 in method 1.

This approach was used to determine experimentally the effect of outlet angle A2 (blade profile) on pump performance. The difficulty of ascertaining A2 analytically has been discussed. This is true because the ideal flow assumptions are not present.

Hence, a number of investigators have tried to correlate the difference between the theoretical magnitude of A2 and that found from experiment. This difference is sometimes called the slip angle. Stepanoff,[6] Pfleider, Busemann, and Kovats[3] have presented procedures to determine the slip quantity when experimental results are known. However, these methods have been calculated from empirical data, which often is not directly applicable when a pump is first designed.

Consequently, three arbitrary values of A2 were selected as criteria for building prototypes. The values of A2 were 15° (prototype 4), 30° (prototype 3), and 55° (prototype 2). These pumps were tested, and the physical nature of blade profile was ascertained to be governed by IFCD hypothesis.

C. Test Apparatus

1. INSTRUMENTATION

A testing apparatus was fabricated in the Fluids Engineering Laboratory of the University of Michigan. Fig. 17-a depicts the overall schematic physical characteristics of the test apparatus while Fig. 17 shows the apparatus as it looks in the laboratory.

Incorporated into the test apparatus is a magnetic pickup to measure shaft speed, a 1/3 horsepower dynamometer to measure reaction torque, an orifice calibrated to determine flow rate, and a mercury manometer to measure pressure head.

2. CIRCUIT

A reservoir holding approximately 25 gallons of water is used as a head tank. From the reservoir, the water flows to a plenum chamber where flow irregularities are removed. The smoothed flow is fed to the inlet side of the pump. Downstream from the pump outlet is an orifice plate and straight pipe where flow rate is measured by the pressure differential depicted on a mercury manometer. Subsequent to the orifice plates and preceding the plenum chamber are throttle valves which regulate the flow. From this point the fluid returns to the reservoir, hence completing the cycle.

3. DYNAMOMETER

The unit must be sensitive to small changes in pump load; bearings and other friction losses must be maintained at a minimum. Therefore, it was decided to use low friction air bearings to support the cradle. Only minor

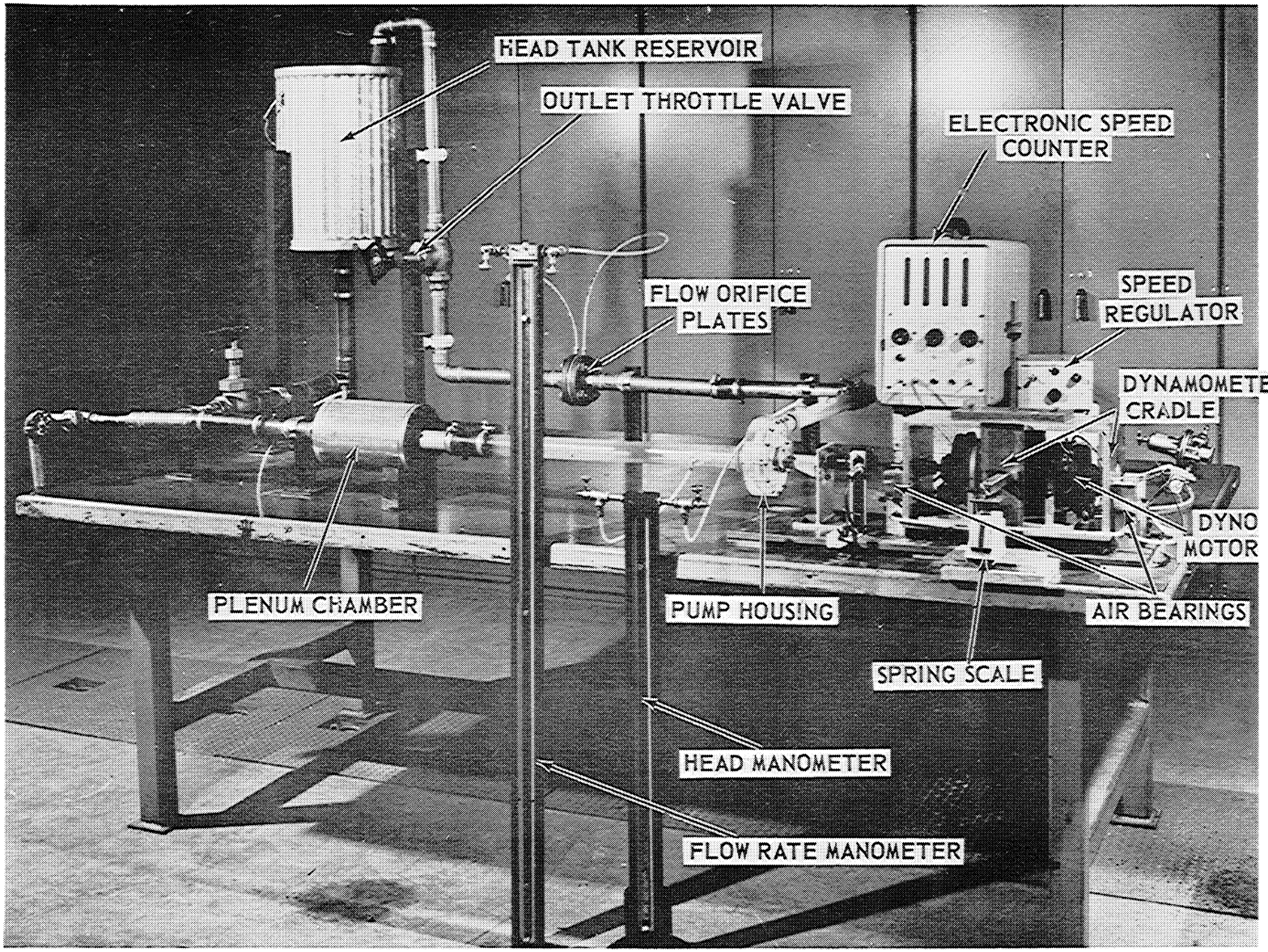

Fig. 17. Pump test apparatus installation.

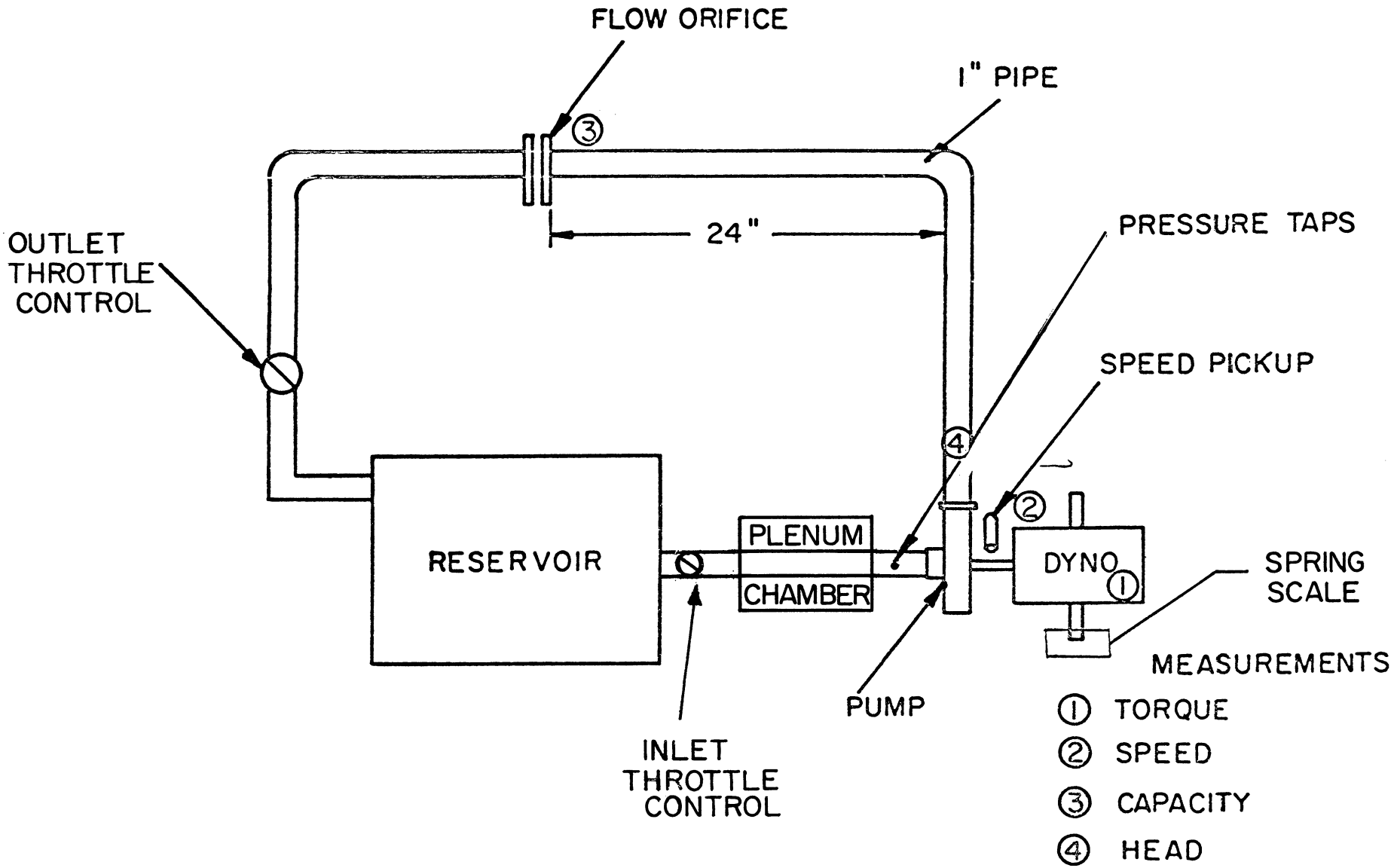

Fig. 17A. Test flow circuit schematic.

problems were encountered and dynamometer operated smoothly.

4. PLENUM CHAMBER

The plenum chamber used to smooth and remove the irregularities in the inlet flow to the pump consists of a steel tube with a series of metal screens to damp out any turbulence, vortices, etc., in the flow which would seriously effect pump inlet performance.

5. TEST PROCEDURE

a. Apparatus was assembled and checked for leaks. Air bearings were actuated.

b. The system was stabilized at a constant speed by the variable speed control.

c. Inlet throttle valve was opened to maximum position.

d. The dynamometer was calibrated dynamically to reach zero deflection at zero load at the required speed.

e. The outlet throttle valve was opened to the test condition setting. Head (manometer), speed (magnetic pickup), flow rate (manometer), and dynamometer torque (spring scale) were measured.

f. These four readings were noted for each fixed outlet throttle setting. Approximately five positions of flow range were recorded between shut-off and maximum flowrate at speeds of 1350, 1750, 2100, and 2400 rpm for each impeller and the same volute casing.

g. The readings were inputed to the data reduction computer program which converted the readings to appropriate units and performed the necessary

calculations. Values of head, flow rate, speed, and efficiency are depicted in Figures 21-24. A sample calculation is included in the computer program section.

h. After each complete run, the dynamometer was checked to ascertain if it was still operating at the calibration point.

6. EXPERIMENTAL ERRORS

Approximate errors encountered in measuring speed, flow rate, head, and dynamometer follow:

a. Speed was measured with a magnetic pickup, which sensed the number of impulses from a gear on the pump shaft. An electronic pulse counter was used to display the rpm every 2 sec. A reasonable estimate of the error would be approximately .5%.

b. Flow rate was measured with an .675 in. orifice plate on the outlet side of the pump. According to ASME standards the error should be less than 2%. In addition actual measurement of flow rate with a weighting tank and stop watch gave points that coincided with the calculated calibration curve.

c. Head was determined directly with a mercury manometer which was accurate within 1% when measuring heads in excess of 2 ft of water.

d. Dynamometer load, measured with a spring scale, represented a large percentage of error because the spring scale was not accurate. A reasonable value of error here would be 3%; however, a larger error probably exists.

IV. DESIGN CALCULATIONS

The calculation section essentially covers parts 2-b and 2-c of the testing program and the data reduction computer program. Part 2-b deals with pumps designed by similarity principles while part 2-c presents the details of method 1. The calculations in part 2-c have been determined by computer computation. A print-out of these calculations is given on page (reference to computer program 2-c, a', b', c').

A. Impeller Prototype 1

The design approach employed to specify prototype 1 in 2-B is based upon conventional scaling techniques. This principle is founded upon a group of nondimensional parameters which are assumed approximately constant for a family of geometrically similar pumps. Normal practice consists of using modeling laws to design a small scale model which is then tested. The model results and geometry are scaled for use in a specific application. Here, the same procedure will be employed in reverse since we are trying to obtain a pump with lower flow rate and lower head. Therefore, a large pump is used as a model with the dimensions scaled down to obtain the smaller geometry.

The dimensionless quantities employed in the scaling technique have been encountered before. They are the head and flow coefficients, i.e.,

$$S = \frac{Hg}{(SN)^2 D_2^2} = \text{const} \qquad (30)$$

$$FL - CO = \frac{Q}{SN*D^3} = \text{const} \qquad (44)$$

The prototype designed is shown in Figure 1C, number 1. The model characteristics will be indicated by the symbol P.

Fl-CO and S are constant for geometrically similar pumps under the assumptions of incompressible, nonviscous, and noncavitating fluids. The model used had the following properties at the design point (maximum efficiency).

H 84 ft Q = 500 gal/min

SN = 1750 rev/min D1 = 4.0 in. D2 = 10.0 in.

After converting the subsequent quantities to appropriate units, i.e., Q in cu fps, H in ft, SN in radians/sec, and diameters in ft., FL - CO and S can be evaluated.

$$SN = 1750 \frac{\text{rev}}{\text{min}} \frac{3.1416}{30} = \frac{1750 \times 3.1416}{30.} \frac{\text{rad}}{\text{sec}} = 183.3 \frac{\text{rad}}{\text{sec}}$$

$$Q = 500 \frac{\text{gal}}{\text{min}} \frac{.1337 \text{ ft}^3}{\text{gal}} \frac{1 \text{ min}}{60 \text{ sec}} = \frac{500(.1,337)}{6.0} \frac{\text{ft}^3}{\text{sec}}$$

$$D_2 = \frac{10 \text{ in.}}{12 \text{ in.}} \text{ ft} = \frac{5}{6}$$

$$D_1 = \frac{4 \text{ in.}}{12 \text{ in.}} \text{ ft} = \frac{1}{3}$$

Head is already in required units of feet.

The design point conditions to be obtained by the prototype are:

H = 10 feet Q = 20 gpm

SN = 1750 RPM D1 & D2 unknown

Consequently, the quantities to be ascertained are the prototypes inlet and outlet diameter. D2 can be found from the head coefficient (30), i.e.,

$$S = \frac{H}{(SN)^2 D^2}\Big|_p = \frac{H}{SN^2 D^2}\Big|_M$$

Since the speeds for both model and prototype are the same, they can be canceled on both sides and removed.

Thus

$$\frac{H}{D^2}\Big|_p = \frac{H}{D^2}\Big|_M$$

Substituting

$$\frac{10}{D2^2}\Big|_p = \frac{84}{10}\Big|_M$$

yields

$$D2_p = \underline{3.44 \text{ in.}}$$

The flow coefficient, which takes into account the capacity, gives these diameter sizes

$$\frac{Q}{SND}\Big|_p = \frac{Q}{SN\ D^3}\Big|_M = \text{const}$$

Again speed cancels.

Hence:

$$\frac{Q}{(3.44)^3} = \frac{500}{(10)^3}$$

$$Q = \frac{(500)\ (40)}{1000} = 20$$

Consequently, the calculations predict the desired operating conditions for a D2 = 3.44 in.

To find inlet diameter, D1, relationship 30 is again used.

$$\frac{H}{D^2}\Big|_p = \frac{H}{D^2}\Big|_M$$

$$\frac{10}{D^2} = \frac{84}{42}$$

$$\frac{160}{84} = D^2 = 1.90$$

yields D1 = 1.37 in.

Since inlet and outlet angles and blade taper are nondimensional quantities, they can be determined directly from model measurement. The values are:

$$A1 = 18°$$

$$A2 = 33°$$

$$T = 8°$$

The blade height dimensions must still be ascertained. These were found from direct scaling ratios as indicated below (Eqs. (35) and (35-A)).

$$SR = \frac{\text{blade height}}{\text{diameter}}\Big|_{p}^{\text{outlet}} = .06 = \frac{\text{blade height}}{\text{diameter}}\Big|_M$$

This gave a value of

$$BH = .275$$

$$B5 = .412$$

We now have found the quantities B5, BH, A1, A2, D1, D2, and T.

The blade profile can be approximately determined by attempting a trial and error procedure to fit a curve to the model's blade profile. The first attempt was to assume the general equation of a logarithmic spiral given as

$$R = f(BETA) = R_1 e^{n*BETA} \tag{59}$$

Table VI shows the calculations necessary for checking a logarithmic curve with the model's blade profile. First accurate measurements were

TABLE VI

SCALING CALCULATION SUMMARY TO DETERMINE N

R	R_1	R/R_1	$\ln(R/R_1)$	n	Angle Beta	Angle Beta
2.78	2.1	1.325	.282	.538	$\pi/6$	.524
3.62	2.1	1.721	.544	.520	$\pi/3$	1.048
4.66	2.1	2.220	.798	.508	$\pi/2$	1.570
5.00	2.1	2.380	.866	.514	97°	1.690

taken from the model in polar coordinates along the blade. For each individual point, a value of radius and angle were noted. When these values were substituted in Eq. 59, the quantity, n, was determined. Fortunately the value of n was approsimately constant for each point used. Hence another attempt at selecting an equation was not necessary. This equation was then employed to determine the blade profile for the prototype. A sample calculation appears below.

For

$$R = 3.62 , \quad R_1 = 2.1 , \quad R/R_1 = 1.72$$

$$\text{at BETA} = 3.1416/3 = 60°$$

and

$$\text{Ln}(\frac{R}{R_1}) = .544$$

Substituting these quantities into Eq. (59) gives n = .520.

Therefore the resulting form of the equation was

$$R = R_1 \cdot e^{.52 \text{ Beta}}$$

Employing values of beta until R = R2, the following table resulted.

TABLE VII

BLADE PROFILE SUMMARY—PROTOTYPE 1

R_1	R_1	Beta[8]	Beta (rad)	$e^{.52 \text{ Beta}}$
.685	1.720	101.5°	1.770	2.420
.685	1.550	90.0°	1.570	2.260
.685	1.350	75.0°	1.310	1.970
.685	1.180	60.0°	1.050	1.725
.685	1.030	45.0°	.785	1.505
.685	0.900	30.0°	.525	1.313
.685	0.785	15.0°	.262	1.146

In conclusion, this impeller (Prototype 1) was noted to have high performance characteristics. Although it did not produce the exact qualities predicted, it did have a high efficiency value. The table below shows its primary operational characteristics.

TABLE VIII

IMPELLER ONE OPERATION AT MAXIMUM EFFICIENCY

Speed	H	Q	Nay
1750	7.50	20.0	65.0
1750	10.00	13.2	72.0
1750	10.75	10.0	64.5

As the original discussion points out, the number of blades is usually picked as a compromise of two factors, with the ultimate decision based on experience. Therefore, I selected a value of six as a reasonable number, the same number as the model.

B. Volute Prototype 1

1. METHOD 1

The preceding analysis dealt only with specification of the impeller dimensions. The subsequent discussion will investigate the volute.

The volute design follows essentially that outlined in the discussion. The first step is to solve for the quantity tan (Y). From Eq. (45)

$$Q = .0223 \text{ ft}^3/\text{sec} \qquad \tan(y) = NHY \cdot \frac{FL-CO}{S}$$

$$W2 = 26.2 \text{ fps} \qquad \text{area} = \pi D_2 B H \epsilon$$

where ϵ is the restriction factor.

The head coefficient was determined from Eq. (30).

$$S = \frac{gH}{\frac{W_2^2}{2}} = \frac{(32.2)(10)}{(24.6)\frac{2}{2}} = 1.06$$

The flow coefficient becomes

$$FL\text{-}CO = \frac{Q}{A_2 W_2} \quad \frac{.0223 \times 2}{(2.06 \times 10^{-2})(26.2) \cdot \epsilon}$$

Noting a value of N_H equal to .73 from Figure 13 and e = .96

$$\tan(Y) \text{ equal to } .0594 = \frac{(.0223)(.73)(2.0)}{(.0206)(26.2)(.92)(1.06)}$$

Therefore Eq. (54) becomes

$$R = R_2 e^{.0594 * Beta}$$

2. METHOD 2

Another mode of determining the value of the constant tan(Y) is to rely on experience. A value of volute exit velocity is assumed and the diameter D3 calculated from the continuity equation. Church[5] notes that a reasonable value for this exit velocity is 7.5 ft/sec for small pumps. Assuming that the cross-sectional area at the cut water area is equal to a circle with diameter D3 the area of the section can be expressed as $3.1416 * D3^2/4$. Mathematically

$$Area = \frac{(.785) D3^2}{144}$$

from continuity

$$Area \cdot Vel = Q$$

or

$$\frac{.785\ D_3^2}{144}\ (7.5\ \text{ft/sec}) \;=\; 2.23 \times 10^{-2}\ \frac{A^3}{\text{sec}}$$

$$D_3 \;=\; \frac{2.23 \times 1.44}{.785\ (7.5)}^{1/2} \;=\; .74\ \text{in.}$$

The value at the cut water area of R_3 can be determined as

$$R_3 \;=\; R_2 + D_3$$

$$R_3 \;=\; 1.72 + 74 \;=\; 2.46$$

Again from (54)

$$R_3 \;=\; R_2\ e^{\tan(y)\theta}$$

$$\text{lu}\ \frac{R_3}{R_2} \;=\; \tan(y)\ 6.283$$

Gives

$$\tan(y) \;=\; .0594$$

Therefore Eq. (54) becomes

$$R \;=\; R_2 e^{.0594 * \text{Beta}}$$

which is identical to that found in the previous part.

The results of calculating values of radius from Eq. (54) for beta equal to 60, 90, 120, 180, 240, 300, and 360 are tabulated in Table IX.

TABLE IX

VOLUTE CALCULATION SUMMARY

	π	R2	Beta	$e^{\tan \theta}$
R_o	= 1.72	1.72	0	1
R_{60}	= 1.83	1.72	$\pi/3$	1.064
R_{90}	= 1.88	1.72	$\pi/2$	1.091
R_{120}	= 1.95	1.72	$2\pi/3$	1.132
R_{180}	= 2.07	1.72	π	1.205
R_{240}	= 2.20	1.72	$4\pi/3$	1.282
R_{300}	= 2.35	1.72	$5\pi/3$	1.364
R_{360}	= 2.49	1.72	2π	1.450

C. Impeller Prototypes 2, 3, and 4

The next part of this report concerns part 2-c of the experimental program. It essentially follows directly from the impeller formulation equations listed listed under the topic impeller design. The method is based on the constant loaded impeller concept with constant taper passage height impeller method. The results of the calculations are tabulated as computer output. The computer language is MAD. (On the right hand side of the enclosed computer output is a number corresponding to the number designating the equation in the report). The following is a summary of the specific statements in the computer program.

First the data is read by a read input statement. Data read were values for T, H, Q, SN, S, B5, A1, D1, A2 and NN.

The relationship W = 3.1416*SN/30 changes the given rotational speed (rev/min) into angular speed (rad/sec) Eq. (29-b).

PNS (specific speed) is Eq. (29-a).

D2 is determined from expression (31).

R1 and R2 are simply the radius at inlet and outlet determined by halving the respective diameter.

U1 and U2 are linear velocities at inlet and outlet found by multiplying the appropriate radius by W.

to calculate inlet angle	Area	is Eq. (38)	A1 read in this case
	Flow	conversion of discharge from gpm to cu fps	
	Anvel	Eq. (39)	
	A1	Eq. (40)	
to calculate outlet angle	Den	Denominator in Eq. (42)	A2 read as Data case
	Bun	numerator in Eq. (42)	
	A2	Eq. (42)	

F3 calculation parameter for blade profile development Eq. (25)

F2 part of the first term of relation (25)

F1 Eq. (24) squared

Through Statement (IMP)—iteration loop to find Beta as a function of (radius)

G4 through G7 constants appearing in Eq. (25)

F4 through F13 variable terms appearing in Eq. (25)

F numerator in Eq. (26)

P denominator in Eq. (26)

CL Eq. (26)

B1 through B4 Eqs. (21), (22), (23), and (24), respectively

F11 constant in Eq. (25)

Beta 1 Eq. (25) in radians

Beta Eq. (25) in degrees

Rad specific radius in inches

Print results statements call for the values of the parameters listed.

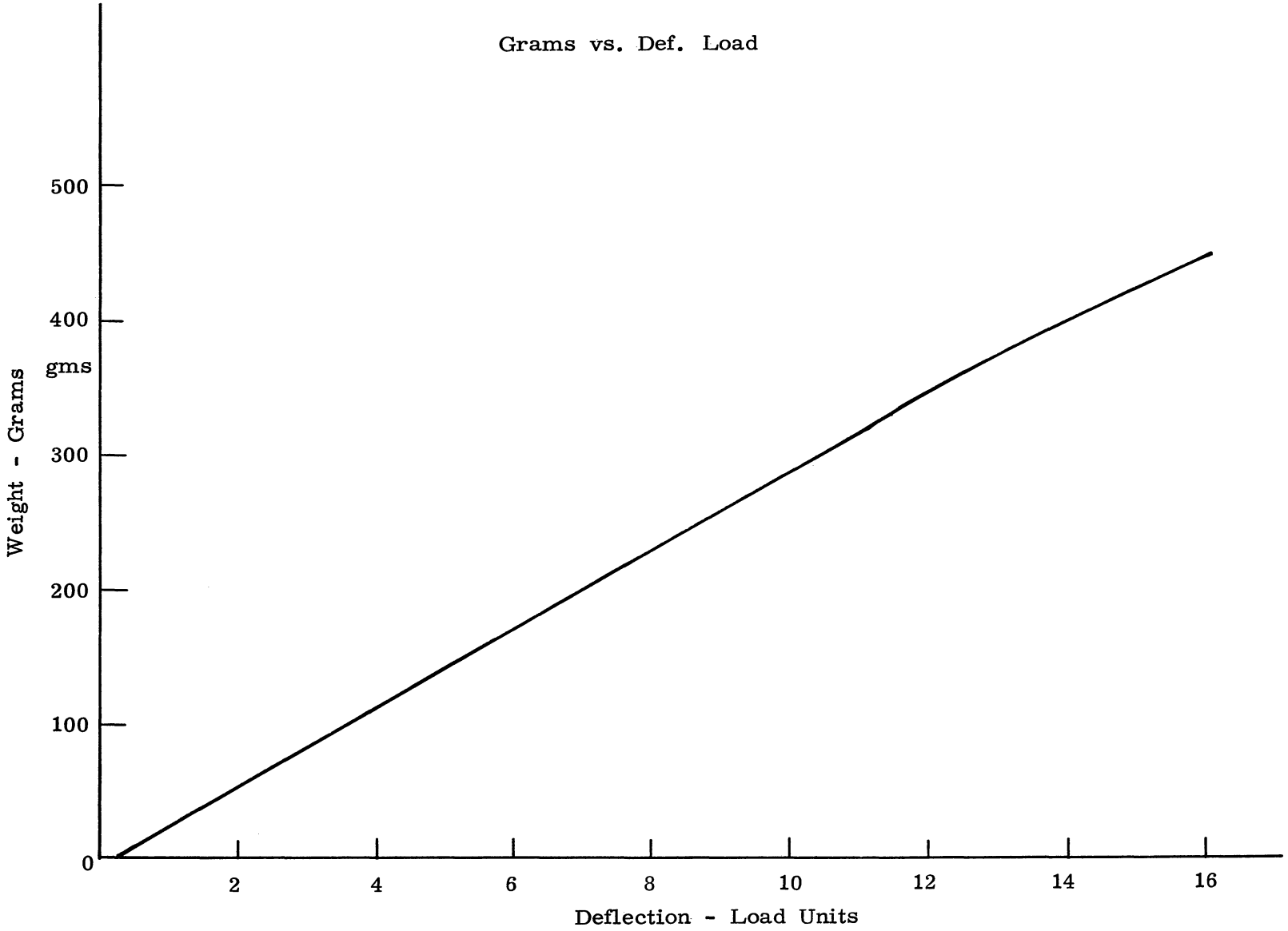

Fig. 18. Calibration curve for dyno spring scale.

D. Calibration

A calculation summary has been given below to demonstrate the relationships and equations employed to arrive at the experimental results. These calculations were used to ascertain the calibration curves and reduce the data.

1. DYNAMOMETER SPRING SCALE CALIBRATION

The dynamometer scale was calibrated by placing know quantities of gram weights on the scale's platform and recording the subsequent deflection. The curve (Fig. 18) was approximately linear throughout most of the deflection range. An equation of this line was defined by employing the general equation of a straight line, measuring the slope and noting the y intercept. The ultimate equation is given below.

$$L1 = ((200*H2)/6.8) - 7.0 \qquad (60)$$

2. ORIFICE PLATES CALIBRATION

The calibration equation was determined from the procedure given in Ref. 14, page A-19, for an orifice plate with do = 0.875, d_1 = 1.50 where Fig. 18 shows do and dl.

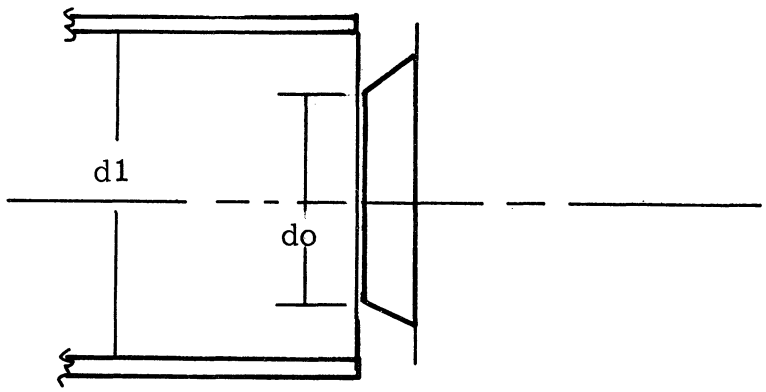

Fig. 19. Orifice Schematic.

Ref. 14 (pp. 4-15), can be employed to determine the flow rate by measuring pressure differential across the orifice. The equation that calculates the flow rate through an orifice for a corresponding ΔP measured across the flange tap is:

$$Q = 236.0\ d\ C\sqrt{\frac{\Delta P}{d}} \qquad (61)$$

where

$$\Delta P = \frac{Hl*d}{12.0*144.0} \qquad (61\text{-a})$$

$$d = dw(Shg - Sw) \text{ at } 60°F \qquad (61\text{-b})$$

for mercury Shg = 13.57
for water Sw = 1.00
density of water is 62.4 lb/ft^3

Hence

$$d = 62.4\ (13.54 - 1.00)$$

$$d = 784\ lb/ft^3$$

therefore

$$\Delta P = \frac{Hl*784.0}{12.0*144.0} = 0.454*Hl$$

for

$$dl = 1.50; \qquad do = .875\ ;$$

$$c = 0.645$$

consequently

$$Q = 236.0*(0.875)^2*0.645 \quad \frac{.454*Hl}{62.34} \tag{61}$$

$$Q = 10.0* \quad Hl \tag{62}$$

This is the equation employed to plot Fig. 20 which is the calibration curve for converting mercury manometer differential to flow rate in gallons per minute.

Furthermore, the flow rate was determined experimentally by using a weight tank and stop watch. The data, depicted below, was very close to that calculated from Equation (62).

TABLE X

FLOW RATE CALIBRATION DATA

Q gpm	t seconds	Weight lbs	Hl
10.24	73.2	100	1.05
10.24	73.0	100	1.05
15.95	47.0	100	2.55
15.95	47.0	100	2.55
18.70	40.0	100	3.55
18.70	40.2	100	3.55
12.85	58.4	100	1.70
12.85	58.6	100	1.70
23.65	31.5	100	5.60
23.65	32.2	100	5.60
23.65	31.7	100	5.60

3. SAMPLE CALCULATION

$$\frac{lbs}{sec} * \frac{60sec}{1\ min} * \frac{1gal}{8\ lb} = \frac{7.5gals*sec}{lb\ *\ min}$$

hence

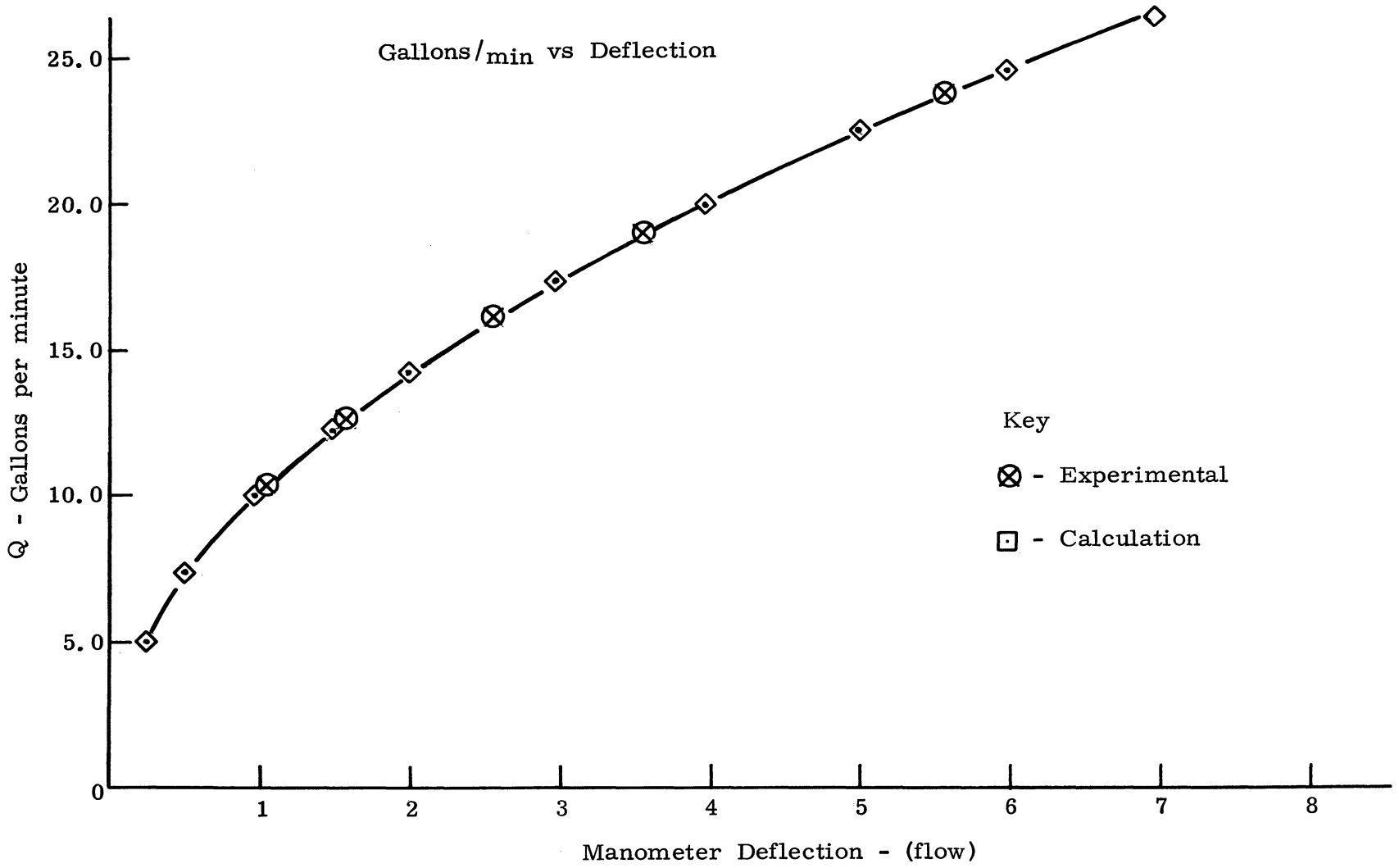

Fig. 20. Calibration curve for flow orifice plate.

$$\frac{100 \text{ lb}}{73.2 \text{sec}} \quad \frac{7.5 \text{ gal-sec}}{\text{lb*min}} \Rightarrow 10.24 \text{ gpm}$$

4. SPEED CALIBRATION

The shaft speed was simply read directly in rpm with an electronic counter.

5. HEAD CALIBRATION

The head manometer reading was converted from inches of mercury to feet of water by employing Equation (67).

6. HYDRAULIC EFFICIENCY

Hydraulic Efficiency (NHY) is defined as:

$$\text{HPout}/(\text{HPin} - \text{HPmech}) \tag{63}$$

The subsequent equations are employed to determine HPin, load, Torque, and NS.

To determine HPin

$$\text{Load} = \frac{\text{scale deflection m grams}}{453.0 \text{ grams/lb}} = \frac{L}{} \tag{64}$$

where

$$L = L1 \tag{64-a}$$

$$\text{Dynanometer moment arm} = \frac{\text{arm length}}{12 \text{ in./ft}} = .716 \text{ ft}$$

$$\text{arm length} = 8.593 \text{ in.}$$

$$\text{Torque} = \text{moment arm*load}$$

$$\text{Torque} = \frac{L}{453.0} \text{ *0.716 ft} = 1.58 \times 10^{-3} \text{*L ft-lb} \tag{65}$$

$$SN = SN\left(\frac{rpm}{min}\right) * \frac{6.28}{60} = SN \cdot \left(1.045 * 10^{-1}\left(\frac{rad}{sec}\right)\right)$$

$$HPin = Torque * SN$$

$$HPin = 1.58 \times 10^{-3} * L * SN * 1.045 \times 10^{-1}$$

$$HPin = 3.00 \times 10^{-7} * SN * L \qquad (66)$$

The value of HPout can be obtained from the subsequent equations. HPout is defined as the product of head times flow rate in horsepower units, i.e., (HPout = H*Q/k).

$$H = 62.4 \frac{lb}{ft^2} \cdot H \qquad (66\text{-a})$$

$$Q = Q(gpm) * \frac{0.1337\ ft^3}{gal} * \frac{1\ min}{60\ sec} = Q * 2.23 \times 10^{-3} \frac{ft^3}{sec} \qquad (66\text{-b})$$

$$HPout = \frac{62.4\ lb}{ft^2} * 2.23 \times 10^{-3}\ \frac{ft^3}{sec} * H * Q \qquad (66\text{-c})$$

$$HPout = 2.53 * 10^{-4} * H * Q(HP)$$

Hence froms Eqs. (63), (66) and (66-c)

$$NHY = \frac{2.54 * 10^{-4} * H * Q}{L * SN * 3.0 * 10^{-7}} \qquad \frac{.844 \times 10^{3} * H * Q}{L * SN} \qquad (63)$$

Similarly NOA can be found to be

$$NOA = \frac{.844 * 10^{3} H * Q}{L1 * SN} \qquad (68)$$

7. SAMPLE CALCULATION OF DATA REDUCTION PROGRAM

data readings — N1 = 875.0 rpm (electric counter)
Prototype L — H2 = 4.40 inches(spring scale-wet)
H3 = 10.60 inches(head manometer)
H1 = 0.65 inches(flow rate manometer)
Def = 1.85 (spring scale-dry)

Employing Eqs. (60) through (68)

$$L1 = ((200.*H2)/6.8) - 7.0 \qquad (60)$$
$$L1 = 122.41 \text{ grams}$$

$$L2 = ((200.*DEI)/6.8) - 7.0 \qquad (60)\ (\text{altered})$$
$$L2 = 47.41 \text{ grams}$$

$$Q = 10.0*)H1)^{1/2}$$
$$Q = 8.06 \qquad (62)$$

$$H = 1.05*H3 + 0.1666$$

where

$$H = \frac{(62.4)(SHy-Sw)*34*H3}{14.7*144.0*12.0} = 1.05\ H3 \qquad (67)$$

and .1666 is the height differential between inlet and outlet.

therefore

$$H = 11.2966 \text{ ft of water}$$

$$N = SN = N1*2.0 \text{ (thirty-tooth gear)}$$
$$SN = 1750. \text{rpm} \qquad (67\text{-a})$$

Consequently NOA and NHY can be determined i.e.,

$$NOA = (.844*10^3*H*Q)/SN*L1) = 35.88\% \qquad (68)$$

$$NHY = (.844*10^3 H*Q)/(SN*L) = 58.56\% \qquad (63)$$

V. BIBLIOGRAPHY

1. Peck, J.R., "Investigation Concerning Flow Conditions in a Centrifugal Pump, and Effect of Blade Loading on Head Slip," English Society of Mechanical Engineers, April 1950.

2. Addison, H., Centrifugal and Other Rotodynamic Pumps, Chapman and Hall, London, 1955.

3. Kovats, A., Design and Performance of Centrifugal and Axial Flow Pumps, Wiley, New York, 1957.

4. Csanady, G.T., Theory of Turbomachines, McGraw-Hill, New York, 1964.

5. Church, A., Centrifugal Pumps and Blowers, Wiley, New York, 1929, 1944.

6. Stepanoff, A. J., Centrifugal and Axial Flow Pumps, Wiley, New York, 1957.

7. Murata, S., "Research on the Flow in a Centrifugal Pump Impeller," Six reports, Bulletin of JSME, 1960.

8. Acosta, A., and R. Bowerman, "An Experimental Study of Centrifugal Pump Impellers, ASME Paper No. 56-A-41, 1957.

9. Final Report, Project P5)2, NASA.

10. Lichtenstein, J., "A Method of Analyzing the Performance Curves of Centrifugal Pumps," ASME Paper No. HYD-50-3, 1927.

11. Fisher, K., and D. Thoma, "Investigation of Flow Conditions in a Centrifugal Pump," ASME Paper No. HYD-54-8, 1932.

12. Duong, M., unpublished report.

13. Shephard, R. K., "Centrifugal Pumps," Wiley, New York, 1952.

14. Crane Co., Technical Paper No. 410, 1957, Crane Copyright.

15. Pfliederer, C., Die Kreiselpumpen, Julius Springer, Berlin, 1932.

16. Busemann, A., Pressure Head Ratio of Radial Centrifugal Pumps with Logarithmic-Spiral Blades, Kaiser-Wilhelm Institut fur Stroemungsforschung. Z. Angew. Math. Mech., Vol. 8, 1928.

VI. APPENDIX

A. Computer Programs

1. INTRODUCTION

Four computer programs, programmed in Mad computer language, were developed. Two aid in calculating impeller and volute geometry. The third predicts the head and flow rate for a predetermined speed. The fourth expedites data reduction calculations. Each program includes a brief introduction of its purpose, content, and output format.

2. IMPELLER PROGRAM

a. Introduction

One major aspect of the analytical study was to develop a computer program to aid a designer in establishing pump impeller geometry and eliminate detailed and time-consuming calculations. The work consisted of writing a program based on impeller analysis one (p. 55). Given the head, flow rate, inlet and outlet angles, blade taper, head coefficient, and speed requirements, the program defines the impeller blade profile geometry in polar coordinates. A print-out of the impeller program is attached.

The computer program's purpose was to make blade profile design calculations for impellers 4, 3, and 2. All input values were the same in each case except for A2. A2 = 15.0° for prototype 4, A2 = 30.0 for prototype 3, and A2 = 55.0° for prototype 2.

The computer output format is given below. The forst eight lines correspond to the iteration loop for radius (rad), beta, and T. The three columns are indicated respectively as rad, beta, and T.

rad (inches)	beta (deg)	blade taper (T)
1		
2		
3		
4		
5		
6		
7		
8		

The remainder of the data corresponds to the following layout as designated on the data sheet.

F9	F13	F	P
C1	B1	B2	B3
B4	F11	A1	A2
PNS	.	.	.
W	.	.	.
.	.	.	.

In summary, the program was run with three values of A2 inputed as data. The results of those runs are enclosed. The data input was

T = 8	H = 10.	Q = 10.	A1 = 12.
SN = 1750	S = 1.06	D1 = 1.37	B5 = .412

NN is dummy expression and A2 was given values of A2 = 15°, prototype 4; 30°, prototype 3; and 55°, prototype 2.

b. Impeller Program

```
                    F3 IS TERM IN EXPRESSION (25 )
                    F1 IS TERM IN EXPRESSION (25 )
                    F2 IS TERM IN EXPRESSION (25 )
                    F9 IS TERM IN EXPRESSION (25 )
                    G4 IS TERM IN EXPRESSION (25 )
                    G5 IS TERM IN EXPRESSION (25 )
                    F3 IS TERMIN EXPRESSSION (25)
                    G6 IS TERM IN EXPRESSION (25 )
                    G7 IS TERM IN EXPRESSION (25 )
                    F13 IS A TERM IN EXPRESSION ( 25 )
                    F  IS THE NUMERATOR IN EXPRESSION (26 )
                     P  IS THE DENOMNATOR IN EXPRESSION (26)
                    B1  IS THE CONSTANT EXPRESSION (21)
                    B2  IS THE CONSTANT EXPRESSION (22)
                    B3  IS THE CONSTANT EXPRESSION (23)
                    B4  IS THE CONSTANT EXPRESSION (24)
                    R  IS THE RADIUS IN POLAR COORDINATES
                    BETA IS THE ANGLE IN POLAR COORDINATES
TOP                 READ DATA
          W = 3.1416*SN/30.
          PNS = (SN*SQRT.(Q))/ (H.P..75)
          D2 = (1840.*SQRT.(H/S))/SN
          R1 =D1/2.
          R2 =D2/2.
          U1 =(R1*W) /12.
          U2=(R2*W)/12.
          F3 = SIN.((T *3.1416)/180.)/COS.((T *3.1416)/180.)
          F2= (5.0*4.*3.1416*B5*U1.P.2) / (.1337*W*Q)
          F1 = F3.P.2
          THROUGH IMP, FOR R=1.,.2, R.G.NN
          G4 = (R2 -1.)
          G5 = (R2.P.3 -1.)
          G6 =  (R2.P.2 -1.)
          G7 = (R2.P.4 -1.)
          F4= (R - 1)
          F5 =( R .P.3- 1)
          F6 =(R .P.2 - 1)
          G7 = (R2.P.4 -1.)
          F4= (R - 1)
          F5 =( R .P.3- 1)
          F6 =(R .P.2 - 1)
          F7 =( R .P.4- 1)
          F8 = SIN.(( A2*3.1416)/180.) / COS.((A2*3.1416)/180.)
          F9 = SIN.(( A1*3.1416)/180.) / COS.((A1*3.1416)/180.)
          F13 = ELOG.(R )
          F = F8-F9-F2*((G6/2.) -F3*(G5/3.-G6/2.)) + F3*G4
          P = -2.*F3*(G5/3. -G6/2.) + F1*(G7/4.-2.*G5/3. +G6/2.) +G6/2.
          C1 = -F/P
          B1 =(C1*F3.P.2)/4.
          B2 =-F2*F3/3. +2.*C1*F3/3.-2.*C1*F3.P.2/3.
          B3 = F2*(F3 +1.)/2.-C1*( 1.+ 2.*F3)/2. +  C1*F1/2.
          B4 =-F3
          F11 = B1+B2+B3+B4
          BETA1= B1*F7/4.0 +B2*F5/3.0 +B3*F6/2.0 +B4*(F4)+(F9 -F11)*F13
          BETA = BETA1*180.0/3.1416
          RAD = R*R1
IMP       PRINT RESULTS RAD, BETA, T
          PRINT RESULTS F9,F13,F,P,C1,B1,B2,B3,B4,F11,A1,A2 ,PNS
          PRINT RESULTS W,SN,D2,R1,R2,U1,U2,F1,F2,F3,F4,F5,F6,F7,F8
          PRINT RESULTS B5, Q, H,S,   D1
          TRANSFER TO TOP
          END OF PROGRAM
```

c. Impeller Program Output

a'. Prototype 4

RAD =	.685000,	BETA =	-.000000,	T =	8.000000		
RAD =	.822000,	BETA =	1.814435,	T =	8.000000		
RAD =	.959000,	BETA =	3.096781,	T =	8.000000		
RAD =	1.096000,	BETA =	4.788622,	T =	8.000000		
RAD =	1.233000,	BETA =	7.740641,	T =	8.000000		
RAD =	1.370000,	BETA =	12.764855,	T =	8.000000		
RAD =	1.507000,	BETA =	20.661811,	T =	8.000000		
RAD =	1.644000,	BETA =	32.235891,	T =	8.000000		
F9 =	.212557,	F13 =	.875469,	F =	-8.717276,	P =	.731021
C1 =	11.924797,	B1 =	.058884,	B2 =	.418613,	B3 =	-.927086
B4 =	-.140541,	F11 =	-.590130,	A1 =	12.000000,	A2 =	15.000000
PNS =	984.097374						
W =	183.259996,	SN =	1750.000000,	D2 =	3.229437,	R1 =	.685000
R2 =	1.614719,	U1 =	10.461091,	U2 =	24.659443,	F1 =	.019752
F2 =	11.562001,	F3 =	.140541,	F4 =	1.400000,	F5 =	12.823998
F6 =	4.760000,	F7 =	32.177595,	F8 =	.267950		
B5 =	.412000,	Q =	10.000000,	H =	10.000000,	S =	1.060000
D1 =	1.370000						

b'. Prototype 3

RAD =	.685000,	BETA =	-.000000,	T =	8.000000		
RAD =	.822000,	BETA =	2.262531,	T =	8.000000		
RAD =	.959000,	BETA =	4.768922,	T =	8.000000		
RAD =	1.096000,	BETA =	8.322199,	T =	8.000000		
RAD =	1.233000,	BETA =	13.668780,	T =	8.000000		
RAD =	1.370000,	BETA =	21.535694,	T =	8.000000		
RAD =	1.507000,	BETA =	32.649956,	T =	8.000000		
RAD =	1.644000,	BETA =	47.749480,	T =	8.000000		
F9 =	.212557,	F13 =	.875469,	F =	-8.407874,	P =	.731021
C1 =	11.501551,	B1 =	.056794,	B2 =	.384531,	B3 =	-.660160
B4 =	-.140541,	F11 =	-.359376,	A1 =	12.000000,	A2 =	30.000000
PNS =	984.097374						
W =	183.259996,	SN =	1750.000000,	D2 =	3.229437,	R1 =	.685000
R2 =	1.614719,	U1 =	10.461091,	U2 =	24.659443,	F1 =	.019752
F2 =	11.562001,	F3 =	.140541,	F4 =	1.400000,	F5 =	12.823998
F6 =	4.760000,	F7 =	32.177595,	F8 =	.577352		
B5 =	.412000,	Q =	10.000000,	H =	10.000000,	S =	1.060000
D1 =	1.370000						

c'. Prototype 2

RAD =	.685000,	BETA =	-.000000,	T =	8.000000		
RAD =	.822000,	BETA =	3.494720,	T =	8.000000		
RAD =	.959000,	BETA =	9.367027,	T =	8.000000		
RAD =	1.096000,	BETA =	18.038936,	T =	8.000000		
RAD =	1.233000,	BETA =	29.970154,	T =	8.000000		
RAD =	1.370000,	BETA =	45.654007,	T =	8.000000		
RAD =	1.507000,	BETA =	65.615318,	T =	8.000000		
RAD =	1.644000,	BETA =	90.409219,	T =	8.000000		
F9 =	.212557,	F13 =	.875469,	F =	-7.557071,	P =	.731021
C1 =	10.337695,	B1 =	.051047,	B2 =	.290810,	B3 =	.073844
B4 =	-.140541,	F11 =	.275160,	A1 =	12.000000,	A2 =	55.000000
PNS =	984.097374						
W =	183.259996,	SN =	1750.000000,	D2 =	3.229437,	R1 =	.685000
R2 =	1.614719,	U1 =	10.461091,	U2 =	24.659443,	F1 =	.019752
F2 =	11.562001,	F3 =	.140541,	F4 =	1.400000,	F5 =	12.823998
F6 =	4.760000,	F7 =	32.177595,	F8 =	1.428155		
B5 =	.412000,	Q =	10.000000,	H =	10.000000,	S =	1.060000
D1 =	1.370000,						

3. VOLUTE PROGRAM

a. Introduction

The other component of the system (volute) was programmed according to the procedure starting on page 106. The results appear as computer output. The statements and output format are given below.

Read Data	NJ = 6.5, H = 10.0, S = 1.06, BH = .279, NHY = .90, Q = 10.0, SN = 1750
Flow	Conversion of Q to ft^3/sec
Area 2	Area at section two
FLCO	Eq. (44)
Y	Eq. (45)
EX	Eq. (45) as tan.
THROUGH VOL	Iteration loop to determine value of radius at given values theta
PRINT RESULTS	Output statement

Output format

	VORA	THETA	FLCO
1	-	-	-
.	-	-	-
.	-	-	-
.	-	-	-
.	-	-	-
.	-	-	-
14	-	-	-
	D2	FLOW	AREA2
	FLCO	NHY	EX

The volute program follows.

b. Volute Program

```
      PROGRAM TO COMPUTE VOLUTE PROFILE
      FLOW IS EQ FOR CHANGING GPM TO FT3/SEC
      AREA2 IS EQ FOR OUTLET AREA
      FLCO IS EQ  (44)
      Y IS EQ (45)
      VORA IS THE VOLUTE RADIUS
      THETA IS THE ANGLE COMPATIBLE WITH ANGLE BETA IN IMPELLER
      PROGRAM
TOP             READ DATA
      W =  3.1416*SN/30.
      D2 = (1840.*SQRT.(H/S))/SN
      R2 =D2/2.
      U2=(R2*W)/12.
      FLOW = Q*.1337/60.0
      AREA2 = 3.1416*D2*BH*.80/144.
      FLCO  =  (FLOW)/ (AREA2*U2)
      Y =NHY*FLCO/S
      EX = SIN.(Y)/COS.(Y)
      THROUGH VOL, FOR THETA = 0.0,.5, THETA.G.NJ
      VORA = R2*EXP. (EX* THETA)
VOL   PRINT RESULTS VORA, THETA, FLCO
      PRINT RESULTS D2,FLOW,AREA2 ,S,FLCO,   EX ,Y    ,NHY
      TRANSFER TO TOP
      END OF PROGRAM
```

c. Volute Program Output

VORA =	1.614719,	THETA =	.000000,	FLCO =	.057463		
VORA =	1.654625,	THETA =	.500000,	FLCO =	.057463		
VORA =	1.695519,	THETA =	1.000000,	FLCO =	.057463		
VORA =	1.737422,	THETA =	1.500000,	FLCO =	.057463		
VORA =	1.780362,	THETA =	2.000000,	FLCO =	.057463		
VORA =	1.824363,	THETA =	2.500000,	FLCO =	.057463		
VORA =	1.869451,	THETA =	3.000000,	FLCO =	.057463		
VORA =	1.915653,	THETA =	3.500000,	FLCO =	.057463		
VORA =	1.962998,	THETA =	4.000000,	FLCO =	.057463		
VORA =	2.011512,	THETA =	4.500000,	FLCO =	.057463		
VORA =	2.061225,	THETA =	5.000000,	FLCO =	.057463		
VORA =	2.112167,	THETA =	5.500000,	FLCO =	.057463		
VORA =	2.164369,	THETA =	6.000000,	FLCO =	.057463		
VORA =	2.217860,	THETA =	6.500000,	FLCO =	.057463		
D2 =	3.229437,	FLOW =	.022283,	AREA2 =	.015726,	S =	1.060000
FLCO =	.057463,	EX =	.048828,	Y =	.048789,	NHY =	.900000

4. PREDICTION PROGRAM

a. Introduction

The third computer program was employed to predict head and flow for a given shaft speed. The results of this program are shown (Fig. 1D) where predicted and experimental head—flow rate characteristics were noted.

The statements are as follows:

READ DATA	data input statements, SN = 1750, S = 1.06
H	Eq. (30) solved for H
Q	Eq. (29-A) solved for Q
PRINT RESULTS	output statement
TRANSFER TO TOP	loop return statement
END OF PROGRAM	terminating

Output format

H	Q	SN
-	-	-
-	-	-
-	-	-
-	-	-
-	-	-
-	-	-
-	-	-

b. Prediction Program

```
$ COMPILE MAD, EXECUTE, PRINT OBJECT, DUMP

TOP     READ DATA
        H = S*(D2*SN/1840.).P.2
        Q = (984.097 *H.P..75/SN).P.2
        PRINT RESULTS   H, Q, SN
        TRANSFER TO TOP
        END OF PROGRAM
```

c. Prediction Program Output

```
H =      5.990013,    Q =      7.790223,    SN =   1350.000000
H =     10.065522,    Q =     10.098436,    SN =   1750.000000
H =     14.494352,    Q =     12.118123,    SN =   2100.000000
H =     18.931399,    Q =     13.849284,    SN =   2400.000000
```

5. DATA REDUCTION PROGRAM

a. Introduction

The final computer program was used to reduce the data to H, Q, SN = N, L1, NHY, and NOA in the appropriate dimensional units. The statements are explained throughly in the latter part of the calculation section.

STATEMENTS

L	Relationship (60)
L2	Relationship (60) altered
Q	Relationship (62)
H	Relationship (67)
N	Used to convert gear rpm to actual rpm
NOA	Expression (68)
L	Difference between measured load, pump wet and pump dry
NHY	Expression (63)

The remaining statements have previously been explained. The apparatus readings inputed were H1, H2, H3, and N1 and DEF. Where

H1 - flow rate manometer reading

H3 - head

H2 - spring scale reading (wet)

N1 - shaft speed/2

Def- spring scale reading (pump dry)

Only a sample of the actual program calculations are included here. The results of this program were employed to define the graphs shown in Figs. 21-24.

b. Data Reduction Program

```
$ COMPILE MAD, EXECUTE, PRINT OBJECT, DUMP

TOP     READ DATA
        L1 = ((200.*H2)/6.8)-7.
        L2 = ((200.*DEF)/6.8)-7.
        Q = 10. *SQRT.(H1)
        H = 1.05*H3 + 0.16666
        N = N1*2.
        NOA =( 844.00 *H*Q )/(N*L1)
        L = L1 - L2
        NHY =( 844.00 *H*Q )/(N*L )
        PRINT RESULTS  Q,H,N,NOA,NHY
        PRINT RESULTS L1,L2,N1,H1,H2,H3,DEF
        TRANSFER TO TOP
        END OF PROGRAM
```

c. Data Reduction Program Sample Output

```
Q =      .000000,  H =     6.309160,  N =  1350.000000,  NOA =     .000000
NHY =    .000000

L1 =    69.470587,  L2 =   38.588235,  N1 =   675.000000,  H1 =     .000000
H2 =     2.600000,  H3 =    5.850000,  DEF =    1.550000

Q =      7.416198,  H =     5.574160,  N =  1350.000000  NOA =     .318145
NHY =    .606011

L1 =    81.235294,  L2 =   38.588235,  N1 =   675.000000,  H1 =     .550000
H2 =     3.000000,  H3 =    5.150000,  DEF =    1.550000

Q =     10.000000,  H =     5.101660,  N =  1350.000000,  NOA =     .342955
NHY =    .586175

L1 =    92.999999,  L2 =   38.588235,  N1 =   675.000000,  H1 =    1.000000
H2 =     3.400000,  H3 =    4.700000,  DEF =    1.550000

Q =     12.247449,  H =     4.576660,  N =  1350.000000,  NOA =     .354392
NHY =    .581203

L1 =    98.882352,  L2 =   38.588235,  N1 =   675.000000,  H1 =    1.500000
H2 =     3.600000,  H3 =    4.200000,  DEF =    1.550000

Q =     14.491377,  H =     3.789160,  N =  1350.000000,  NOA =     .318729
NHY =    .496675

L1 =   107.705881,  L2 =   38.588235,  N1 =   675.000000,  H1 =    2.100000
H2 =     3.900000,  H3 =    3.450000,  DEF =    1.550000

Q =      .000000,  H =     10.456660,  N =  1750.000000,  NOA =     .000000
NHY =    .000000

L1 =    98.882352,  L2 =   53.294117,  N1 =   875.000000,  H1 =     .000000
H2 =     3.600000,  H3 =    9.800000,  DEF =    2.050000
```

B. Graphs

The subsequent figures have been referred to in the previous discussion. Their major significance is that they represent the operating and performance characteristics of the prototypes and other machinery tested. These graphs were drawn from the data reduction program output (Figs. 21-26).

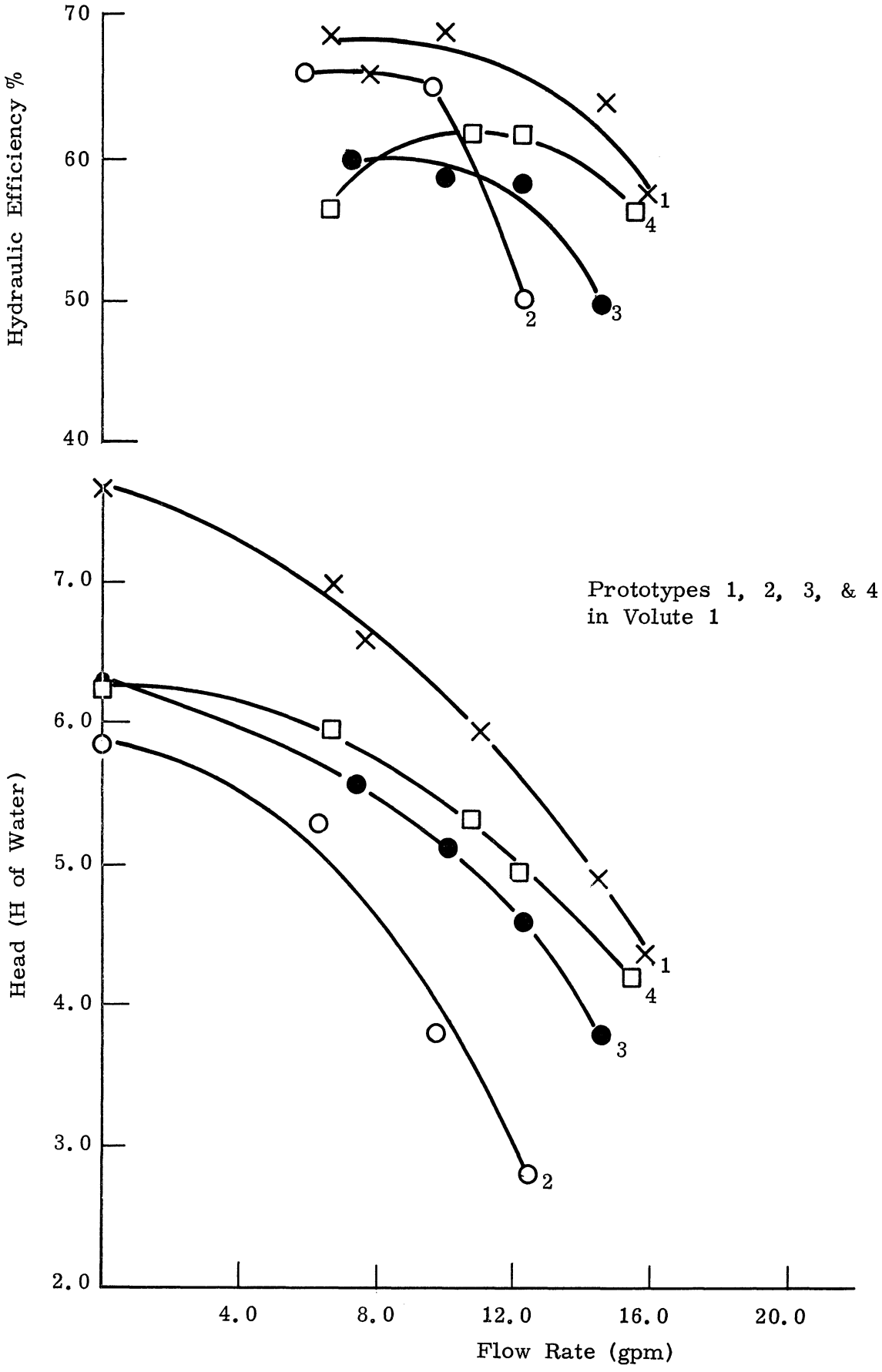

Fig. 21. H & NHY vs. Q at 1350 rpm.

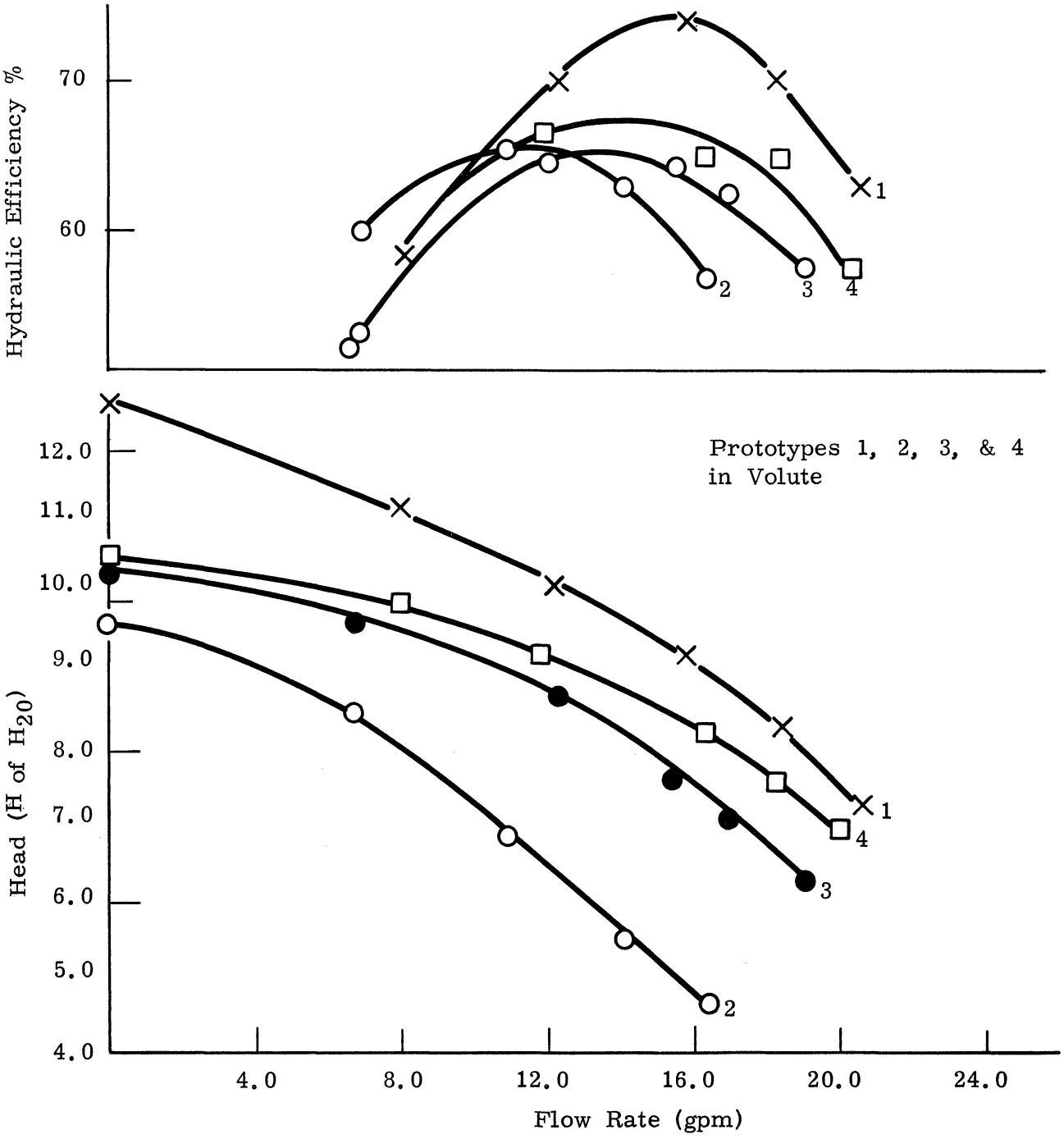

Fig. 22. H & NHY vs. Q at 1760 rpm.

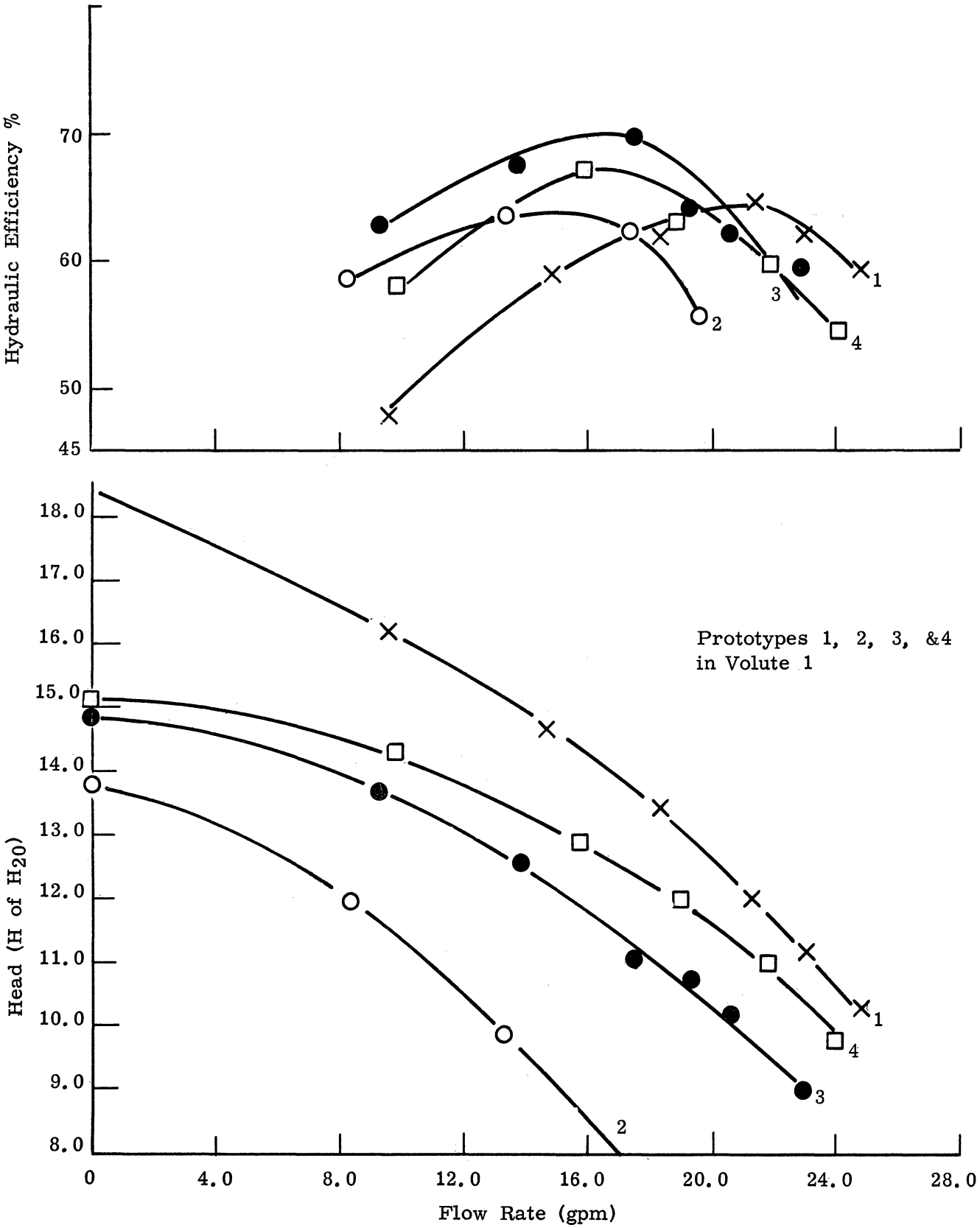

Fig. 23. H & NHY vs. Q at 2100 rpm.

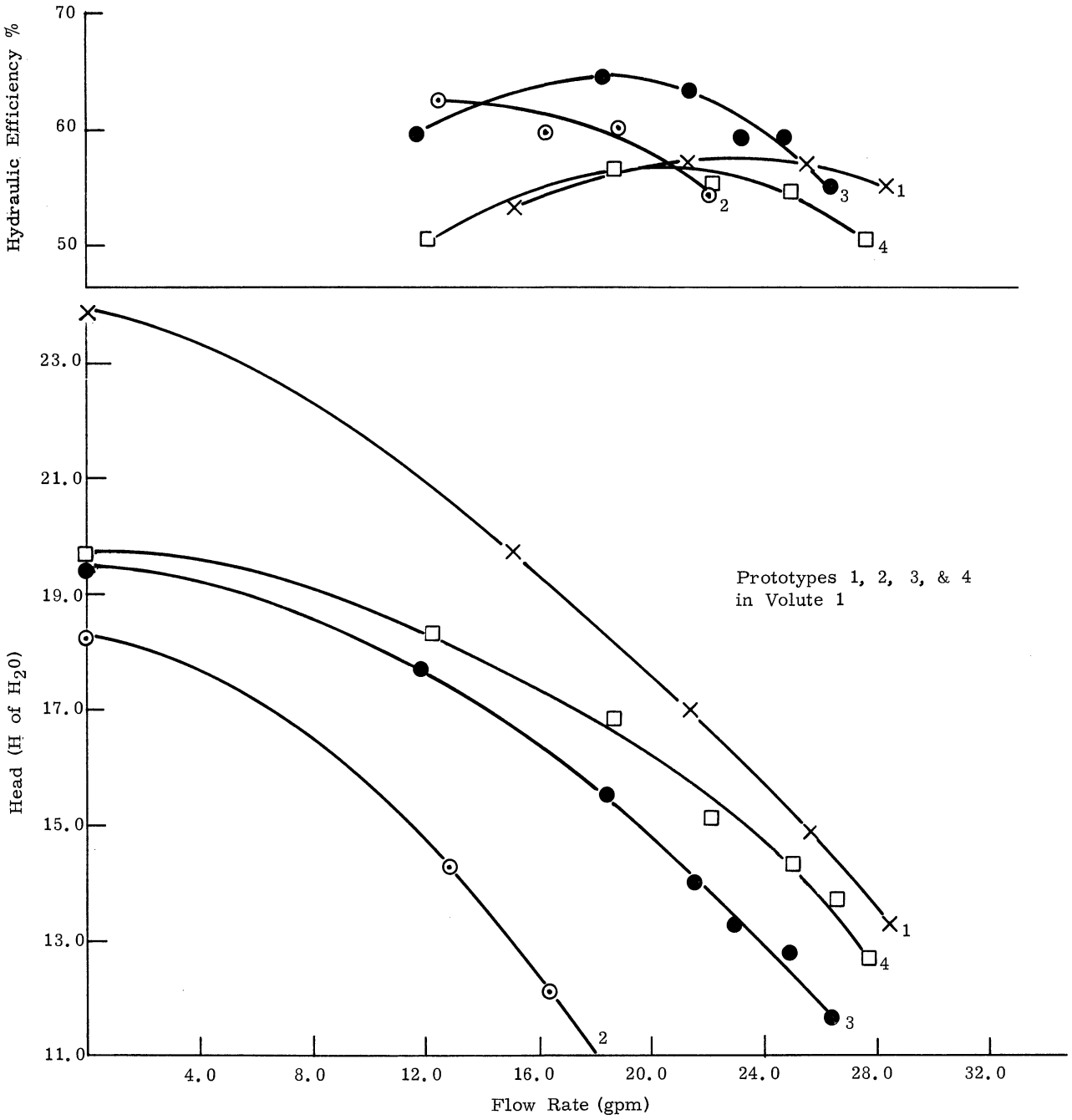

Fig. 24. H & NHY vs. Q at 2400 rpm.

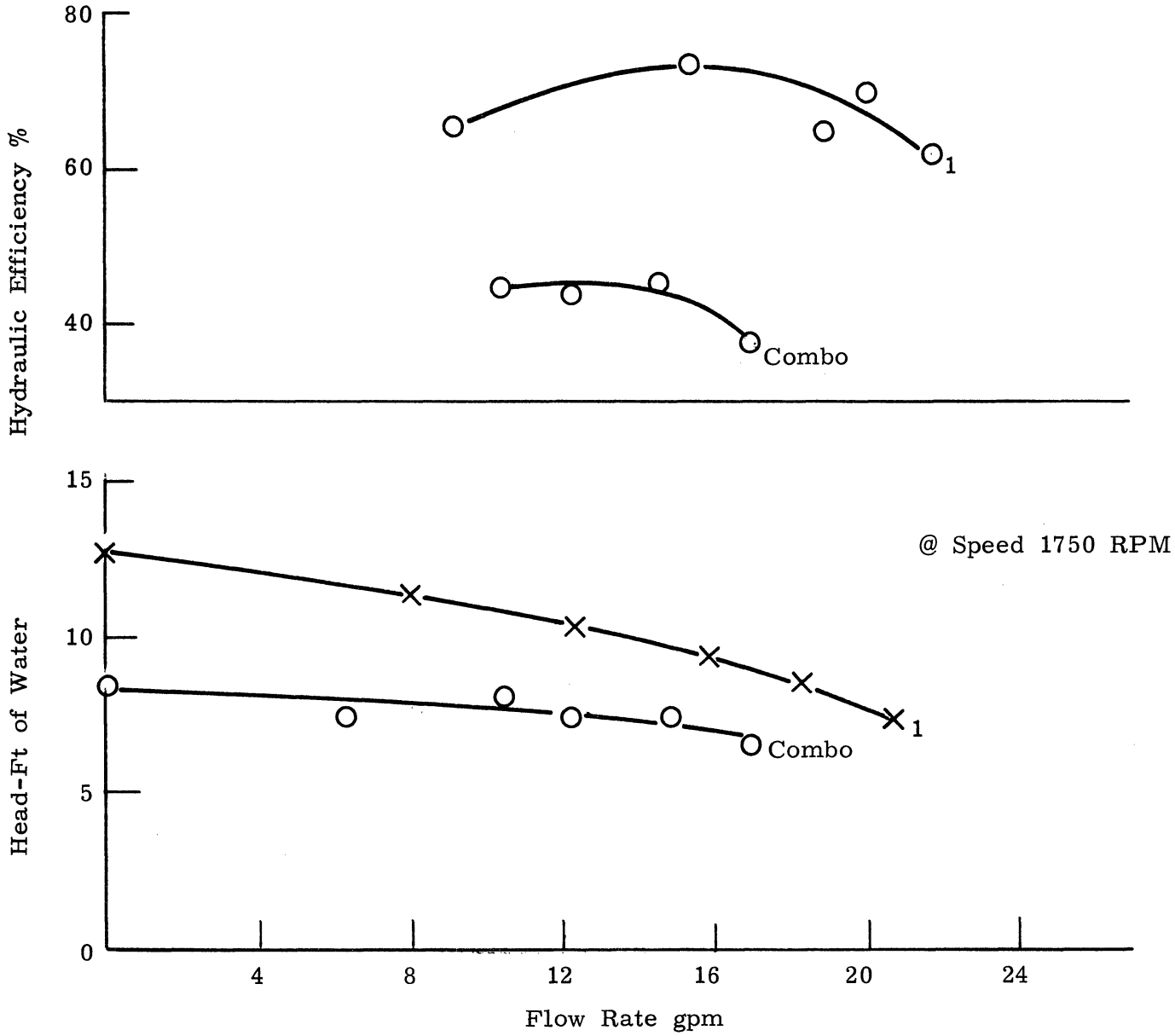

Fig. 25. Comparison of Prototype 1 vs. Whirlpool combo.

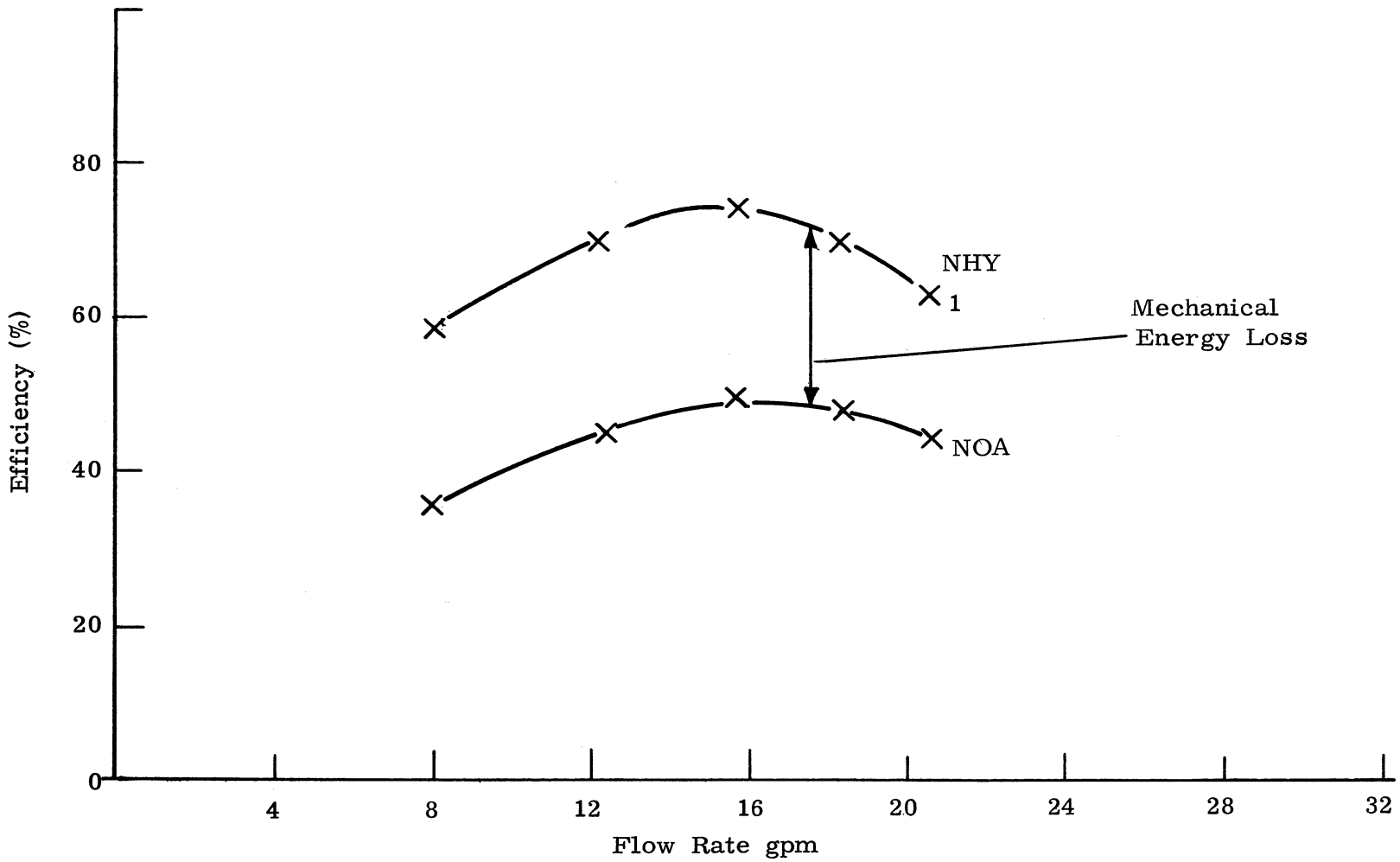

Fig. 26. NHY & NOA vs. Q mechanical energy loss at 1750 rpm.

VII. SUPPLEMENT

A. Centrifugal Pump Design Procedure

1. INTRODUCTION

The following procedure is based on the design and experimental work done on impeller number four. The primary requirement is to ascertain the input data, i.e., parameters A1, A2, T, H, Q, SN, and S for the impeller computer program, and NHY and NJ for the volute computer program. The method for determining these quantities has been and is subsequently reviewed. The purpose of this supplement is to give a quick review of the design procedure.

2. PROCEDURE-IMPELLER

Step 1. Calculate the head (H), flow rate (Q), and shaft speed (NS) required by conventional techniques.

2. Set T equal to 8.0.

3. Calculate PNS from relationship (29-A) and obtain S from Fig. 8.

4. Select A1 from report discussion or from Eqs. (37)-(41).

5. Select A2 to be equal to 15°.

6. Select the number of blades to be between 4 and 8. The guiding principal should be a result of previous discussion and hypothesis.

3. PROCEDURE-VOLUTE

Step 1. Employ the same values o H, Q, and SN as above.

2. Select NHY from Fig. 13 based on the PNS calculation.

3. Set NJ equal to 6.5.

Once this general procedure is completed, the input data can be used in the appropriate computer program.

4. DISCUSSION

a. Impeller

After the computer output has been obtained make a plot of rad vs. beta on polar coordinate paper for two adjacent blade profiles. Then by visual inspection, determine if the resultant flow channel fits the criteria of Hypothesis A. If it does, the impeller design is complete. However, if it violates Hypothesis A, a new value of A2 should be selected between (12°-24°) and the results imputed and rechecked. Once the points are plotted, the blade profile is defined by drawing a smooth curve through these points.

b. Volute

After the computer output has been obtained, make a plot of VORA vs. theta on polar coordinate paper. A smooth curve through these points defines the volute profile.

5. EXAMPLE

Consider selecting a pump which will generate sufficient head to cause water to flow from tank(a) to tank (b).

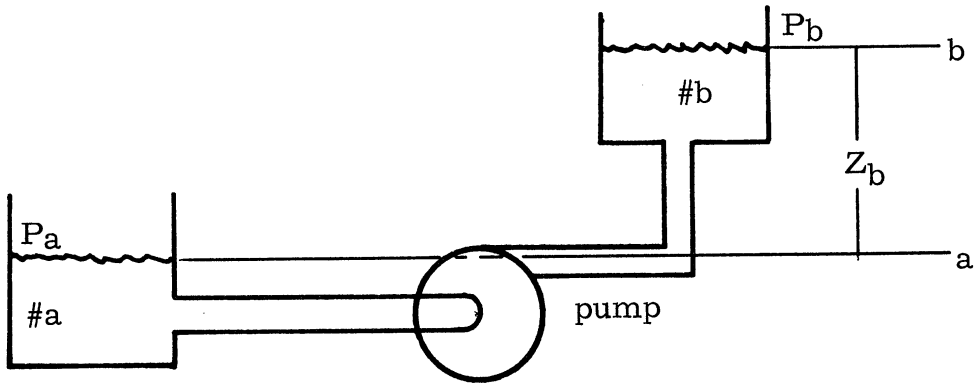

Fig. 27. Hypothetical pumping situation.

Using the simplified energy equation

$$H = \underset{(1)}{Zb - Za} + \underset{(2)}{\frac{Pb-Pa}{S}} + \underset{(3)}{\frac{Vb^2-Va^2}{2}} + \underset{(4)}{\text{losses}} \qquad (69)$$

Assume terms 2 and 3 are approximately zero because for all practical purposes

$$Pa = Pb = Patom. \quad \text{and} \quad Va = Vb = 0$$

Hence

$$H = Zb - Za + \text{losses} . \qquad (70)$$

The losses are composed primarily of pumping loss and pipe friction factor. The losses encountered in the pump can be determined very conservatively by doubling the head calculated by adding Zb-Za and the pipe losses, i.e.,

$$Ha = Zb - Za + \text{losses}_{pipe}$$

$$H = 2 \cdot Ha$$

Although this particular example is quite simple, in any given situation adequate information and data is generally available to ascertain head.

Let us assume H was determined to be 10 ft. The flow rate desired was to pump 10 gallons from (a) to (b) in 1 min, and the motor operates at a constant speed of 1750 rpm.

Consequently:

H = 10.0, Q = 10.0 and NS = 1750 rpm. PNS = 984.0 and from Fig. 28 S was given a value of 1.06. A1 was set at 12°, A2 set at 15°, and the number of blades selected to be six. The volute parameters were determined by selecting NHY = 73.0 (Fig. 13) and NJ equal to 6.5. Using these values for input, the resultant impeller blade profile and volute profiles are shown in Fig. 28.

a. Impeller Program Output (Example)

```
 RAD =      .645887, BETA =     -.000000,    T =     8.000000
 RAD =      .775065, BETA =     1.891223,    T =     8.000000
 RAD =      .904242, BETA =     3.302384,    T =     8.000000
 RAD =     1.033420, BETA =     5.035514,    T =     8.000000
 RAD =     1.162597, BETA =     7.810322,    T =     8.000000
 RAD =     1.291775, BETA =    12.310506,    T =     8.000000
 RAD =     1.420952, BETA =    19.207877,    T =     8.000000
 RAD =     1.550130, BETA =    29.175924,    T =     8.000000
  F9 =      .212557,  F13 =      .875469,    F =    -7.266729,   P =      .731021
  C1 =     9.940521,   B1 =      .049086,   B2 =      .347514,   B3 =     -.755261
  B4 =     -.140541,  F11 =     -.499202,   A1 =    12.000000,   A2 =    15.000000
 PNS =   984.097374
   W =   183.259996,   SN =  1750.000000,   D2 =     3.229437,   R1 =      .645887
  R2 =     1.614719,   U1 =     9.863777,   U2 =    24.659443,   F1 =      .019752
  F2 =     9.668885,   F3 =      .140541,   F4 =     1.400000,   F5 =    12.823998
  F6 =     4.760000,   F7 =    32.177595,   F8 =      .267950
  B5 =      .387532,    Q =    10.000000,    H =    10.000000,    S =     1.060000
  BH =      .258355,   D1 =     1.291775,   NN =     2.500000
```

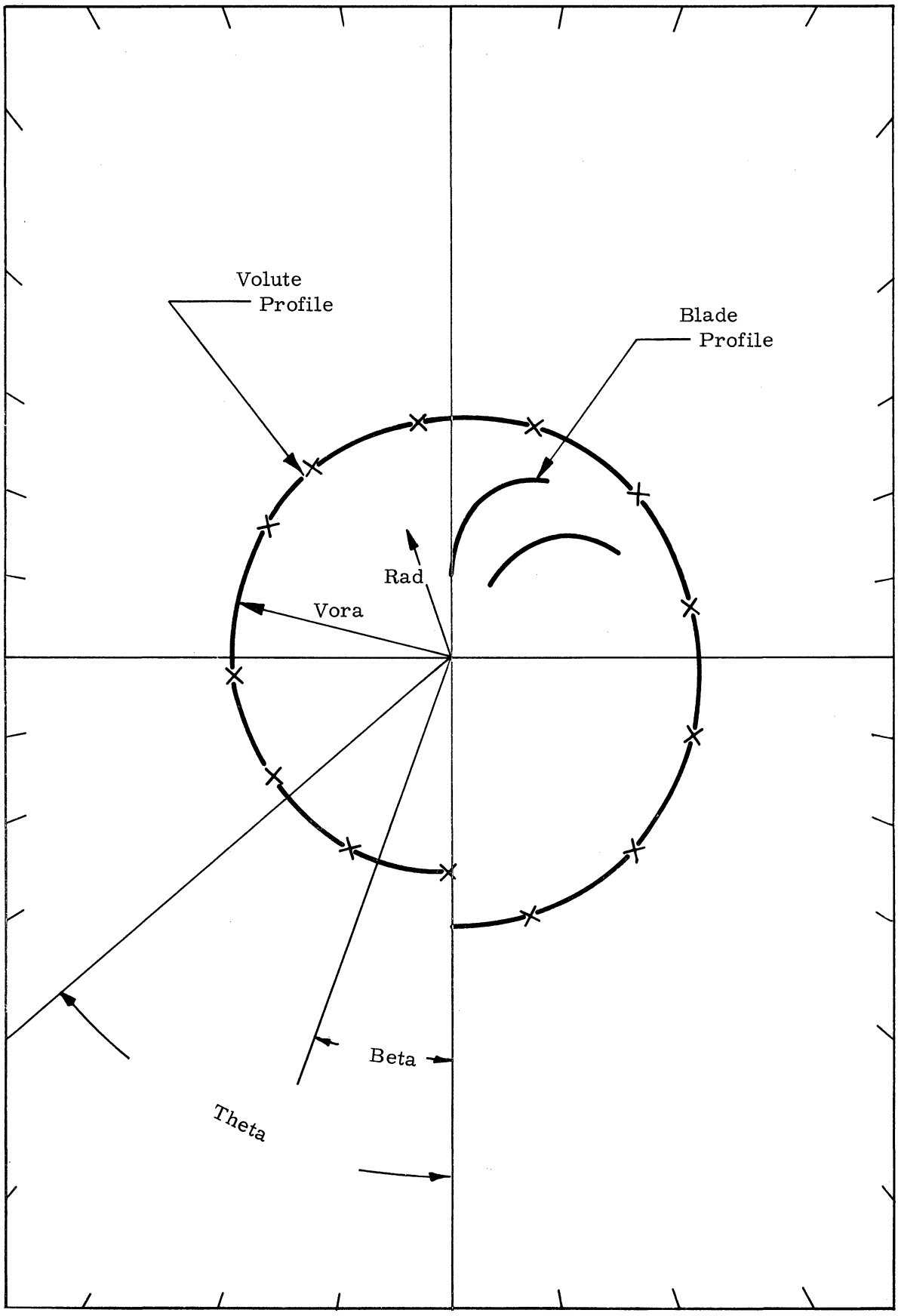

Fig. 28. Example impeller and volute layout.

b. Volute Program Output (Example)

```
VORA =     1.614719,   THETA =      .000000,   FLCO =      .062055
VORA =     1.649614,   THETA =      .500000,   FLCO =      .062055
VORA =     1.685264,   THETA =     1.000000,   FLCO =      .062055
VORA =     1.721685,   THETA =     1.500000,   FLCO =      .062055
VORA =     1.758893,   THETA =     2.000000,   FLCO =      .062055
VORA =     1.796904,   THETA =     2.500000,   FLCO =      .062055
VORA =     1.835737,   THETA =     3.000000,   FLCO =      .062055
VORA =     1.875410,   THETA =     3.500000,   FLCO =      .062055
VORA =     1.915939,   THETA =     4.000000,   FLCO =      .062055
VORA =     1.957345,   THETA =     4.500000,   FLCO =      .062055
VORA =     1.999645,   THETA =     5.000000,   FLCO =      .062055
VORA =     2.042860,   THETA =     5.500000,   FLCO =      .062055
VORA =     2.087008,   THETA =     6.000000,   FLCO =      .062055
VORA =     2.132111,   THETA =     6.500000,   FLCO =      .062055
  D2 =     3.229437,   FLOW =       .022283,   AREA2 =      .014562,   S =      1.060000
FLCO =      .062055,     EX =       .042762,      Y =      .042736,   NHY =      .730000
```

COMPUTER SIMULATION OF VELOCITY EXTRACTION DRYING EQUIPMENT

John Robinson

I. INTRODUCTION

The following is a brief résumé describing a computer program, both its mechanical and theoretical aspects, which is intended to simulate the dry and high velocity extract cycles in a Whirlpool combination washer-dryer.

The program theoretically describes any system composed of six basic component types. These components can be put together in any configuration, and with a minimum of descriptive data as input, the computer will return an approximate time response curve. Different configurations can be programmed and compared. It is hoped that the results of the program will be accurate enough to save the designer time and money.

This report is organized in the following manner.

II. THE REQUIRED INPUT DATA DECK

To describe the system ALL the following parameters and ONLY the following parameters must be specified in the exact manner as described below. To illustrate this, an example data deck will be written describing the system along with the term descriptions.

A. REQUIRED DATA FOR THE SYSTEM IN GENERAL

NUMCOM

The total number of components that comprise the system excluding the drum.

FOR EXAMPLE:
In the example system, there are eight components. Therefore the first card in the data deck should read:

```
NUMCOM = 8,
```

TIME

Actual test time of the configuration in seconds.

FOR EXAMPLE:
If we would like to describe the example system for three seconds of actual running time, the data card should read:

```
TIME = 3.0,
```

Note: Care should be taken in the selection of this parameter because it sets the length of the computer run, and, consequently, its cost.

AREA(1)...AREA(N)

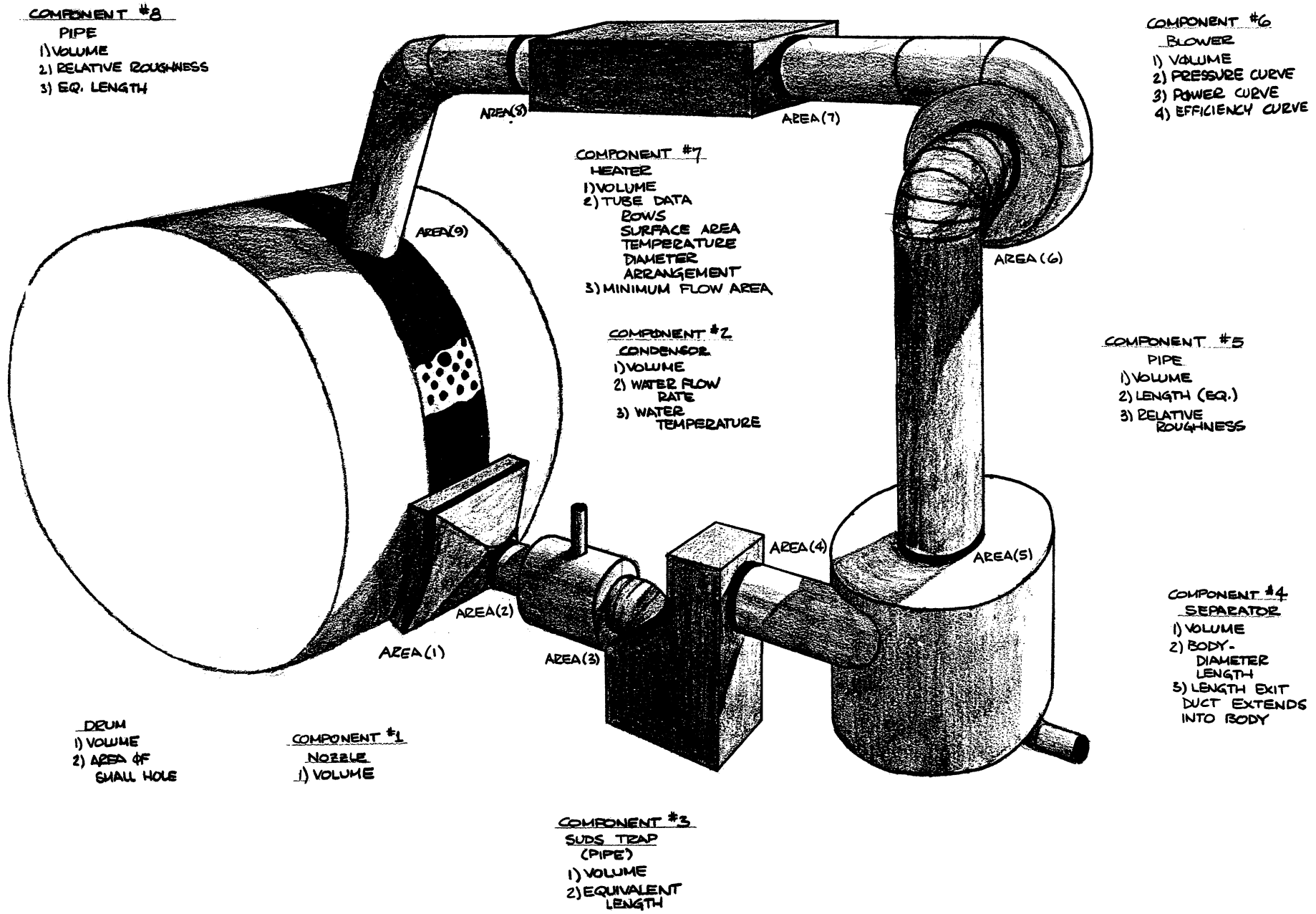

Fig. 1. Example system.

Property array that gives the areas in square feet for all transitional pieces (equal area links between two components).

FOR EXAMPLE:
In Fig. 1, all these areas are indicated by an orange band, and should be given in feet^2. AREA(1) is the first of these areas encountered by the flow, and AREA (9) is the exit area. The data cards should be:

```
AREA (1) = .0650, AREA (2) = 0.0156, AREA (3) = 0.0156,
AREA (4) = .0156, AREA (5) = 0.0180, AREA (6) = 0.0180,
AREA (7) = .0162, AREA (8) = 0.0162, AREA (9) = 0.0162,
```

Note: For accurate results, consecutive transitional areas should not vary unless the component between is a nozzle, separator, or blower. The program will work, but its accuracy will suffer since the other component analyses are based on constant cross-sectional area.

TYPE(1)...TYPE(N)

The array that informs the computer of the order and type of components that comprise the system. There are six different types of components listed below with their corresponding TYPE(N) value.

COMPONENT	TYPE(N)
Heater	1
Frictional elements	2
Separator	3
Condensor	4
Nozzle	5
Blower	6

Fig. 2.

Generally TYPE(N) = K, where the N index refers to the component's location in system, and the K index is taken from the values given in Fig. 2.

FOR EXAMPLE:
The first component is a nozzle, the second a condensor, third a suds trap (a frictional element), fourth a separator, fifth a pipe (frictional element), sixth a blower, seventh a heater, and eighth another pipe. Using T 2, the data cards would be:

```
TYPE(1) = 5,    TYPE(2) = 4,    TYPE(3) = 2,
TYPE(4) = 3,    TYPE(5) = 2,    TYPE(6) = 6,
TYPE(7) = 1,    TYPE(8) = 2,
```

Note: Care should be taken to omit the decimal points.

TBOWL

Initial temperature of the drum. To examine the system at startup, TBOWL should be atmospheric temperature in Degrees Rankin. If an examination of the system during operation is required, TBOWL should be set considerably higher. If this is the case, the first sets of output data will be somewhat inaccurate and should be disregarded.

FOR EXAMPLE:
The system in Fig. 1 is being examined at startup, therefore, the temperature of the drum will be about 70 degrees Fahrenheit or 530 degrees Rankin. The data card should be:

```
TBOWL = 530.0,
```

In addition to the data required for the total system, more specific information about each component must be read into the computer. The required information for the six types of components is listed below.

B. DATA REQUIRED BY THE COMPONENTS

1. Heat Exchangers

The program is written for a heater of the type shown in Fig. 3. This heat exchanger is a simple tube-type exchanger with tubes in staggered

rows perpendicular to the flow. This exchanger, while different in configuration from the Calrod Heaters normally used, is the same basic tube type exchanger. An engineer could take other configurations and transform them into equivalent exchangers of the programmed type. The required input data is:

HTWALL(N)

Surface temperature of the tubes in degrees Rankin. For steam generated heat, HTWALL(N) would be 212 degrees Fahrenheit or 672 degrees Rankin, for a Calrod Heater much more. (N refers to the location of the component in the system.)

HAMIN(N)

The minimum flow area in square feet, obtained by subtracting the projected area of a row of tubes from the total duct area.

HDO(N)

The diameter of the heating tubes in feet.

VOLUME(N)

The volume of the component in cubic feet.

HATUBE(N)

The total surface area of the tubes in square feet.

SL(N) & ST(N)

Configuration parameters in feet describing how the tubes are arranged in the duct (Fig. 5).

HNTUBE(N)

Refers to the number of horizontal rows of tubes (Fig. 3 has four rows).

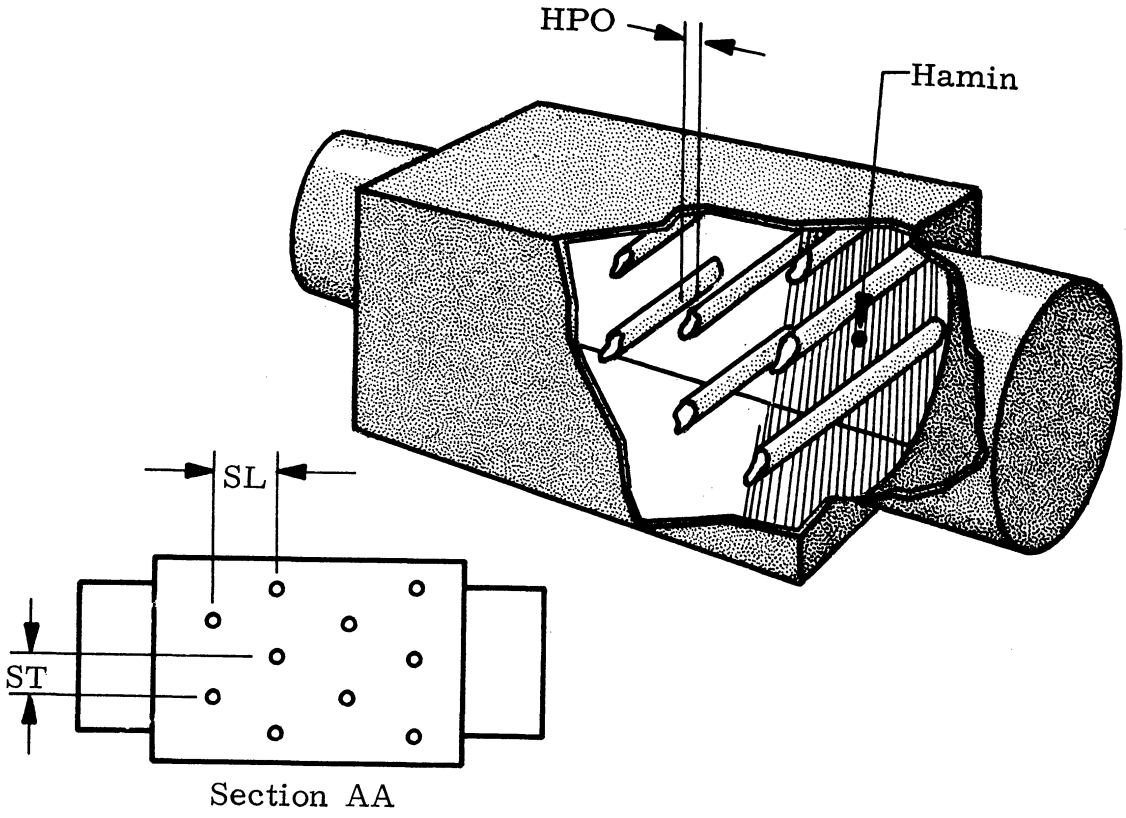

Fig. 3.

FOR EXAMPLE:
In an exchanger with four rows of 1/2 inch diameter tubes, the rows will be staggered with 3-2-3-2 number of tubes per row. Heat will be provided by steam (wall temperature = 212°F). The distance between rows is one and a quarter inches. The distance between tubes in a row is one inch. The heater will be enclosed in a 2" x 3" x 6" LG. duct, and is the seventh component in the system, therefore N = 7.

Since the wall temperature equals 212 degrees Fahrenheit or 672 degrees Rankin,

HTWALL(7) = 672.0

HAMIN(N) is the duct area minus the projected tube area.

PROA = (maximum number of tubes per horizontal row) x Length x Diameter

PROA = (3.0)(3.0)(0.5)/(144.0) = 0.032

HAMIN(7) = AREA - PROA = (3.0)(2.0)/144.0) - .032

HAMIN(7) = 0.0096

HDO(N), the tube diameter is equal to 1/2".

HDO(7) = 0.0417

HATUBE(N) is the total surface area of the tubes and is computed as follows.

$$\text{HATUBE(N)} = \left(\begin{matrix}\text{number of}\\ \text{tubes}\end{matrix}\right)\left(\begin{matrix}\text{tube}\\ \text{diameter}\end{matrix}\right)\left(\begin{matrix}\text{tube}\\ \text{length}\end{matrix}\right)\pi$$

HATUBE(7) = (10.0) (π) (0.5/12.0) (3.0/12.0)

HATUBE(7) = 0.326

In Fig. 3 we see that SL(N) is the distance between rows and ST(N) is the distance between tubes in a row. Therefore,

SL(7) = 0.104 (1.25")

ST(7) = 0.0417 (0.50")

Since there are 4.0 rows,

HNTUBE(7) = 4.0

And the volume of the component is (3) (2) (6)/(12^3) or

VOLUME(7) = 0.0208

The data card deck would then be:

HTWALL(7) = 672.0,	HAMIN(7) = 0.0096,	HDΦ(7) = 0.0417,
HATUBE(7) = 0.326,	SL(7) = 0.104,	ST(7) = 0.0417,
HNTUBE(7) = 4.0,	VOLUME(7) = 0.0208,	

2. Frictional Elements

This includes all types of purely friction loss devices, i.e., those with no heat transfer, work, or cross-sectional area changes. Data required

by the computer for each component of this type is:

RR(N)

This parameter gives the relative surface roughness of the element in question. Some typical roughness figures (e) are listed in Table I. relative roughness can be obtained by dividing by the equivalent diamiter in inches.

Table I

MATERIAL	e
Drawn Tubing	0.00006
Steel	0.002
Rubber tubing	---
Plastic tubing	---

X2(N)

The length of the flow path through the component.

KK(N)

KK(N) is the parameter that allows the user to take into consideration other friction devices such as elbows, tees, etc. Values of KK(N) for these different devices are listed in Table II.

VOLUME(N)

The volume of the component in cubic feet.

Note: In the frictional element the inlet area (AREA (N)) and the outlet area (AREA (N+1)) must be equal for accurate results.

Table II

ITEM	KK(N)
STANDARD TEE	1.80
CLOSE RETURN BEND	2.20
STANDARD ELBOW	0.90
MEDIUM SWEEP	0.75
LONG SWEEP	0.60
45° ELBOW	0.42

FOR EXAMPLE:
Here there are three such friction devices, components 3, 5, and 8.

Component 3- (N = 3)
Component 3 is essentially a close return bend and is made out of plastic. (See Fig. 4 for dimensions.)

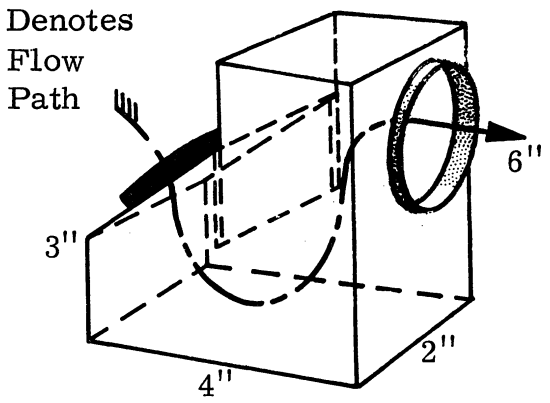

Fig. 4.

The equivalent flow length of this component is about 9". Since it is made out of plastic, its RR(N) value is computed as follows:

e = 0.00006 (From Table I)

AREA = (2)(2) = 4 inch^2

Since AREA = $(\pi)\ (D^2)/(4)$, D = 2.27"

RR(N) = (e)/(D) / 0.0000265

RR(3) = 0.0000265
X2(3) = 0.75 (Flow length = 9")

From Table II, we see that KK(N) for a close return bend equals 2.20,

therefore,

KK(3) = 2.20

The volume of the suds trap in cubic feet is 0.026, and

VOLUME(3) = 0.026

Component 5- (N=5)

Component 5 is just a pipe with a standard 90° elbow. Its input data should be as follows.

X2(5) = 2.0 (pipe length plus flow length through the elbow)

RR(5) = 0.00003 (pipe diameter equals 2", and the pipe material is plastic)

KK(5) = 0.90 (From Table 2)

VOLUME(5) = 0.057

Component 8- (N=8)

Component 8 is the same as component 5 except there is a 45° elbow instead of the 90° elbow.

X2(8) = 1.5

RR(8) = 0.000030

KK(8) = 0.42

VOLUME(8) = 0.038

The sample input data cards for these three components would then be:

```
X2(3) = 0.75,   RR(3) = 0.0000265,   KK(3) = 2.20,
VOLUME(3) = 0.026,
X2(5) = 2.0,    RR(5) = 0.000030,    KK(5) = 0.90,
VOLUME(5) = 0.057,
X2(8) = 1.50,   RR(8) = 0.000030,    KK(8) = 0.42,
VOLUME(8) = 0.038,
```

3. Separators

The program is written for cyclone separators of the type shown in Fig. 5. The required input is as follows. The location of the parameters on the separator can be seen in the figure.

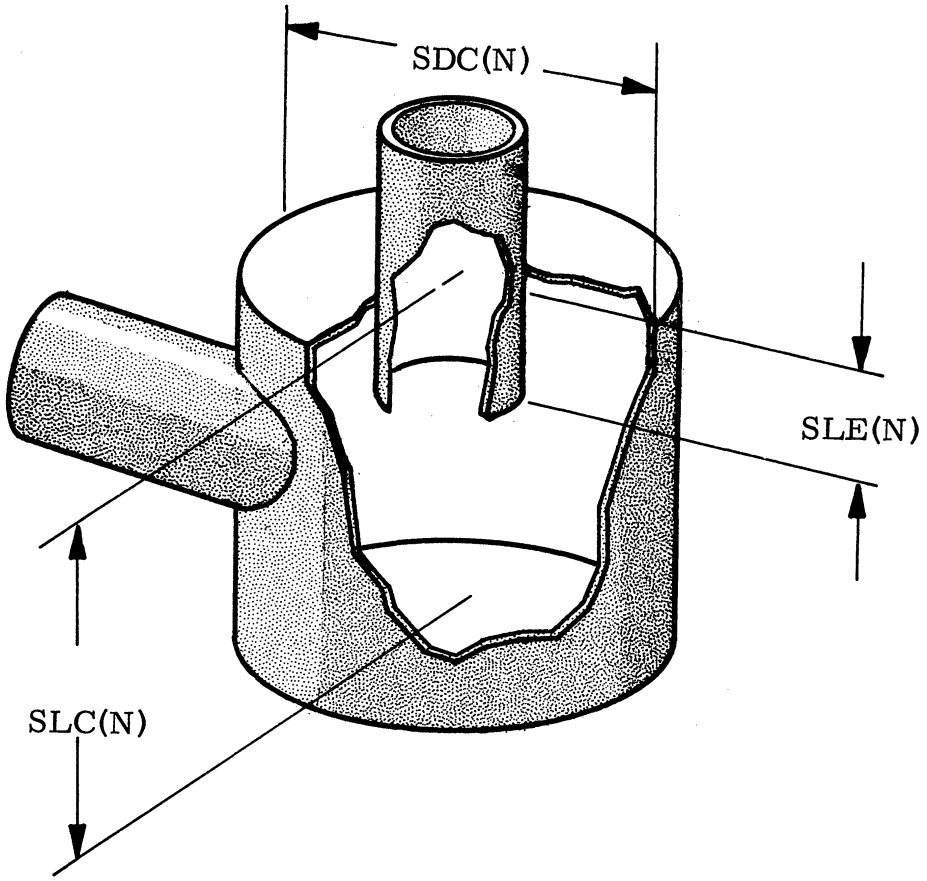

Fig. 5.

SDC(N)

The diameter of the cyclone chamber in feet.

SLC(N)

The length of the chamber in feet.

SLE(N)

Length the exit duct extends into the separator chamber in feet.

VOLUME(N)

The volume of the separator in cubic feet.

SDQ(N)

Amount of heat added to the fluid in the separator in feet-pound/second.

In most cases this term will be zero.

FOR EXAMPLE:
The fourth component is a separator (N=4) that has a chamber diameter of 6", a height of 5", and the exit duct extends 2-1/2" into the chamber. There is no heat added during operation. The above parameter list would become,

SDC(4) = 0.50 (6")

SLC(4) = 0.417 (5")

SLE(4) = 0.203 (2-1/2")

SDQ(4) = 0.0

Since the volume equals $(0.5)^2 (\pi/4.0)(0.416) = 0.082$

VOLUME(4) = 0.082

The data cards will be:

```
SDC(4) = 0.5,     SLC(4) = 0.417,     SLE(4) = 0.208,
SDQ(4) = 0.0,     VOLUME(4) = 0.082,
```

4. Condensers (Spray)

CTW1 (N)

Temperature of the condensing (spray) water, in degrees Rankin.

MCW (N)

Spray water mass rate of flow in pounds per second.

VOLUME (N)

Component volume in cubic feet.

FOR EXAMPLE:
The second component is a condenser, therefore, N = 2. Our condenser happens to be 4" long and 3" in diameter. Water is sprayed into the chamber at a rate of 0.0333 pounds per second and at a temperature of 65 degrees Fahrenheit. The above parameters become,

$$\underline{CTW1(2)} = 460.0 + 65.0 = \underline{525.0}$$

$$\underline{MCW(2)} = \underline{0.0333}$$

$$\underline{VOLUME(2)} = (\pi/4.0)(3.0/12.0)^2(4.0/12.0) = \underline{0.0197}$$

The data cards are:

```
CTW1(2) = 525.0,     MCW(2) = 0.0333,     VOLUME(2) = .0197
```

5. Nozzles

This category is for components with nothing more than a simple area change. The only input data required is the component volume.

VOLUME(N)

The component volume in cubic feet.

FOR EXAMPLE:
A nozzle is the first component. Its volume is 0.025 cubic feet. Knowing that N = 1, the data card becomes:

```
VOLUME(1) = 0.025,
```

6. Blowers

Data for the blower should be in the form of three characteristic curves — 1) pressure head vs. flow rate, 2) power vs. flow rate, and 3) efficiency vs. flow rate. Because the computer can not read equations, this information must be stored in array form. Values for the above parameters must be given for every five CFM of flow rate. It

should be noted that the program is equipped to handle only one blower per system. The required data are:

PCNT

Maximum flow rate (ft^3/min) divided by five and rounded off to the nearest integer.

BP(0) ... BP(PCNT)

Pressure (head) array (inches of water).

POWER(0) ... POWER(PCNT)

Power array (watts).

EFF(0) ... EFF (PCNT)

Efficiency array.

VOLUME (N)

Volume of blower in ft^3.

FOR EXAMPLE:
Suppose the blower has the characteristic curves shown below. PCNT is first determined by taking the maximum flow rate (20 CFM), dividing by five and rounding off.

PCNT = 20/5 = 4

Values for the three arrays are then read from the curves at 5 CFM intervals:

BP(0) = 60.0,	EFF(0) = 0.0,	POWER(0) = 600.0,
BP(1) = 46.0,	EFF(1) =12.0,	POWER(1) = 800.0,
BP(2) = 32.0,	EFF(2) =20.0,	POWER(2) =1000.0,
BP(3) = 18.0,	EFF(3) =23.0,	POWER(3) =1150.0,
BA(4) = 0.0,	EFF(4) =21.0	POWER(4) =1200.0,

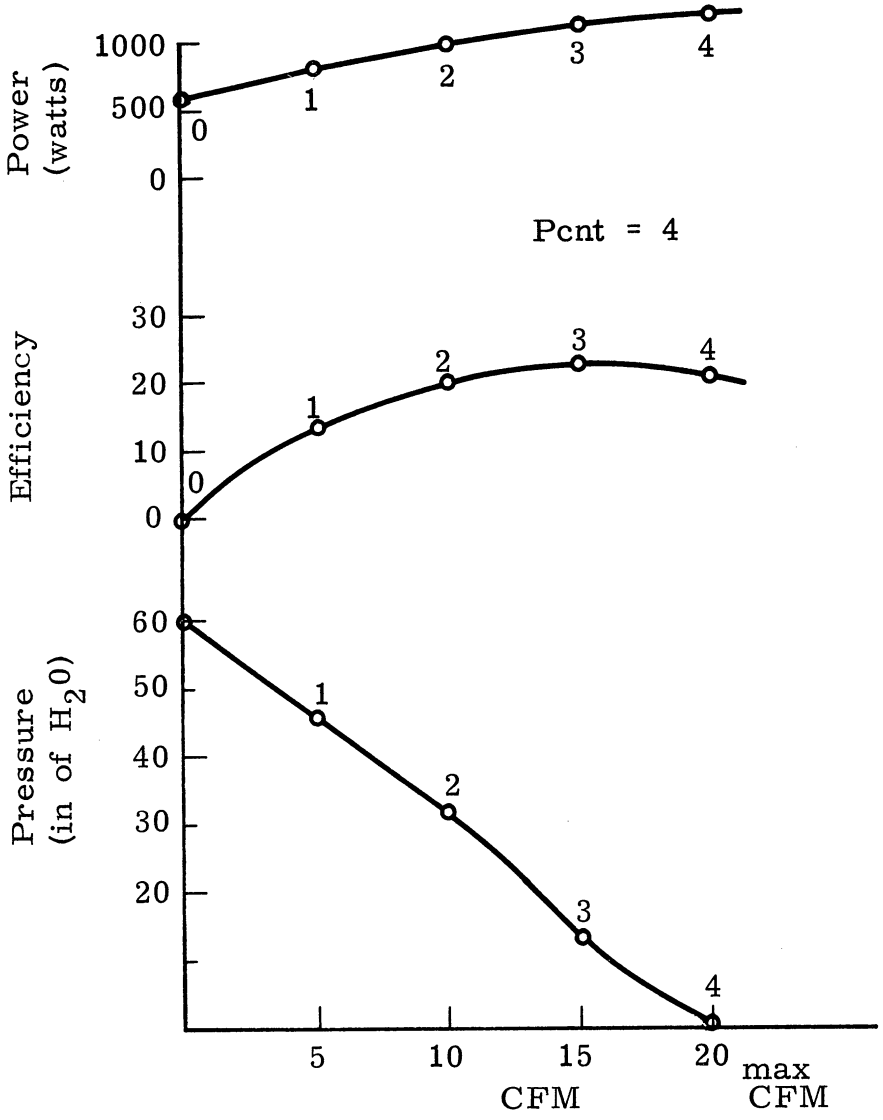

Characteristic Curves

The volume of the blower is calculated

VOLUME(6) = .025 ft^3

The data cards are then:

```
PCNT = 4,      VOLUME(6) = .025,
BP(0) = 60.0,     BP(1) = 46.0,     BP(2) = 32.0,
BP(3) = 18.0,     BP(4) = 0.0,      EFF(1) = 12.0,
EFF(2) = 20.0,    EFF(3) = 23.0,    EFF(4) = 21.0
POWER(0) = 600.0,     POWER(1) = 800.0,     POWER(2) = 1000.0,
POWER(3) = 1150.0,    POWER(4) = 1200.0,    EFF(0) = 0.0,
```

III. HOW TO INTERPRET THE OUTPUT

Below is an example system and its computer output at a certain instant of time.

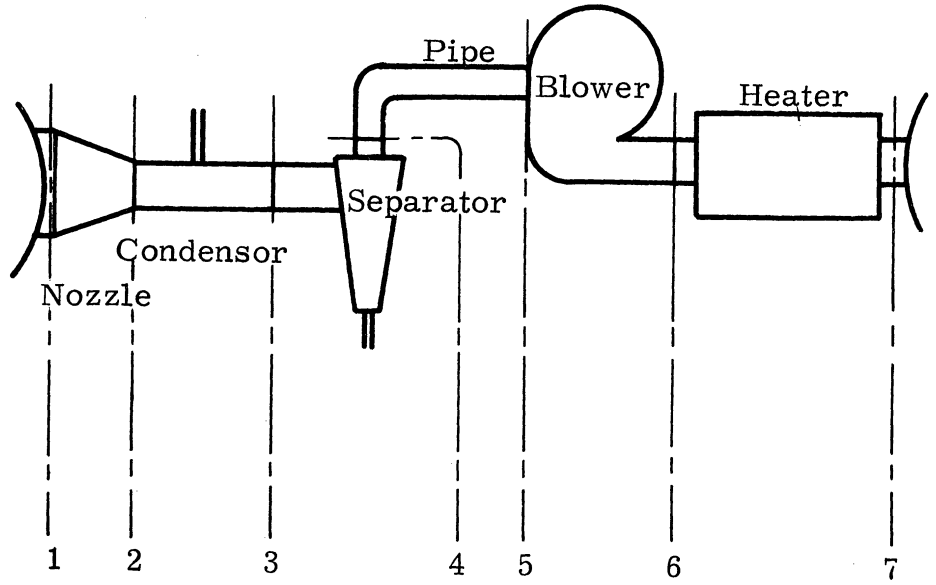

Example System

FLOW PROPERTIES AT TIME(SECONDS) = .000

PRESSURE	2129.141	2113.147	2121.739	2020.309	2019.271	2144.071	2142.398
TEMPERATURE	529.965	528.827	527.459	527.337	527.336	517.388	519.631
VELOCITY	20.743	119.989	119.833	125.909	125.973	80.441	79.294
DENSITY	.074	.074	.074	.071	.070	.076	.076
MASS FLOW	.075	.075	.075	.075	.075	.075	.075
MACH NUMBER	.018	.105	.105	.111	.111	.071	.070
STAG PRESSURE	2129.634	2129.634	2138.293	2037.719	2036.691	2151.745	2149.816
STAG TEMP	530.000	530.000	528.629	528.629	528.629	517.915	520.144
SONIC VELOCIT	1138.893	1137.670	1136.197	1136.066	1136.065	1125.298	1127.735

VELOCITY AT INLET PLATE = 81.612
BOWL TEMPERATURE = 530.000
MASS REMOVED DURING TIME INTERVAL = .000
TOTAL MASS REMOVED = .000

EXAMPLE OUTPUT

The output should be interpreted as follows:

1. Flow Properties at Time (seconds = .000.—These are the properties at t = 0 or t = 2.3 secs., etc. When t = 0, the properties returned are the

steady-state solution; at all other times they are the transient approximation.

2. Property Array.—The properties are returned in array form. The respective properties are listed vertically and their location in the system horizontally. For example, if we wanted to find the pressure between the blower and the pipe at T = 0, we would first pinpoint the location in the system—location 5. We would then go to the pressure row of the flow properties and count 5 spaces over. The desired pressure would be 2019.271 pounds per square foot.

The remaining terms are self-explanatory: the velocity at the inlet plate is the speed of the air travelling through one of the perforated plate holes; the bowl temperature is the drum temperature; the mass removed during the time interval is the mass removed during DELT; and the total mass removed is the sum of these masses from t = 0 to the time indicated.

Units on the properties are:

time	- seconds
temperature	- degrees Rankin
pressure	- pounds per square foot
velocity	- feet per second
density	- pounds per cubic foot
mass flow	- pounds per second
mach number	- dimensionless
stagnation pressure	- pound per square foot
stagnation temperature	- degrees Rankin
sonic velocity	- feet per second

velocity at inlet plate - feet per second

bowl temperature - degrees Rankin

masses - pounds

IV. STEADY STATE ANALYSIS

There are basically six different types of components in the average dryer. They are:

1. PIPES—this includes all of the piping of the dryer in addition to all components that are purely friction loss type components (components with little or no change in cross-sectional area, negligible heat and mass transfer, and zero work input).
2. NOZZLES—pure cross-sectional area change components.
3. HEATERS—heat input devices.
4. CONDENSERS—spray condensers.
5. SEPARATORS—cyclone separators.
6. BLOWERS

Analytical work for the condenser and separator had been done previously and a detailed steady-state analysis for these components can be found in the project reports of Vern Wedeven and Douglass Lane. The detailed analysis for the rest of the components and complementary fluid analysis for the other two is given below. In all cases, it will be assumed that the fluid flow is a continuous one-dimensional flow, obeys the perfect gas law, and has constant specific heats.

A. PIPES

In order to solve the equations resulting from a pure friction analysis the following assumptions must be made:

a. adiabatic flow (no heat transfer)

b. constant mass rate of flow

c. constant cross-sectional area

The equations of motion then become,

Continuity

$$\frac{d\rho}{\rho} + \frac{dv}{v} = 0 \tag{1}$$

First law of thermodynamics

$$C_p\, dT + d\frac{V^2}{2} = 0 \tag{2}$$

Conservation of momentum

$$-dp = \frac{f\rho V^2}{2D}\, dz + \rho V dV \tag{3}$$

Equation of state

$$\frac{dp}{p} = \frac{d\rho}{\rho} + \frac{dT}{} \tag{4}$$

Solving these equations simultaneously we get

$$\int_{M_1}^{M_2} \frac{1 - M^2}{1 + \frac{k-1}{2} M^2} \cdot \frac{dM}{M^3} = \int_0^L \frac{k\lambda}{2D}\, dx \tag{5}$$

Where

M = Mach Number
k = Ratio of specific heats
D = Diameter of pipe
L = Length of pipe
λ = Friction factor (see below)

The friction factor is determined by the following relations

$$KA = 390/\left(R_{ey}\sqrt{0.0032 + \frac{0.021}{R_{ey}^{.237}}}\right) \tag{6}$$

Where

KA = An arbitrary index of flow
Rey = Reynolds Number

Whenever the relative roughness of the pipe wall is greater than KA

$$\lambda = 1.0/(2.0 \log_{10} RR + 1.74)^2 \tag{7}$$

Otherwise

$$\lambda = 0.0032 + \frac{0.221}{R_{ey}^{0.237}} \tag{8}$$

By integrating P-5 using the CRC Handbook tables, we get the following equation that can easily be solved on the computer for the value of the downstream Mach Number.

$$\frac{k\lambda L}{2D} = \left[-\frac{1}{2M^2} - \left(\frac{k+1}{2}\right) \log_e \left(\frac{M^2}{1 + \frac{k-1}{2} M^2}\right)\right]_{M_1}^{M_2} \tag{9}$$

Pressure drop, however, is not caused by wall friction alone. Other factors such as obstructions, bends in the pipe, and changes in height are also important. Because these factors are usually determined empirically, they will be taken into account in the following manner. Since

$$\Delta p \approx \frac{2\lambda}{2D}\frac{U^2}{2g} = KK \frac{U^2}{2g}$$

we see that KK is equivalent to $\lambda L/2D$ where KK is an empirically determined constant for various types of obstructions (see Table 1). We then can alter equation P-7 and it becomes

$$\frac{k}{2}\left(\frac{\lambda L}{D} + 2KK\right) = \left[- \frac{1}{2M^2} - \left(\frac{k+1}{2}\right)\log_e\left(\frac{M^2}{1 + \frac{k-1}{2}M^2}\right)\right]\Bigg|_{M_1}^{M_2} \qquad (10)$$

Or finally

$$\frac{k}{2}\left(\frac{\lambda L}{D} + 2KK\right) = \left[- \frac{1}{2M_2^2} - \left(\frac{k+1}{2}\right)\log_e\left(\frac{M_2^2}{1 + \frac{k-1}{2}M_2^2}\right)\right] - \qquad (11)$$

$$\left[- \frac{1}{2M_1^2} \left(\frac{k+1}{2}\right)\log_e \left(\frac{M_1^2}{1 + \frac{k-1}{2}M_1^2}\right)\right]$$

Then knowing the downstream Mach Number (M_2), the downstream mass rate of flow ($\dot{m}_2$), and the stagnation temperature (TO_2), we can calculate the downstream pressure (P_2) using the following relation

$$P_2 = \frac{\dot{m}}{M_2}\left(\frac{RTO_2}{k\left(1 + \frac{k-1}{2}M_2^2\right)}\right)^{1/2} \qquad (12)$$

Where

R = The perfect gas constant
k = The specific heat ratio

The other properties can be calculated as follows

$$T_2 = {TO_2}/{\left(1 + \frac{k-1}{2}M_2^2\right)} \qquad (13)$$

$$\rho_2 = {P_2}/{RT_2} \qquad (14)$$

$$C_2 = \sqrt{k8RT_2} \qquad (15)$$

$$PO_2 = P_2 \left(1 + \frac{k - 1}{2} M_2^2\right)^{k/k - 1} \tag{16}$$

$$V_2 = C_2 M_2 \tag{17}$$

Flow diagram and program listing for this steady-state analysis can be found in the appendix. Its relation to the total program can also be seen in the flow diagram (Appendix).

B. HEATERS

In Principles of Heat Transfer by Frank Kreith, the following empirical equations were developed for a heat exchanger with air flow over small diameter tubes. The equation for the heat transfer coefficient ($\bar{h}_c$) was given as follows,

$$\bar{h}_c = \frac{kf}{D_o} (0.033) C_H \left(\frac{G_{max} D_o}{M_f}\right)^{0.6} P_{r_f}^{0.3} \tag{18}$$

Where

C_H = an empirical coefficient (equal to 1.0 if the number of tube rows is greater than 10.0, slightly less if less)
G_{max} = mass velocity at the minimum area
D_o = tube diameter
K_f = thermal conductivity of the film near the wall (subscript f denotes film)
u_f = fluid viscosity of the film
Pr_f = Prandtl Number of the film (equal to 0.72 for all cases we will be considering)
$\bar{h}_c$ = heat transfer coefficient

Then

$$Q = \bar{h}_c A (T_f - T_w) \tag{19}$$

Where

Q = heat transfered to the fluid
A = tube surface area
T_f = film temperature (an average of the wall and fluid temperature)
T_w = tube wall temperature

Since from thermodynamics

$$dT/T = d\Phi + \frac{dU}{c_p T} + dW \qquad (20)$$

Therefore, equating heat input to enthalpy change

$$T2 = T1 + \Phi/c_p \dot{m} \qquad (21)$$

Where

c_p = constant pressure specific heat of air
T = temperature of fluid
$\dot{m}$ = mass rate of flow through the exchanger

An empirical relation was also developed for the pressure drop resulting from flow over the tubes. This equation is

$$\Delta p = \frac{f' G_{max}^2 N}{\rho(2.08 \times 10^9)} \times \left(\frac{M_S}{M_B}\right)^{0.14} \qquad (22)$$

Where

dp = the frictional pressure drop
N = number of tubes
ρ = fluid density (taken as the inlet density in computer calculations
u_s = fluid viscosity of the stream
u_b = fluid viscosity of the fluid at the wall
f' = given below,

$$f' = \left[0.44 + \frac{0.08\, S_L/D_O}{\left(\frac{S_T - 1}{D_O}\right)^{0.43 + 1.13\, D_O/S_L}}\right]\left(\frac{G_{max} D_O}{\mu B}\right)^{-0.15} \qquad (23)$$

where

S_L and S_T are the distances shown in Fig. 3.

With these calculated values and knowing the mass rate of flow is constant, one

can calculate the other downstream properties in the following manner. Assuming 1) the heat transfer phenomena is confined to an area within the component and the ends are essentially isentropic, 2) there is no change in cross-sectional area, and 3) the mass rate of flow is constant, the following equation can be used to determine the downstream Mach Number(M_2)

$$M_2 \sqrt{\frac{1 + \frac{k-1}{2} M_2^2}{1 + kM_2^2}} = M \sqrt{\frac{1 + \frac{k-1}{2} M_1^2}{1 + kM_1^2}} \quad \frac{TO_2}{TO_1} \tag{24}$$

This can be solved by an iterative type solution on the computer. When M_2 is determined P_2 can be solved for using

$$P_2/P_1 = 1 + kM_1^2/1 + kM_2^2 \tag{25}$$

But this does not take into account the frictional pressure loss due to flow over the tubes, so this must be subtracted from P_2 and then the other downstream properties (C_2, V_2, PO_2, and TO_2) can be easily calculated with the relations below,

$$\rho_2 = \sqrt{kgRT_2} \tag{26}$$

$$V_2 = M_2 C_2 \tag{27}$$

$$\rho_2 = P_2/RT_2 \tag{28}$$

$$Po_2 = P_2\left(1 + \frac{k-1}{2} M_2^2\right)^{k/k-1} \tag{29}$$

C. NOZZLES

For flow through a nozzle, the following assumptions will be made,

a. No heat transfer

b. Frictionless flow

The equations of motion then become,

CONTINUITY

$$\frac{A_2}{A_1} \quad \frac{P_1 V_1}{P_2 V_2} \tag{30}$$

Plugging in the following,

$$V = MC \tag{31}$$

$$C = \sqrt{kRTg} \tag{32}$$

Isentropic relations,

$$\frac{P_2}{P_1} = \left(\frac{1 + \frac{k-1}{2} M_1^2}{1 + \frac{k-1}{2} M_2^2} \right)^{k/k-1} \tag{33}$$

$$\frac{T_2}{T_1} = \left(\frac{1 + \frac{k-1}{2} M_1^2}{1 + \frac{k-1}{2} M_2^2} \right) \tag{34}$$

$$\frac{\rho_2}{\rho_1} = \left(\frac{1 + \frac{k-1}{2} M_1^2}{1 + \frac{k-1}{2} M_2^2} \right)^{1/k-1} \tag{35}$$

We can derive the following equation and solve for the downstream Mach Number

$$\frac{A_2}{A_1} = \frac{M_1}{M_2} \left(\frac{1 + \frac{k-1}{2} M_1^2}{1 + \frac{k-1}{2} M_2^2} \right)^{\frac{k+1}{2(k-1)}} \tag{36}$$

Knowing M_2 and using the above equations, we can calculate P_2, T_2, and ρ_2. From these V_2, C_2, $\dot{m}_2$, TO_2, PO_2 can be found.

$$C_2 = \sqrt{kRg\ T_2} \tag{37}$$

$$V_2 = M_2 C_2 \tag{38}$$

$$\dot{m}_2 = \dot{m}_1 \tag{39}$$

$$TO_2 = T_2\left(1 + \frac{k-1}{2} M_2^2\right) \tag{40}$$

$$PO_2 = P_2\left(1 + \frac{k-1}{2} M_2^2\right)^{k/k-1} \tag{41}$$

where,

A = area
ρ = density
V = velocity
M = Mach Number
c = acoustic velocity
P = pressure
$\dot{m}$ = mass rate of flow
TO = stagnation temperature
PO = stagnation pressure
R = gas constant
g = gravitational constant
k = specific heat ratio

The subscripts 1 and 2 refer to conditions at the inlet and exit of the component, respectively.

D. CONDENSERS

This program was written for direct contact or spray condensers. The initial analytical work was done by Vern Wedeven in 1966. He developed a program in which the downstream temperature provided that the inlet temperature, air mass rate of flow, and water flow rate (spray) were known. The other

downstream properties can then be calculated. Assuming (1) the condensing phenomena is confined to an area within the component (the ends are therefore isentropic) (2) there is no change in cross-sectional area (3) the mass rate of flow is constant, the following equation can be used to calculate the downstream Mach Number.

$$\frac{M_2}{1 + kM_2^2} = \frac{M_1}{1 + kM_1^2} \sqrt{\frac{T_2}{T_1}} \tag{42}$$

Where,

M = Mach Number
T = temperature
(subscripts 1 and 2 refer to inlet and exit conditions, respectively)

This equation can be solved by the computer using an iterative solution technique. The downstream mass rate of flow can then be found knowing the inlet and exit temperatures and equation C-2. (The derivation of this equation can be found in the Constant and Mass Rate of Flow Corrections section of this report.)

$$\mathring{m}_2 = \mathring{m}_1 \left(\frac{1 + W_2}{1 + W_1} \right) \tag{43}$$

Where,

$\mathring{m}$ = mass rate of flow
W = vapor to air ratio (mass)

Note: W is a function of the temperature alone. For the actual determination of values for W, see Vern Wedeven's report, 07494-2-P.

Using the following sequence of equations, the rest of the downstream properties can be calculated.

$$TO_2 = T_2 \left(1 + \frac{k - 1}{2} M_2^2 \right) \tag{44}$$

$$C_2 = \sqrt{kgRT_2} \tag{45}$$

$$V_2 = M_2 C_2 \tag{46}$$

$$\rho = \frac{\dot{m}_2}{A_2 V_2} \tag{47}$$

$$P_2 = \rho_2 R T_2 \tag{48}$$

$$PO_2 = P_2 \left(1 + \frac{k - 1}{2} M_2^2\right)^{k/k - 1} \tag{49}$$

where,

A = area
ρ = density
V = velocity
M = Mach Number
c = acoustic velocity
P = pressure
m = mass rate of flow
TO = stagnation temperature
PO = stagnation pressure
R = gas constant
g = gravitational constant
k = specific heat ratio

E. SEPARATORS

Initial steady-state analytical work was done by Douglas Lane for a cyclone separator. He developed a program that would return a downstream pressure figure when the diameter, height, and exit duct length were provided. (For details see his report, 07494-2-P.)

Since there is no heat transfer, the stagnation temperature is constant across the separator. The mass rate of flow is also constant because our control volume is only the gaseous part of the fluid mixture and this does not change appreciably. Knowing the downstream pressure, stagnation temperature,

and mass rate of flow, we can calculate M using the internal function CALMAC.

The other necessary properties can be calculated using the following two equations.

$$T_2 = \frac{TO_2}{1 + \frac{k - 1}{2} M_2^2} \tag{50}$$

$$PO_2 = P_2 \left(1 + \frac{k - 1}{2} M_2^2\right)^{k/k - 1} \tag{51}$$

Where,

T = temperature
TO = stagnation temperature
M = Mach Number
PO = stagnation pressure
P = pressure
k = specific heat ratio

F. BLOWERS

The steady-state analysis of the blower is based on the characteristic curves of the blower itself. These curves—pressure head, efficiency, and power versus volumetric flow rate—are used in the following manner.

Initially an inlet flow rate is determined. Using this valve and the blower curves, pressure head, efficiency and power input are determined. The second law of thermodynamics is then reduced to the following form assuming (1) no heat transfer, (2) no height change, and (3) constant mass rate of flow.

$$0 = \frac{V_2^2 - V_1^2}{2g} + \frac{Cp}{k} (T_2 - T_1) + \frac{\dot{w}}{\dot{m}}$$

$$0 = \frac{VdV}{g_c} + \frac{Cp}{k} (T_2 - T_1) + \frac{\dot{w}}{\dot{m}} \tag{52}$$

where

V = velocity
T = temperature
C_p = constant pressure specific heat
k = specific heat ratio
$\dot{w}$ = power
$\dot{m}$ = mass rate of flow
V = velocity

Since (1) $VdV = \frac{P_2 - P_1}{\rho}$ and $P_2 - P_1$ equals the head developed by the blower and (2) $\dot{w}$ = Power time Efficiency, we can, assuming a constant valve for the density and using an iterative solution, determine a valve for T_2.

Then knowing ρ_2, P_2, T_2, m_2 the other downstream properties are calculated using the following series of equations,

$$V = \frac{m_2}{\rho_2 A_2} \tag{53}$$

$$C_2 = kgRT_2 \tag{54}$$

$$M_2 = \frac{V_2}{C_2} \tag{55}$$

$$TO_2 = T_2\left(1 + \frac{k - 1}{2} M_2^2\right) \tag{56}$$

$$PO_2 = P_2\left(1 + \frac{k - 1}{2} M_2^2\right)^{k/k - 1} \tag{57}$$

V. THE TIME RESPONSE APPROXIMATION

In order to examine a proposed system properly, a method for determining a transient solution had to be developed. The nature of the differential equations made a conventional solution impossible for the wide variety of cases encountered in a dry cycle. Programming the solution also imposed limitations. The method that was finally decided upon is listed below.

STEP 1. Determine the average values of the inlet and outlet stagnation temperatures and pressures at Time 1.

STEP 2. Compute a value for the density using these two parameters and the Perfect Gas Law.

STEP 3. Using this density and the volume of the component, determine the mass of the gas in the component at Time 1.

STEP 4. Assuming the inlet and outlet mass rates of flow are constant over a predetermined time interval, calculate the change in component mass.

STEP 5. Using this value for the mass, obtain a new density figure by dividing by the volume.

STEP 6. Using a steady-state analysis with the inlet conditions those of the inlet properties at Time 1, determine values for DPO, DTO, DMDOT. These parameters are measures of the frictional losses and energy and mass rate of flow changes caused by the component. The value of the outlet stagnation temperature at Time 2 can then be found by adding DTO to the average stagnation temperature at Time 1.

STEP 8. Because we know the average value of the stagnation pressure at Time 1, and can calculate the average value of the stagnation pressure at Time 2 without the use of any flow information (stagnation properties are properties of the fluid at aero velicity), we can calculate these two values for the next component in the same manner. Since we know that the flow rate is directly proportional to the square root of the pressure drop, we can calculate a new value for the mass rate of flow at Time 2 using the following equation.

$$\frac{MDOT_1}{(POA1_1 - POA2_1)^{1/2}} = \frac{MDOT_2}{(POA2_2 - POA2_2)^{1/2}}$$

Where

$MDOT_1$ = Mass rate of flow at Time 1
$MDOT_2$ = Mass rate of flow at Time 2
$POA1_1$ = Average value of the stagnation pressure at Time 1 in the first component
$POA1_2$ = Average value of the stagnation pressure at Time 2 in the first component
$POA2_1$ = Average value of the stagnation pressure at Time 1 in the second component
$POA2_2$ = Average value of the stagnation pressure at Time 2 in the second component

Use of the stagnation pressures instead of the total pressures is valid here because we are considering the flow across the short connector piece between the components. Since the velocity will be the same for both components (See Fig. 6 for the indicated velocities), the stagnation pressure ratio will be equal to the total pressure ratio and the assumption relatively accurate.

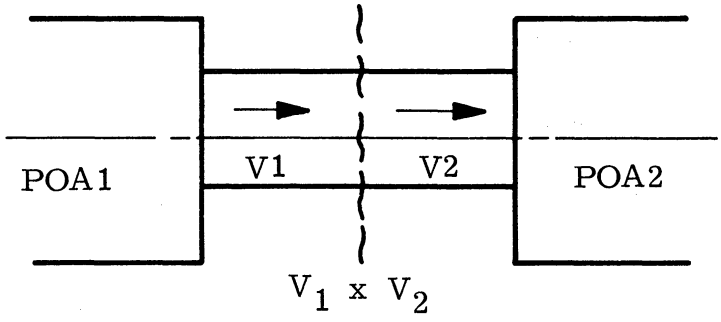

Fig. 6.

STEP 9. Knowing the outlet stagnation temperature and pressure and downstream mass rate of flow at Time 2, we can calculate the other properties at Time 2.

VI. THE INLET PHENOMENA

To determine the system's transient response, three parts of the inlet phenomena had to be understood and approximated. The first was the effect of clothes blockage on the system. Since the clothes blockage is nothing more than a change in the inlet area, it was approximated by varying the area as it would occur during operation.

Because this prototype washer-dryer required a novel inlet system, consideration had to be given to its physical characteristics. In approximating what actually occurs, the perforated drum plate was assumed to be a large number of flat plate orifices. Knowing the pressure drop (to be explained later), the configuration of the notes, and the number of holes opened, one can calculate the inlet mass rate of flow, and the new exit pressure (drum pressure minus the loss across the orifice) using basic orifice equations. Assuming the stagnation temperature is constant, the rest of the inlet conditions could be calculated for the nozzle, using the nozzle's inlet area and an internal function CALMAC.

The orifice equations are as follows:

$$GAM = \frac{P_2}{P_1} \qquad ARE = \frac{AREO}{A_2}$$

$$DZZ = \sqrt{\frac{((ARE)^2 - 1)(3.5)(1 - GAM^{.285})(GAM^{2/1.4})}{(1-GAM)((ARE)^2 - GAM^{2/1.4})}}$$

$$CD = 0.914 - 0.306\ GAM$$

$$\Delta P = P_2 - P_1$$

$$M_1 = CD \cdot N \cdot AREAO \cdot G \cdot DZZ \sqrt{\frac{2\rho(ARE)^2 \Delta P}{ARE^2 - 1}}$$

where

N	= number of holes opened
CD	= discharge coefficient
AREAO	= area of orifice
G	= gravitational constant
DZZ	= compressibility correction factor
ρ	= density
ΔP	= pressure drop across the orifice
ARE	= area ratio (orifice/downstream)
m_1	= mass rate of flow
GAM	= pressure ratio

The Inlet Phenomena

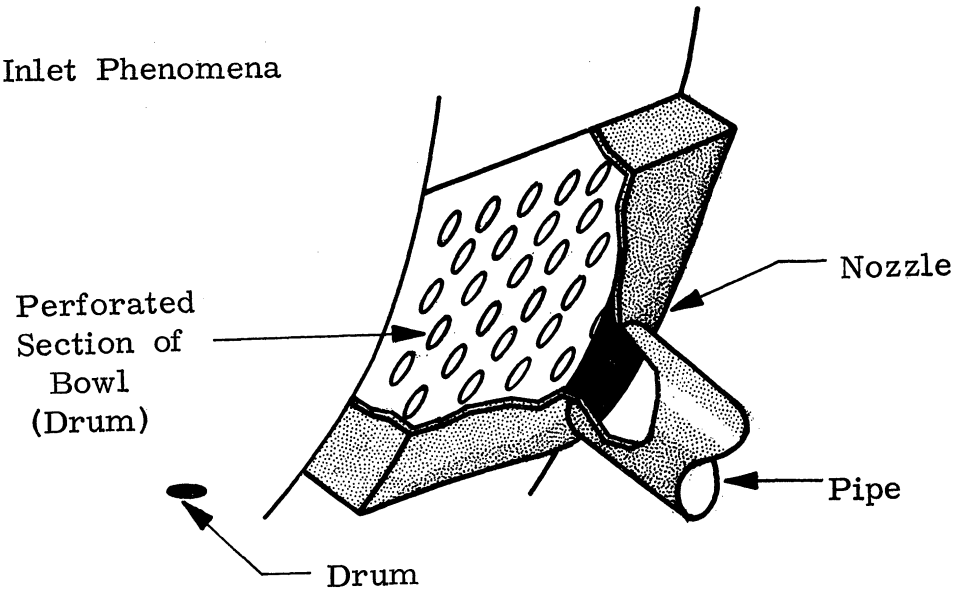

Fig. 7.

These equations enable us to calculate all of the inlet properties, provided the pressure across the plate is known. But the pressure drop across the plate is dependent upon the pressure head developed by the blower downstream, which is in turn dependent upon the mass flow rate throuth the system.

Consequently, a vicious cycle exists; but because pressure waves travel at the acoustic velocity (1150 fps) and the mass at speeds much less (200 fps), the system can be approximated in the following manner:

Knowing the flow rate at the blower, a value for the pressure head can be determined. By summing all the pressure losses in the system at that instant of time and subtracting them from the pressure head, a value for the pressure differential at the orifice plate can be found. With this parameter and the above equations, inlet conditions for the first component can be determined and the system readied for the rest of the analysis.

A. INTERNAL FUNCTIONS

To solve for downstream conditions knowing some of the downstream properties, two internal functions, SOLVE. and CALMAC., were written. These derivations are as follows—

1. CALMAC

CALMAC calculates the Mach Number at a point when the calculator knows the mass rate of flow, the pressure, stagnation temperature and the area. The derivation is:

Knowing

$$p = \rho RT$$
$$\dot{m} = \rho AV$$
$$M = V/C$$
$$C = \sqrt{kRgT}$$

Known Quantities

$$A, p, T\Phi, \dot{m}$$

$$T = \frac{T\Phi}{\left(1 + \frac{k-1}{2} n^2\right)}$$

we get

$$\frac{k-1}{2} M^4 + M^2 - \left(\frac{\dot{m}}{Ap}\right)^2 \left(\frac{RT\Phi}{kg}\right) = 0$$

solving by the quadratic equation

$$M^2 = \frac{-1 \pm \sqrt{1 + 4\frac{k-1}{2}\left(\frac{m}{Ap}\right)^2 \frac{RT\Phi}{kg}}}{2\frac{k-1}{2}}$$

Knowing that M can never be negative, we can eliminate the negative root and the program becomes:

```
INTERNAL FUNCTIONS CALMAC (MDOTS, PS, TOS, AS)
RS  = 53.34
KS  = 1.4
GS  = 32.20
CMA = (KS - 1.0)/2.0
CMC = -((MDOTS/(AS*PS)).P.2.0)* (RS*TOS/)KS*GS))
CMM = (-1.0 + SQRT. (1.0-4.0*CMA*CMC))/(2.0*CMA)
MS  = SQRT. (CMM)
FUNCTION RETURN MS
END OF FUNCTION
```

2. SOLVE

SOLVE is an external function used to solve for the Mach Number at a point if the stagnation temperature, stagnation pressure, area, and mass rate of flow are known at that point. Using the following relations,

$$\dot{m} = \rho AV$$

$$p = \rho RT$$

$$PO = P\left(1 + \frac{k-1}{2}M^2\right)^{k/k-1} \qquad TO = T\left(1 + \frac{k-1}{2}M^2\right)$$

we can derive the following equation,

$$PO = \frac{\dot{w}}{A}\sqrt{\frac{RT\Phi}{k}}\, M \left(1 + \frac{k-1}{2}M^2\right)^{\frac{1-3k}{2(k-1)}}$$

Where,

$\dot{m}$ = mass rate of flow
ρ = density
A = area
V = velocity
T = temperature
R = gas constant
PO = stagnation pressure
TO = stagnation temperature
M = Mach Number
k = specific heat ratio

This equation can be used by the computer to solve for M, the Mach Number, using an iterative technique. (For listing see Appendix.)

VII. DRUM TEMPERATURE CALCULATION

The determination of the drum temperature after every time interval is done in the following manner.

1. The mass of the gas in the drum is calculated.

$$MASS = \rho VOL + (\dot{m}_1 - \dot{m}_2)DELT$$

Where,

MASS = mass of gas in the drum
ρ = density
VOL = volume of the drum
$\dot{m}_1$ = mass rate of flow into the drum
$\dot{m}_2$ = mass rate of flow out of the drum
DELT = time interval

2. Next the heat transfered into the drum during the time is calculated.

$$Q = DELT\ (TO_{in} - TO_B)Cp\dot{m}_1$$

Where,

Q = heat transferred into the drum
TO_{in} = stagnation temperature of incoming fluid
TO_d = temperature of the gas in the drum
c_p = specific heat

3. Assuming the system is a closed system, a new value for the internal energy can be calculated.

$$E2 = Q + E1$$

Where,

E1 = initial internal energy of the drum
E2 = final internal energy

4. Then

$$E2 = MASS \cdot U$$

where U, the internal energy, is a function of T

$$U = \left(78.36 + \frac{3.47}{20.0}\,(T - 460.0)\right)778$$

solving for T we get

$$T = \frac{20.0}{3.47}\left(\frac{Q + E1}{778 \times MASS} - 78.36\right) + 460$$

where T is the new temperature of the drum.

VIII. COMPUTER PROGRAM

This computer program describes any dryer system composed of six basic component types. Up to twenty of these components can be arranged in any order to form a system and the computer will return a steady-steady and transient solution describing the system's reaction to a standard or selected input.

The manner in which the computer does this will be listed in steps below and reference will be made to both the program listing and flow diagram. Each step will be marked on the listing and flow diagram. A more detailed description of some of the separate parts and their theoretical basis are included elsewhere in the report.

A. COMPUTER DECLARATIONS

These statements set aside locations in memory for the arrays used in the program and sit the mode for all variables used.

B. CONSTANTS AND INITIAL CONDITIONS

This part of the program initializes all the constants (k, Cp, R, etc.) used in the program and specifies or calculates other initial properties such as the drum conditions. Included in this part are statements that locate the blower and separator in the system.

C. TIME LOOP

Because identical calculations will be performed over and over for each time interval until the time limit is reached, a loop labeled STIME was used.

This loop allows the program to make all the calculations between this statement and the one labeled STIME for each increment of time beginning at zero and ending at the time limit.

D. STEADY-STATE ANALYSIS

Because the initial specification of the property arrays was found to be important for the time response approximation, initial values for the properties throughout the system were the result of a steady-state analysis, assuming wide open conditions at the inlet. This steady-state solution was arrived at in the following manner:

1. When time (ATM) equaled 0, an index (SWIT) was set to allow the program to make a steady-state analysis—(SWIT = 1).
2. An assumed value for the pressure drop across the perforated plate was then used to calculate a set of inlet conditions. Using these as initial conditions for the first component, a steady-state analysis was made by (1) transferring to the first component in the system, (2) calculating the S.S. outlet properties, (3) changing the outlet properties into inlet properties for the next component, etc. through the system.
3. Upon completion of the solution, the pressure drops across all the components were summed and compared to the pressure developed by the blower. Using a half-interval method on the perforated plate pressure difference (the loss controlling factor), steady-state calculations were repeated

until the loss equaled the head.

E. TIME RESPONSE

The drum conditions, constants, and property arrays having been initialized, the program is ready to begin the transient calculations.

1. The inlet area are the specified time is determined, a pressure drop across the perforated plate calculated, and the inlet conditions found. (See the Inlet Phenomena.)
2. The program then transfers to the SYSTEM loop which successively does the following for each component throughout the system.
    a. The program transfer to the component, and a steady-state analysis is used to determine DPO, DTO, DMDOT measures of the work, loss, heat and mass addition to the system.
    b. Given these values, a transient analysis is performed (see TIME RESPONSE APPROXIMATION) and new downstream property values determined.
    c. These properties are then stored in an array and calculations on the next component made until there are no more components.

F. PRINT RESULTS

The results were then printed for this instant of time and the program returned to the STIME loop.

G. INTERNAL FUNCTION AND FORMAT SPECIFICATIONS

These are the internal functions written to aid in calculation of downstream properties. The format specifications were used in printing out the data.

Term Dictionary (parameters not specified, self explanatory—see prog)

ACTM - STIME loop limiting index. Equal to the desire simutation time divided by the time interval

ALPHAM - parameter used in pipe calculations—refer to program listing and SS analysis report

ARE - orifice area ratio

AREA - transitional area array (ft^2)

AREAO - orifice cross sectional area (ft^2) i.e., area of a single hole in perforated plate

ARK - index used in FIND loop to locate the blower and separator in the system

ART - intermediate variable used to calculate pipe diameter

ATM - index used to increment time in the STIME loop

AS - area in the internal function SOLVE

BLW - location of blower in the system

BLWR - pressure head developed by the blower

BP - blower pressure head array

C1 - inlet acoustic velocity

C2 - exit acoustic velocity

CCT - argument of internal function W (temperature in degrees R).

CD - discharge coefficient (orifice)

CDDT - error measure in flow calculations for the condenser

CE - parameter used in W—see Vern Wedeven's writeup

CKLW - variable used in condenser Mach Number calculations

CMA, CMM, CMC - parameters used in internal function CALMAC

CMCW - array specifying water flow rate to condenser

CND - minimum temperature of the system

CNT - index used to count the number of calculations

CNTA - likewise

COM - statement label array used for transferring to the correct component for steady-state results.

CP - constant pressure specific heat

CPF - film specific heat (heat exchanger)

CPV - parameter used in W (see Vern Wedeven's report)

CT - see Wedeven's report

CTC - see Wedeven's report

CTNI - temperature of condenser water (°R)

CT2R - see Wedeven's report

CT2L - see Wedeven's report

CWC - see Wedeven's report

CX - see Wedeven's report

D - pipe diameter

DDMDOI - mass removed during one time interval
DEL - pressure differential (across plate) array
DELL - parameter used in nozzle Mach Number calculations
DELMW - see Vern Wedeven's report
DELT - length of time interval
DELTAP - perforated plate pressure differential
DELTAΦ - heat transfer rate into the drum
DFRIC - parameter used in pipe steady-state analysis
DLMACH - error measure in pipe mach number calculations
DMDOI - change in mass rate of flow through a component
DMMM - total mass removed
DP - pressure drop across component
DPO - stagnation pressure change across component
DR - error measure in blower temperature calculations
DTO - stagnation temperature charge across component
DZZ - compressibility factor—orifice calculations
E1 - drum internal energy at t = 1
E2 - drum internal energy at t = 2
EFF - blower efficiency array
ER - error measure—steady-state calculations
ERS - error measure—pipe calculations
ERRS - error measure—nozzle calculations
ERRRS - error measure—heater calculations
FPRIME - friction factor for heater pressure drop calculations
FRIC - friction factor—pipes
G - gravitational constant
GAM - area ratio (orifice)
HAMIN - minimum area through the heater
HATUBE - surface area of heat exchanger tubes
HBARC - heat transfer coefficient (heater)
HCAL - variable used in heater flow calculations
HDELL - variable used in heater flow calculations
HDELP - pressure loss across the heater
HDO - heater tube diameter
HGMAX - maximum flow rate through the heater
HKN - index used to determine blower pressure head
HN - index used to calculate heater's constants
HNTUBE - number of horizontal tube rows in heater
HPRF - Prantt Number of film-heater
HQ - heat added in heater
HTL, HTF - temperatures used to calculate film constants in the heater.
HTWALL - temperature of heater tubes
K - specific heat ratio
KF - heater film specific heat ratio
KK - pipe friction factor array (for obstructions)
KS - specific heat ratio in internal function, SOLVE and CALMAC

M - mach number array
M1 - inlet mach number
M2 - exit mach number
MA1 - mass in the "next" component at t = 2
MA - condenser mass rate of flow (pounds/ minute)
MASS - mass in the component at t = 1
MBOWL - mass in the drum
MCW - condenser water rate of flow (pounds/minute)
MDOTI - inlet mass rate of flow
MDOTZ - exit mass rate of flow
MDOTS - mass rate of flow in internal function, SOLVE and CALMAC
ME - molecular weight of vapor mixture
MS - mach Number in SOLVE and CALMAC
MU - viscosity
MUB - viscosity of fluid-heater
MUF - viscosity of film-heater
MUS - viscosity of fluid at tube surface-heater
MW - see Vern Wedevin's report
N - index used in transfer operation
NC - number of components plus one
NRHOA - new average density
NS - integer used in SOLVE
NUM - index denoting location in system
NUMB - "SYSTEMloop" limiting index
NUMCOM - number of components in the system
NUMO - orifice area array
NWAI - mass in the "next" component at t = 2
NWMASS - mass in the component at t = 2
ONE - parameter used in SOLVE
P1 - inlet pressure
P2 - exit pressure
PBOWL - drum pressure
PC - acoustic velocity preperty array
PI - 3.14159
PM - Mach Number property array
PMD - mass rate of flow property array
PO1 - inlet stagnation pressure
PO2 - exit stagnation pressure
PO25 - stagnation pressure in SOLVE and CALMAC
POA - average stagnation pressure at t = 1
POA1 - average stagnation pressure of the next component at t = 1
POA2 - average stagnation pressure of the next component at t = 2
POWER - blower power array
PP - pressure property array
PPO - stagnation pressure property array
PPO1 - variable used in calculating new mass rate of flow
PRHO - density property array

PT - temperature property array
PTO - stagnation temperature property array
PURDUE - variable used in calculating stagnation properties
PV - velocity property array
Q - heat transferred to drum in DELT
R - perfect gas constant
RC - acoustic velocity print out array
REY - Reynolds number—pipe
RHO - average density—blower
RHO1 - inlet density
RHO2 - exit density
RHOA - average component density at t = 1
RHOB - drum density
RM - mach number print out array
RMD - mass rate of flow print out array
RP - pressure print out array
RPO - stagnation pressure print out array
RR - relative roughness of the pipe
RRHO - density print out array
RS - perfect gas constant in SOLVE
RT - temperature print out array
RTO - stagnation temperature print out array
RV - velocity print out array
SB - see Doug Lane's report
SCON - parameter in SOLVE
SD - see Doug Lane's report
SDC - diameter of separator chamber
SDE - exit duct diameter—separator
SDELP - pressure drop across separator
SDI - inlet duct diameter—separator
SDQ - heat transferred to separator
SEPA - location of separator in the system
SERS - error measure in SOLVE
SK1 - see Doug Lane's report
SK2 - see Doug Lane's report
SK3 - see Doug Lane's report
SK4 - see Doug Lane's report
SL - configuration parameter—heater
SLC - separator chamber length
SLE - length exit duct extends into separator
SM - Mach Number array in SOLVE
SN - see Doug Lane's report
SP - separator pressure in psi
SST - length of time the system has been operating
ST - separator temperature in °F
SUMDP - pressure loss across all components
SWIT - calculation controlling index

T1 - inlet temperature
T2 - exit temperature
TA - area input to SOLVE
TA1 - average stagnation temperature in the "next" component at t = 2.
TB - stagnation temperature
TBOWL - drum temperature
TL - mass rate of flow
TD - stagnation pressure
TIME - length of simulation time
TO1 - inlet stagnation temperature
TO2 - exit stagnation temperature
TO2S - stagnation temperature in SOLVE and CALMAC
TOA - average stagnation temperature in component at t = 1
TOA1 - average stagnation temperature in "next" component at t = 2
TYPE - array specifying the location and type of component in the system
U - internal energy
V1 - velocity
V2 - exit velocity
VELOR - velocity through the perforated plate
VOLUME - component volume
WKNR - variable used in condenser Mach Number calculations
WORK - work per unit time done by the blower
X2 - length of the pipe

DIMENSIONS

The dimensions of all properties and constants in the program are in the following system of units—

distance - feet
time - seconds
mass - pounds
temperature- degrees Rankin

BIBLIOGRAPHY

Arden, Bruce W., The Michigan Algorithm Decoder, rev. ed., 1966.

Berry, Charles H., Flow and Fan, Industrial Press, New York, 1954.

Church, Austin H., Centrifugal Pumps and Blowers, Wiley, New York, 1944.

Favalora, Emile W., Practical Design of Exhaust and Blower Systems, Edwin Scott, New York, 1935.

Kreith, Frank, Principles of Heat Transfer, International Textbook Co., Scranton, Pa., 1965.

Loitsianskii, L.G., Mechanics of Fluids and Gases, Pergamon, New York, 1966.

Shapiro, Ascher H., The Dynamics and Thermodynamics of Compressible Fluid Flow, vols. I and II, Ronald Press, New York, 1953.

Shames, Irving H., Mechanics of Fluids, McGraw-Hill, New York, 1962.

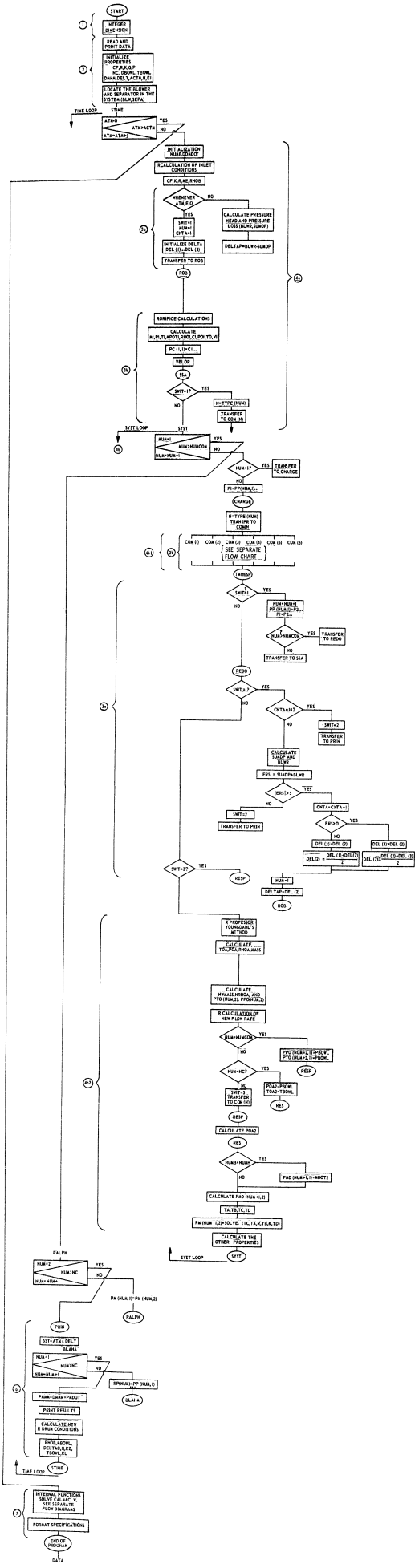
START
INTEGER DIMENSION
READ AND PRINT DATA
INITIALIZE PROPERTIES CP,R,K,GFI NC, DBOWL, TBOWL DMAX, DELT, ACTR, U, EI
LOCATE THE BLOWER AND SEPARATOR IN THE SYSTEM (BLR,SEPA)
TIME LOOP
STIME
ATWO
ATR=ACTR
ATR=ATR+1
YES
NO
INITIALIZATION NUMB,SOMDP
RECALCULATION OF INLET CONDITIONS
CP, K, R, AE, RHOS
WHENEVER ATR.EQ.0
YES
NO
SWIT=1 IRUN=1 CNT A=1
INITIALIZE DEL T, DEL I, DEL I-1, DEL I-2, DEL I-3
TRANSFER TO 1006
CALCULATE PRESSURE HEAD AND PRESSURE LOSS (BLWR, SUMDP)
DELTAP=BLWR-SUMDP
1006
RORIFICE CALCULATIONS
CALCULATE AI, PI, TI, APOTI, RHOI, CI, PDI, TD, YI
PC (I, I)=CI...
VELOR
15A
SWIT=1?
YES
NO
M=TYPE (IRUN)
TRANSFER TO CON (M)
SYST LOOP
SYST
NUM=1
NUM>NUMCON
NUM=NUM+1
YES
NO
NUM=1?
YES
TRANSFER TO CHARGE
NO
PI=PP(NUM,I)...
CHARGE
N=TYPE (NUM) TRANSFER TO COND
COM (1) COM (2) COM (3) COM (4) COM (5) COM (6)
SEE SEPARATE FLOW CHART
TAMESP
SWIT=1
YES
NO
RUN=NUM+1 PP (NUM,I)=PI... PI=I+2...
NUM=NUMCON
YES
TRANSFER TO REDO
NO
TRANSFER TO 15A
REDO
SWIT=1?
YES
NO
CNTA=1ST?
YES
NO
SWIT=2
TRANSFER TO PRIN
CALCULATE SUMDP AND BLWR
ERS = SUMDP+BLWR
IERST>1
YES
NO
SWIT=2
TRANSFER TO PRIN
CNT A=CNT A+1
ERS>0
YES
NO
DEL (1)=DEL (2)
DEL (1)=DEL (2)
DEL (2)
DEL (1)=(DEL (1)+DEL (2))/2
DEL (2)=(DEL (2)+DEL (3))/2
SWIT=3?
YES
RESP
NUM=1
DELTAP=DEL (2)
RUN
R PROFESSOR YOUNG'S(N.Y.) METHOD
CALCULATE VOL,POL,RHOL,MASS
CALCULATE RMASS,WMOL, AND PTO (NUM,I), PPO(NUM,I)
R CALCULATION OF NEW FLOW RATE
NUM=NUMCON
YES
NO
PPO (NUM+1, I)=PBOWL PTO (NUM+1, I)=PBOWL
NUM=NC?
YES
NO
RESP
PDA2=PBOWL TDA2=TBOWL
RES
SWIT=3 TRANSFER TO CON (NC)
RESP
CALCULATE PDA2
RES
NUM3=NUM4
YES
NO
PAD (NUM+1, I)=ADOT2
CALCULATE PAD (NUM+1, I)
TA, TB, TC, TD
PN (NUM 1, I)=SOL VE. (TC, TA, R, TB, 4, TD)
CALCULATE THE OTHER PROPERTIES
SYST LOOP
SYST
RALPH
NUM=2
NUM>NC
NUM=NUM+1
YES
NO
PN (NUM, I)=PN (NUM, 2)
RALPH
PRIN
SST=ATW+DELT
SLAMA
NUM=1
NUM>NC
NUM=NUM+1
YES
NO
RPONUM)=PP (NUM, I)
SLAMA
PAMA=CMAN+PADOT
PRINT RESULTS
CALCULATE NEW R PRIN CONDITIONS
PROBLABOWL, DELTAD, QEZ, TBOWL, EL
STIME
TIME LOOP
INTERNAL FUNCTIONS SOL VE, CALAIC, F, SEE SEPARATE FLOW DIAGRAMS
FORMAT SPECIFICATIONS
END OF PROGRAM
DATA

ANALYTIC STUDY OF DIRECT-DRIVE AUTOMATIC WASHING

Ishwar Lal Thakur

This is an analytic study to determine the optimum motor and control system to power a direct-drive automatic washing machine from a 110 v, 60 cycles, single-phase, household supply. The system must operate in two modes, agitation and spin.

The agitation mode requires the motor to run in forward and reverse directions with an agitation rate variable between 30 and 68 strokes/min with an arc ranging between 70 and 192°. The cycling of the agitation mode is intended to be as shown in Fig. 1.

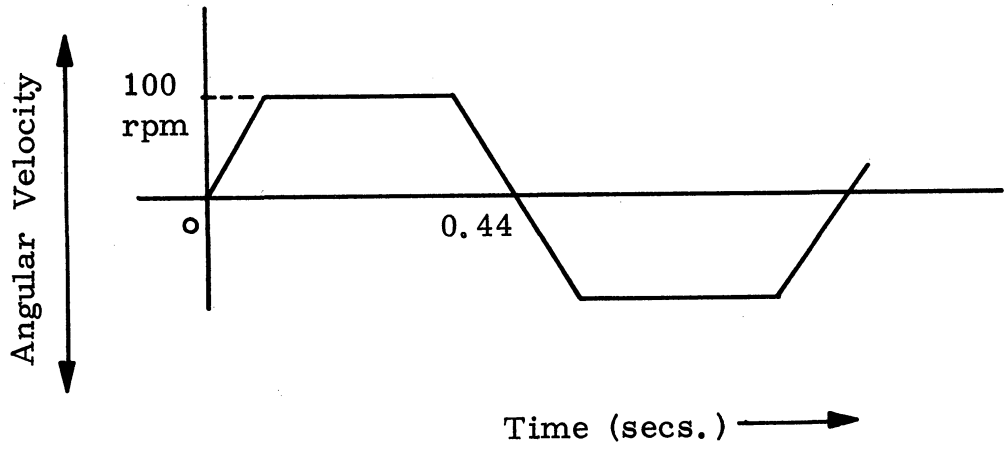

Fig. 1. Agitation mode.

The average power input to the system is restricted to a maximum of 800 watts, with peaks not exceeding 1,000 watts.

An extensive survey of the literature indicates that machines with larger size have been manufactured to run at low speeds, 100 rpm or less, such as train lighting generators. A recent development in the design and manufacture of a gearless low-speed motor is being carried out in Britain by Evershed and Vignoles, Ltd., but this machine handles only small load torques and, therefore, is not suitable for our system.

Inasmuch as our system must operate in reversible mode (Fig.1), problems such as sparking at brush contacts, development of induced voltages in the field windings, and excessive heating have arisen. We have been unsuccessful in designing a direct-drive motor within reasonable limits of power requirements, size, and material cast.

A simple way of reversing the direction of rotation of a ac series motor using plugging relays and contactors is shown in Fig. 2. In this arrangement the direction of current is reversed in the armature winding by simultaneous operation of forward and reversing contactors connected in the armature circuit. The phenomenon of reversing the armature current while the motor is running in one direction is known as plug-reversal. Under the condition of plugging, the e.m.f. generated in the armature acts in the same direction as the line voltage with the result that the current will be excessive unless additional resistance is inserted in the armature circuit. To accomplish this, a plugging relay and contactor C are provided (Fig.2). The plugging relay is shunt wound and is connected across the resistor. When the current through this resistor exceeds a predetermined amount, the relay prevents the closure of plugging contactor C.

It is preferable to reverse the armature current rather than the field current since this avoids the high induced voltage which may be produced in the field winding when it is opened and the machine is running. A sudden collapse of motor field winding may also induce a large current in the armature circuit which could damage the commutator or interrupt the power to the armature circuit.

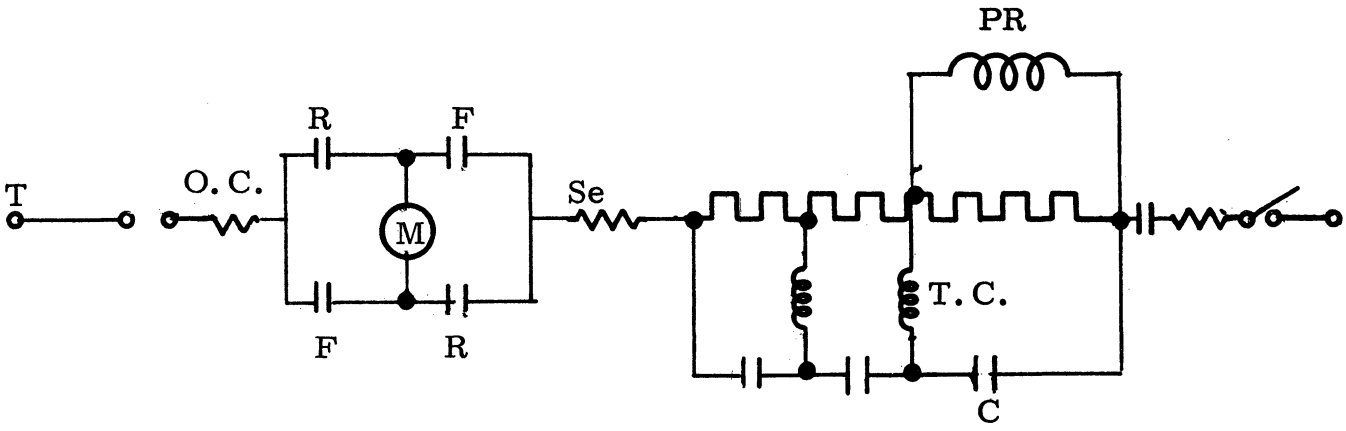

C—Contactor
F—Forward
M—Motor
O.C.—Overload Trip Coil
P.R.—Plugging Relay
R—Reverse
Se—Series Field
T.C.—Time-Current relay

Fig. 2. Reversing of motor.

If a single armature winding is used in a reversing motor, the speeds in two directions are frequently different, causing the arc lengths to differ. To avoid this difficulty, two separate armature or field windings are frequently used. Another difficulty is armature reaction which results in sparking at the commutator due to frequent reversals. This sparking can be minimized by using interpole windings that compensate for the frequent reversals.

Because of these considerations, we decided to design a dc series motor having the double armature and interpole windings. However, our analysis showed that the size of the armature, considering only the single armature winding in the first step, was impractical. Therefore, the next step in the design, the

double armature with interpole windings, was not considered since this would have further increased the size of the machine.

Let us now consider the reason for greater heat losses in the direct-drive system. When the duty cycle of a motor requires frequent starting and reversing, energy stored in rotating masses of both rotor and driven equipment becomes a significant factor in overall performance, especially when the load has high inertia, low speed, and little time for starting and reversing. The mechanical power available at the motor shaft as a result of energy conversion in the motor serves two functions during the starting period. At any instant, part of the power maintains rotation at the speed then attained, and the remainder accelerates this speed. The motor thus does not reach operating speed until the system has had time to convert and store the corresponding amount of energy into the mass. Similarly, stopping the motor demands that an opportunity be provided for the complete dissipation of stored energy, either through friction or through a conversion to electrical energy. In the same way, reversing the rotor demands the complete dissipation of stored mechanical energy, followed by re-storage corresponding to rotation in the opposite direction.

The stored energy (or kinetic energy) in a rotating mass is a function of moment of inertia and angular velocity of the rotating mass, and is given by the relationship $J_c\frac{w^2}{2}$, where J_c is the combined inertia of the load and the rotor. In the direct-drive system the motor rotates at the low speed of the connected load, which requires a larger motor and therefore more rotor inertia and accelerating losses. If J_r is the rotor inertia and J_e the load inertia, then in the direct-drive system $J_c = J_r + J_e$ (Fig.3a). When the load is driven

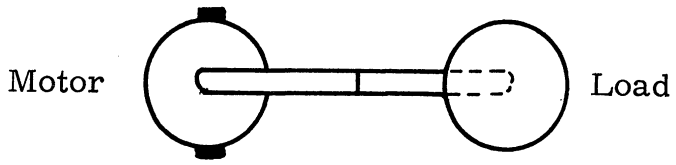

$$Jc = Jr + Je$$

Fig. 3a. Direct-drive system.

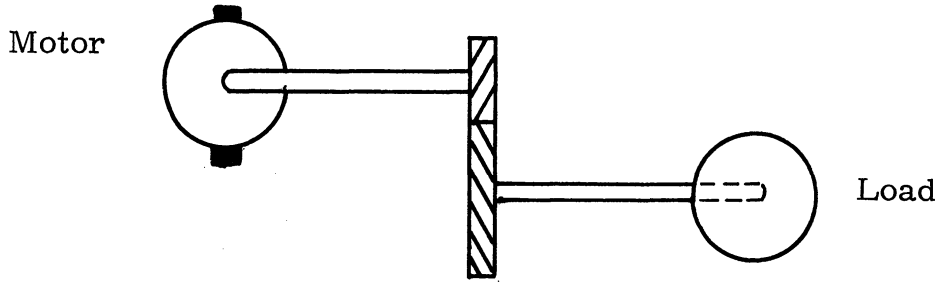

$$Jc = Jr + \frac{Je}{r^2},$$

Fig. 3b. Gear-drive system.

Jc - combined inertia of load and rotor
Jr, Jr' - rotor inertia
Je - load inertia
n - gear ratio

through a gear train, the combined inertia is given by the relation:

$$J_c = J_r' + \frac{J_e}{n^2} \quad \text{(Fig. 3b)}$$

The combined inertia J_c is now considerably smaller than that for a direct-drive system. In the latter case a small high-speed motor is used, resulting in much smaller rotor inertia (J_r') and thus less accelerating loss.

Consideration was also given to a system supplied from a 220 v supply. It was realized after a few calculations that the machine would still be large and therefore would have high rotor inertia and excessive accelerating losses.

The control system, which is necessary to gain the knowledge of the functioning of the complete system, was made.

The Flip-Flop circuit (Fig. 4) can be used to energize one of the double rotor or field windings and do the job of cycling required for our system (Ref. 4). When the collector supply potential v is applied to the circuit, both transistors begin to conduct. One will conduct more heavily than the other, thereby dropping its collector voltage and the base voltage of the other transitor. This will cause the collector current of the other transistor to decrease and its voltage to rise, thereby increasing the base voltage of the first transistor and therefore its collector current. This keeps the other transistor non-conducting. The circuit will remain in this state until some external signal triggers it. Once it is triggered from an external timer circuit (not shown), the conditions reverse. The circuit is based on the principle of two switches connected in a manner so that the output of the first is fed to the input of the second, and the output of the second is connected to the input of the first.

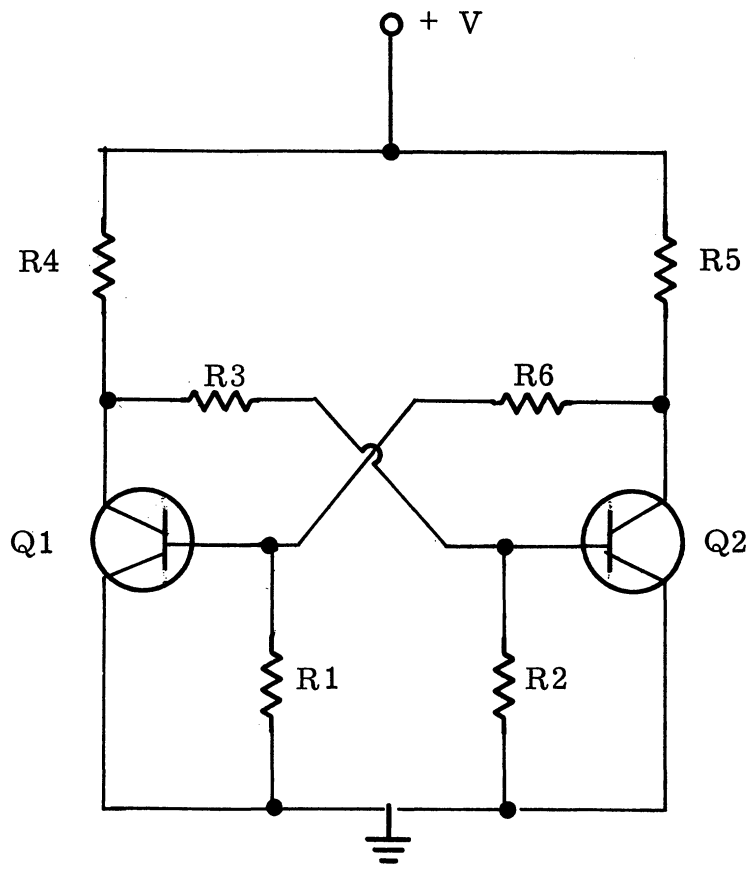

Fig. 4. Flip-flop circuit for motor reversal.

Another control circuit (Fig.5) can be used to control the amount of arc in each direction. This is done by using the feedback principle; a control signal is fed into the control amplifier, which drives the motor (Ref.5). A feedback path is present by which the motor generates an error signal proportional to the difference between its actual position and the position it should be in as indicated by the control signal.

After considerable study of the various possibilities, a design for a dc series motor was made as detailed in the Appendix. It is seen from the calculations that the machine size is very large due to heating, high load torques, rapid reversals in a short interval of time, and the low operating speed of the

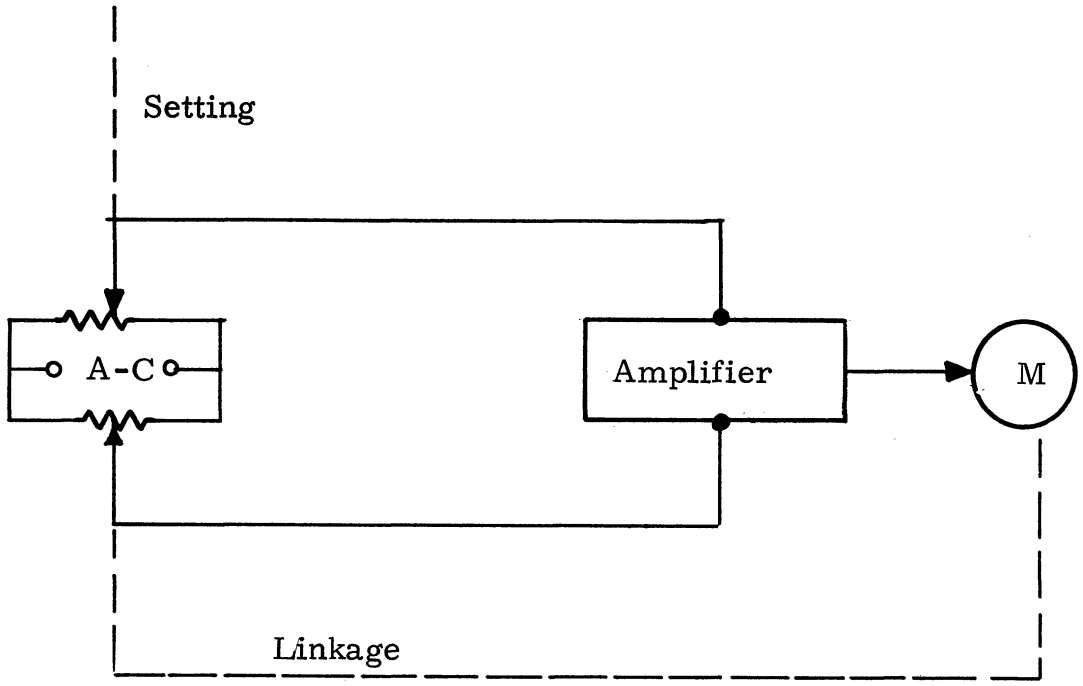

Fig. 5. Control of arc.

system during the agitation mode. The provision for double armature windings and interpole windings is not made in the present design because the motor would have been too large. The overall dimensions and other pertinent data are given below for a brief review of results.

Diameter of machine	= 14.5 in.
Length of machine (rotor only)	= 8 in.
Weight of iron	= 150 lbs.
Weight of copper	= 65 lbs.

NOTE: The above data do not include double armature or field windings, interpole and compensating windings, commutator and shaft dimensions as discussed earlier.

APPENDIX

SYMBOLS

A = area. Subscript identifies part, as s for a slot, cu for copper, sn for n slots, r for tooth root, m for field magnet.

AT = total ampere turns.

at = ampere turns, subscript identifies part, as g for gap, a for armature, m for field poles.

a = no. of parallel paths in armature.

B = flux density, subscript identifies part, as g for air gap, a for armature f for field magnet.

D_a = external diameter of the armature in inches.

D_i = internal diameter of the armature in inches.

D_o = outside diameter of the field yoke in inches.

D_r = diameter at the bottom of slots in inches.

D_d = radial depth of armature core in inches.

d = radial depth of slot in inches.

E = supply voltage in volts.

E_a = generated back e.m.f. in volts.

f = frequency.

g = acceleration due to gravity = 32.2 ft. per sec. per sec.

H = intensity of magnetization

I = current in amperes.

i_a = instantaneous value of a variable armature current.

K = number of commutator bars.

k = percent of power loss.

L_c = axial length of armature core.

l_f = main pole leakage factor.

MT = length of mean turn, subscript a for armature conductor, b for field conductor.

m = shape ratio of armature.

N = number of slots in armature.

N_c = number of armature coils per slot.

n = speed in rpm.

p = number of main poles.

p_w = pole waist.

V = ampere conductors per unit of periphery = $ZI/\pi D_a$.

R = resistance, subscripts, as a for armature, f for field winding, and b for brushes and brush contacts.

S_{Fe} = stacking factor.

s = specific cooling surface.

S_a = cooling surface armature.

T = number of turns per armature coil.

T_f = number of turns for field winding.

t_r = tooth root width.

t_m = thickness of yoke.

v = peripheral speed of armature in ft. per min.

Wm = width of the frame.

W = capacity of motor.

Z = number of armature conductors.

Z_s = number of conductors per slot.

λ = slot pitch.

μ = permeability.

ρ = resistivity.

Φa = useful flux per pole in c.g.s. lines.

ψ = pole enclosure.

π = pole pitch.

I. DETERMINATION OF ARMATURE DIMENSIONS

METHOD (a) Approximate Cooling Surface of Armature: Cooling surface of drum armature is approximately expressed as:

$$Sa = D_n^2 \pi(m + 1/4)$$

Cooling surface in square inches required is:

$$Sa = 8 \times k \times W$$

Thus:

$$D_a = \frac{S \times k \times W}{\pi(m + 1/4)}$$

The data assumed for our problem are:

S = specific cooling surface = 0.75
k = percent of power loss = 50%
W = capacity of the motor = 373 watts (1/2 H.P.)
m = shape ratio of armature = 1.1

Therefore:

$$D_a = \frac{0.75 \times 0.5 \times 373}{\pi(1.1 + 0.25)} = \frac{33}{} = 5.75 \text{ in.}$$

METHOD (b) Peripheral Speed of Armature: An alternate guide in obtaining the diameter of an armature is the fact that the peripheral velocity v, must be kept within the limits established by practice, that is, between 1,500 and 6,000 feet per minute. The most common peripheral velocity being 3,000 ft./min.

Since,

$$v = \frac{\pi D_a}{12} \times n$$

Thus,

$$D_a = \frac{12\ v}{\pi n}$$

For, $v = 3{,}000$ ft/min. and $n = 100$ rpm.

$$D_a = \frac{12 \times 3{,}000}{\pi \times 100} = 11.5 \text{ in.}$$

The actual armature diameter is determined as below by considering the number of armature conductors required to run the motor at a speed of 100 rpm.

METHOD (c) Armature Dimensions: After several trials, the suitable armature dimensions were obtained, by keeping various flux densities within permissible limits, are:

$$D_a = 12 \text{ in. and } L_c = 8 \text{ in.}$$

Thus the peripharal speed $v = \frac{\pi \times 12}{12} \times 100 = 3{,}142$ ft./sec. which is within reasonable limits.

The choice of number of poles is chiefly a matter of number of magnetic cycles per second occurring in the armature core. The lower frequency of about 10 or 15 cycles per second applies to low speed machines for direct-drive systems. Tentative values of resistance drops are taken since,

$$f = \frac{n \times p}{60 \times 2}$$

chosing p = number of main poles = 10 and for n = 100 rpm

$$f = \frac{100 \times 10}{2 \times 60} = 8.32 \text{ cycles/sec.}$$

Which is little less than minimum limit of 10 cycles/sec., but is considered for the design.

$$T = \text{pole pitch} = \frac{\pi D_a}{p} \qquad \frac{\pi \times 12}{10}$$

$$= 3.77 \text{ in.,}$$ corresponding pole enclosure ψ from tables of Ref. 2 is:

$$\psi = 0.5$$

The emprical relation for air gap flux density (Ref.2) is:

$$Bg = 27{,}100\ W^{0.192}$$

Where W = capacity of motor in KW = 0.373 KW

So, $Bg = 27{,}100\ (0.373)^{0.192} = 21{,}000$ lines per square inch.

The useful flux per pole is given by:

$$\Phi_a = \psi \times T \times Bg \times Lc$$

$$= 0.5 \times 3.77 \times 21{,}000 \times 8 = 318{,}000 \text{ lines.}$$

Tentative values of resistance drops are taken to be (Ref.2):

(i) armature = 0.08 v = 8.8 v
(ii) series field = 0.08 v = 8.8 v
(iii) interpole winding = 0.08 v/3 = 2.9 v
(iv) brushes and brush contacts = 3.0 v
total resistance drops = 23.5 v

Thus,

$$E_a = V - IR \text{ drop} = 110 - 23.5 = 86.5 \text{ v}$$

Number of armature conductors are:

$$Z = \frac{a\ Ea \times 60 \times 10^8}{p\ \Phi_a\ n}$$

Simple wave winding is preferred for a motor having more than 2 main poles (Ref.2), and therefore the number of parallel paths = a = 2.

$$Z = \frac{2 \times 86.5 \times 60 \times 10^8}{10 \times 318000 \times 100} = 3260$$

$$\text{Input Current} = \frac{\text{H.P.} \times 746}{V \times N}$$

$$\text{Assuming } N = 50\%$$

$$\text{Input Current} = \frac{0.5 \times 746}{100 \times 0.5} = 6.76 \text{ amps}$$

$$\text{Hence, each conductor must carry} = \frac{6.76}{2}$$

$$= 3.38 \text{ amps}$$

Total Ampere conductors = $3260 \times 3.38 = 11{,}100$

periphery = $\pi D_a = 12\pi = 37.6$ in.

Ampere conductors per inch of periphery

$$= 11{,}100/37.6 = 295$$

Permissible ampere conductors per inch of periphery (Ref.2) are = 395.

Number of slots per pole should be (Ref.2):

$$N/p = \frac{3.5}{1-\psi}$$

$$N = \frac{3.5 \times 10}{1 - 0.5} = 70$$

But making N/2p a whole number, say 4, we require: N = 80.

Conductors per slot $Z_s = \frac{3,260}{80} \simeq 40$

Thus

$$Z = 40 \times 80 = 3200$$

Slot depths more than 2 in. make it difficult to take heat out. When the armature is large enough so that there is no longer sufficient surface to get rid of heat, or ir the slots become too deep, most of the best proportions can no longer be adhered to.

Taking these factors into consideration, the slot depth d is chosen to be 1.5 in.

For best proportions which give maximum power converted (Ref.2).

$$t_r = \frac{1}{Nd}\left[\frac{\pi}{4}(Da^2 - Dr^2) - A_{ns}\right]$$

$$D_r = D_a - 2d = 12 - 2 \times 1.5 = 9 \text{ in.}$$

For $S_r = t_r$, so $\psi_r = 0.5$, $\alpha = 0.25$ from graph (Ref. 2)

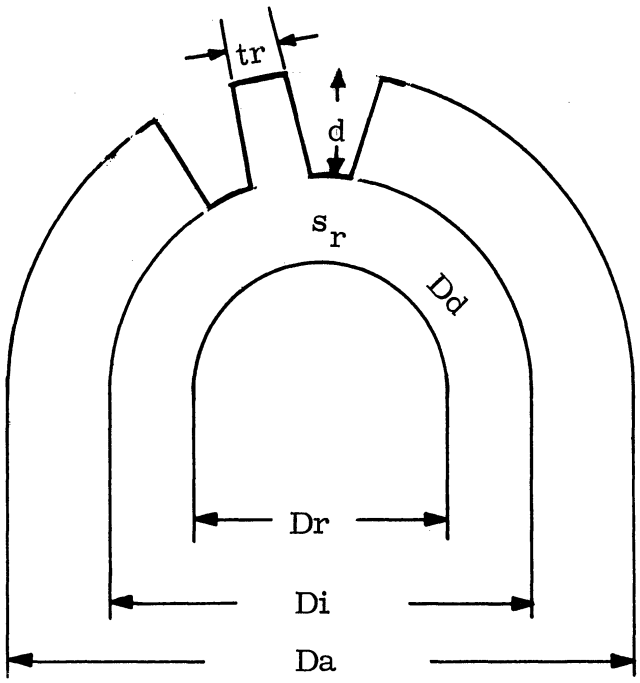

$$Tr = \frac{tr}{Sr+tr}$$

Fig. 6. Rotor details.

$$\alpha = \frac{\text{Slot Area}}{\text{Disc Area}}$$

Thus

$$A_s = 0.25 \times \frac{\pi}{4} \frac{Da^2}{N}$$

$$A_s = \frac{0.25\pi \times (12)^2}{4 \times 80} = 0.353 \text{ sq. in.}$$

S_{cu} = space factor of copper = $\frac{\text{Area of Copper}}{\text{Area of space occupied by winding}}$

= 0.6

Thus

A_{cu} = Area of copper per slot = 0.6 x 0.353

= 0.212 sq. in.

Gross area available per conductor = $\frac{A_{cu}}{Z_s} = \frac{0.212}{40}$

= 0.0053 Sq. in.

Dia. of Conductor = 0.073 sq. in.

Corresponding wire size chosen from table (Ref.1) is AW6 13 whose:

ρ = resistivity is 0.0020 ohms/ft.

and weight is 0.0157 lb/ft.

A_s = Area of copper per slot = $\frac{A_{sn}\, S_{cu}}{N}$

A_{sn} = Area of N slots = $\frac{0.212 \times 80}{0.6}$ = 28.2 sq. in.

Thus

$$t_r = \frac{1}{80 \times 1.5}\left[\frac{\pi}{4}(12^2 - 9^2) - 28.2\right]$$

$$= \frac{1}{120}\left[\frac{\pi}{4}(144 - 81) - 28.2\right]$$

$$= \frac{1}{120}\left[49.6 - 28.2\right] = \frac{21.4}{120} = 0.178 \text{ in.}$$

Length of mean turn $= MT_a \simeq 2\left[L_c + \frac{\pi T(D_a - d)}{N}\right]$

T = number of teeth entraced by coil $= \frac{N}{P}$

$$= \frac{80}{10} = 8$$

$$MT_a = 2\left[8 + \frac{\pi 8(12 - 1.5)}{80}\right]$$

$$= 16 + \frac{\pi \times 10.5}{5} = 16 + 6.6 = 22.6 \text{ in.}$$

$$= 1.88 \text{ ft.}$$

l_a = Total length of armature wire $= \frac{1}{2} ZMT_a$

$$= \frac{1}{2} \times 3200 \times 1.88 = 3010 \text{ ft.}$$

R_c = resistance of the armature circuit

$$= \frac{\rho \times l_a}{a^2} \qquad \frac{0.0020 \times 3010}{2^2} = 1.5 \text{ ohms}$$

D_d = radial depth of armature core $= \frac{\Phi_a}{L_c \times B_a \times S_{Fe}}$

Where B = flux density in armature core = 50,000 lines/sq. in.

$$D_d = \frac{318{,}000}{8 \times 50{,}000 \times 0.925} = 0.38 \text{ in.}$$

A_r = tooth root area under a pole

$$= \psi \frac{N}{P} \text{ tr } L_c \, S_{Fe} \; ; \quad S_{Fe} = 0.925$$

$$= 0.5 \frac{80}{10} \times 0.178 \times 8 \times 0.925$$

$$= 5.27 \text{ sq. in.}$$

B_r = tooth root density = $\frac{\Phi a}{A_2}$

$$= \frac{318{,}000}{5.27} = 60{,}500 \text{ lines per sq. in.}$$

B_r is well within permissible limits 40,000 to 150,000.

II. FIELD WINDING AND STRUCTURE

$$\Phi_a = 318{,}000 \text{ lines}$$

$$l_f = \text{leakage factor} = 1.2$$

Consequently total flux in the field magnet is

$$\Phi_f = 1.2 \times 318{,}000 = 381{,}000 \text{ lines}$$

Let the field magnet be composed of cast iron of flux density 45,000 per sq. in. requiring a cross-section area of

$$A = \frac{\Phi_f}{B_f} \quad \frac{381{,}000}{45{,}000} = 8.48 \text{ sq. in.}$$

An elliptical magnet is preferred with its major axis a = 3 in.

Thus

$$\pi ab = 8.48$$

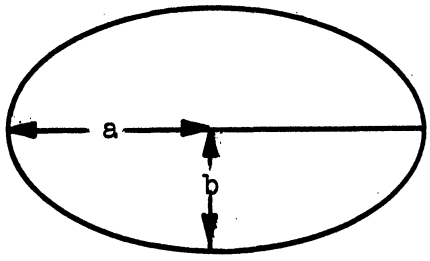

Cross-section of field magnet.

$$b = \frac{8.48}{3\pi} = 0.9 \simeq 1 \text{ in.}$$

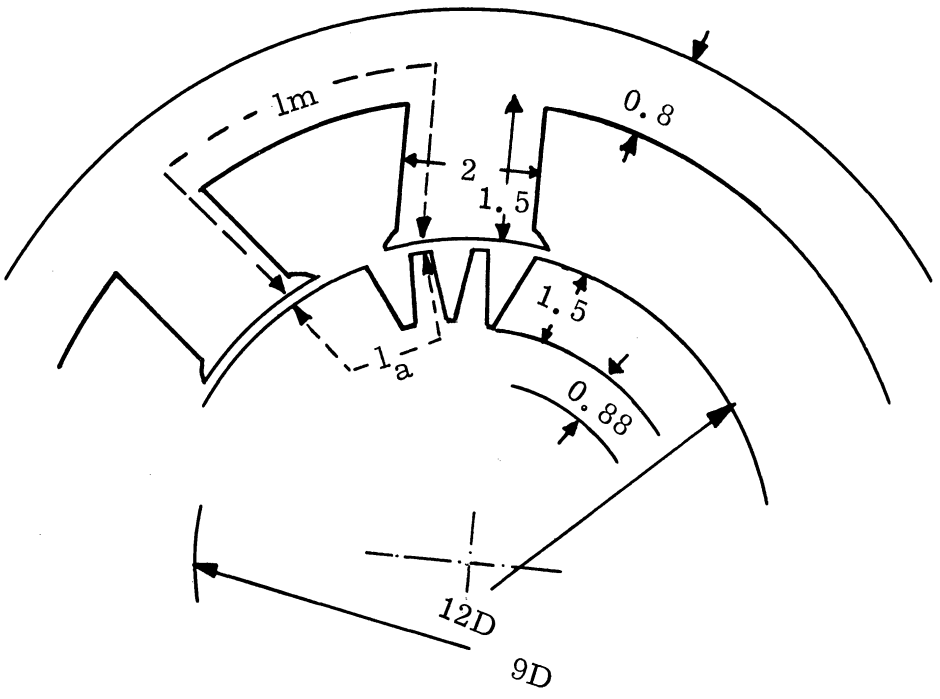

Fig. 7. Motor detailed dimensions. All dimensions are in inches.

The yoke is multiple design and carries half the lines of each magnet; hence, its cross-section need only be 8.48/2 = 4.24 sq. in.

Making a frame W_m = 7 in. wide with overhangs on either side, the radial thickness of the yoke will be t_m = 4.24/7 = 0.6 in., which we will raise to 0.8 in. allowing for rounding, etc., at corners.

Mean length of magnetic paths are:

l_a core = mean length of magnetic path in armature = 2.70 in.

l_m core = mean length of magnetic path in yoke = 5.8 in.

l_g = length of air gap = 1/8 in.

L_m = length of the magnetic pole = 3 in.

D_i = internal diameter of the armature = 12 - (1.5 + 0.88) = 7.24 in.

D_o = external diameter of the yoke = $12 + \frac{1}{8} + 1.5 + 0.8 \approx 14.5$ in.

Determination of total ampere turns is as below:

At_g = ampere turns in gap (Ref.1)
= 0.313 x Φ_a x $2\ell g$
= 0.313 x 21,000 x 1/4 = 1650 ampere turns

at_m = ampere turns for yoke core
= H_m x ℓ_m

Where H_m = 95 is the magnetizing force corresponding to B_m of 45,000 for wrought iron (Ref. 1).

at_m = 95 x 5.8 = 552 ampere turns

at_g = ampere turns for teeth
= H_g x (2d)

Where H_g = 13 is the magnetizing force corresponding to tooth flux density of 60,500 lines per sq. in. (Ref.1)

at_g = 13 x (2 x 1.5) = 39 ampere turns

at_a = ampere turns for armature core

= H_a x la

Where H_a = 9.6 is the magnetizing force corresponding to armature flux density of 50,000 lines per sq. in. (Ref. 1).

$$at_a = 9.6 \times 2.70 = 26$$

Total ampere turns required

$$= AT = 1650 + 552 + 39 + 26$$

$$= 2267 \text{ ampere turns}$$

T_f = number of turns in field winding = $\frac{AT}{I}$

$$= \frac{2267}{6.76} = 335$$

Thus, number of turns per pole

$$= \frac{335}{10} \simeq 34$$

Allowing 1,250 circular mils per ampere, the cross-section of the wire is found to be 1,250 x 6.76 = 8490 circular mils and corresponding AWG wire size is 10, whose diameter is 0.112 in. with double cotton covering.

Also

ρ = resistivity = 0.000992 ohms per ft.

and weight of wire = 0.0323 lbs./ft.

L_m = length of field core = 1.5 in.

Back core will be bound with $\frac{1.5}{0.112} \simeq 12$ turns

$$\text{No. of layers} = \frac{34}{12} \simeq 3$$

The height of winding will be 0.112 x 3 = 0.336 in.

Thus the length of mean turn on the field core is about 17 in. or 1.42 ft.

Total length of the field wire = 10 (3 x 13 x 1.42) = 555 ft.

R_f = resistance of field winding

= 555 x 0.000992 = 0.55 ohms

III. LOSSES

A. COPPER LOSS

Power loss in armature winding = I^2Ra

= $(6.76)^2 \times 1.5$ = 69 watts

Power loss in field winding = $I^2 R_f$

= $(6.76)^2 \times 0.55$

= 25 watts

Total copper losses = 69 + 25 = 94 watts

B. IRON LOSS

V_r = volume of iron in teeth = N tr d L_c S_{Fe}

= 80 x 0.178 x 1.5 x 8 x 0.925

= 156 cu. in.

W_r = weight of iron in teeth = 0.284 V_f

= 0.284 x 156 = 44.2 lb.

V_y = volume of iron in armature yoke

= $(D_r - D_d) \pi \times D_d \times 0.925 L_c$

= $(9 - 0.88) \pi \times 0.88 \times 0.925 \times 8$

= 168 cubic in.

W_y = weight of iron in armature yoke = 0.284 V_y

= 0.284 x 168 = 47.6 lbs.

Weight of armature copper wire = 0.0157 lbs./ft.

Total weight of copper wire in armature winding = 0.0157 x 3010 = 47 lbs.

Flux density in tooth root = B_r = 60,500 lines per sq. in.

Hysteresis factor for teeth: η_r = 0.0128 watts per cu. in.

Hystenesis power loss in teeth = $\eta \times f \times V_\ell$

= 0.0128 x 1.32 x 156

= 16.7 watts

A_r = area of the armature yoke = $D_d \, L_c \, S_{Fe}$

= 0.88 x 8 x 0.925

= 6.38 sq. in.

B_a = flux density in the armature yoke = $\frac{\Phi}{A_r}$ $\frac{318,000}{6.38}$

= 50,000 lines per sq. in.

Hysteresis factor for armature: η_a = 0.0048 watts per cu. in.

Hysteresis power loss in armature = $\eta_a \times f \times V_y$

= 0.0048 x 8.32 x 128

= 5.06 watts

Iron losses = w_h = 16.7 + 5.06 = 21.76 watts

Assume thickness of the laminations = 0.01 in.

w_e = eddy current power loss = $\epsilon \times f^2 \times V_y$

For B_a = 50,000 lines per sq. in., in armature core. ϵ_c = 0.000011 watts per cu. in.

For B_r = 60,500 lines per sq. in., in tooth root, ϵ_r = 0.000015 watts per cu. in.

Thus

$$w_{ec} = 0.000011 \times (8.32)^2 \times 168$$

$$= 0.0127 \text{ watts}$$

$w_{e_r} = 0.000015 \times (8.32)^2 \times 156$

$= 0.163$ watts

Total eddy current loss: $w_e = 0.162 + 0.04$

$= 0.18$ watts

Total Iron losses $= 21.76 + 0.18 = 21.94$ watts

V_p = volume of the field poles

$= \pi ab L_m = \pi \times 2 \times 6 \times 3 = 113$ cu. in.

W_p = weight of the field pole $= 0.284 \times 113$

$= 32.2$ lbs.

V_f = volume of the field yoke

$\simeq \frac{\pi}{4} D_o^2 - (D_o - t)^2 W_m$

$= \frac{\pi}{4} 14.5^2 - (14.5 - 0.6)^2 7$

$= \frac{7\pi}{4} 210 - 194 = \frac{7\pi}{4} \times 16 = 88$ cu. in.

W_f = weight of field yoke $= 0.284 \times 88$

$= 25$ lbs.

Weight of field copper wire $= 0.0323$ lbs. per ft.

Total weight of field copper wire $= 0.0323 \times 550$

$= 17.8$ lb.

C. STORED ENERGY LOSSES (ACCELERATION AND DECELERATION LOSSES)

Moment of inertia of the load $= 32.2$ lb.-ft.^{2}

Weight of copper on armature $= 47$ lbs.

Weight of armature yoke $= (44.2 + 47.6)$

$= 91.8$ lbs.

Considering the weight of spider and shaft as 10% of the weight of armature yoke the total weight of armature: $W_a = 47 + 1.1 \times 91.8$

$= 47 + 101 = 148$ lbs.

K_a = radius of gyration of the armature $= \sqrt{\frac{(12)^2 + (7.24)^2}{2}} = 9.9^2$ in.

$= 0.828$ ft.

Moment of inertia of the armature $= W_a K_a^2$

$= 148\ (0.828)^2$

$= 102$ lb.-ft.^{2}

Wk^2 = total moment of inertia of load + motor

$= 32.2 + 1(2 = 134.2$ lb.-ft.^{2}

w = speed in radians per sec. $= \frac{2\pi n}{60} = \frac{2\pi \times 100}{60}$

$= 10.45$ radians per sec.

During starting and accelerating the load, the equation of motion is:

$$T_m - T_e = \text{Acceleration torque} = \frac{Wk^2}{g}\frac{dw}{db}$$

Where

T_m = motor torque in lb.-ft.

T_e = load torque in lb.-ft.

W_k^2 = total moment of inertia of load and motor combined

The energy consumption equation or work done in raising the load to w rps in time + sec. is:

$$\frac{T_m w_t}{2} = \frac{T_e w_t}{2} t + E_1$$

Where E_1 = kinetic energy = $\frac{W_k^2}{g} \frac{w^2}{2}$

This kinetic energy is dissipated as heat during every start and plug reversal.

Thus energy loss during one cycle is:

$$2E_1 = 2\frac{Wk^2}{g} \frac{w^2}{2} = \frac{Wk^2}{g} w^2$$

$$= \frac{134.2}{32.2} \times (10.45)^2 = 455 \text{ watts-sec.}$$

Total energy losses in one cycle of period T sec.

= (copper losses + iron losses)T + $2E_1$

Consistency duration of one cycle: T = 0.44 sec.

Total energy loss = $\left\{(94 + 22)\ 0.44 + 455\right\}$ watt-sec.

= (51 + 455) watt-sec.

= 506 watt-sec.

Average losses during one cycle = $\frac{506}{0.44}$

= 1150 watts

Input power = output + losses

= 373 + 1150 = 1523 watts

Thus, it is seen that the input power required is more than an allowable limit of 1,000 watts.

$$\text{Efficiency of the motor during agitation mode} = \frac{\text{output}}{\text{output and losses}} \times 100\%$$

$$= \frac{373}{1523} \times 100 = 24.4\%$$

IV. TRANSIENT ANALYSIS

The equations describing the behavior of the motor and load during transient period are:

$$V = E_a + (R_a + R_f)\, i_a + (L_a + L_f)\, \frac{dia}{dt} \qquad (1)$$

but

$$E_a = \frac{\rho z}{2\pi a}\, \Phi w = K\Phi w$$

where

$$K = \frac{\rho z}{2\pi a} = \text{a constant}$$

Substitute $R = R_a + R_f$, $L = L_a + L_f$ and value of k in (1) we get:

$$V = K\Phi w + R\, i_a + L\, \frac{dia}{dt} \qquad (3)$$

Also, during starting and accelerating, the equation of motion is:

$$T = J\frac{dw}{dt} + \alpha w + T_L \qquad (4)$$

but

$$T = \frac{\rho z}{2\pi a}\, \Phi\, i_a = k\Phi\, i_a$$

Thus Eq. 4 becomes:

$$K\, \Phi\, i_a = J\frac{dw}{dt} + \alpha w + T_e \qquad (5)$$

Where αw is the loss due to friction and windage.

The solution of Eqs. (3) and (5) will give us the required transient analysis of the system. It is seen from these equations that Φ, w, i_a, copper losses and core losses are the variables and these are important for the solution of transient problems since they vary twice every cycle during a start and and a plug-stop in the agitation mode.

The solving of these differential equations is difficult and may involve cut and try method. The complexity of the problem makes it worthless to solve these equations for the transient analysis.

REFERENCES

1. Crocker, F.B. and Torda, T., Direct and Alternating Current Machine Design, McGraw-Hill, New York, 1908.

2. Puchstein, A.F., The Design of Small Direct Current Motors, Wiley, New York, 1961.

3. Langsdorf, A.S., Principles of Direct Current Machines, Sixth Ed., McGraw-Hill, New York, 1959.

4. Donald, J.K. and Alvarez, E.C., Pulse and Switching Circuits, McGraw-Hill, New York, 1965.

5. Lytel, A.H., Industrial Electronics, McGraw-Hill, New York, 1962.

6. Langlois, Berthelot, R., Electromagnetic Machines, Philosophical Library, New York, 1955.

7. Fitzgerald, A.E. and Kingslay, C., Electric Machinery, MeGraw-Hill, New York, 1952.

BIBLIOGRAPHY

Books:

Wiener, A.E., Dynamo-Electric Machines, McGraw-Hill, New York, 1901.

Baily, B.F. and J.S. Gault, Alternating Current Machinery, McGraw-Hill, New York, 1951.

Gray, A., Electrical Machine Design, McGraw-Hill, New York, 1913.

Perry, J.H., ed., Chemical Engineer's Handbook, Fourth Ed., McGraw-Hill, New York, 1966.

Kuhlmann, J.H., Design of Electric Aparatus, Wiley, New York, 1950.

Spreadbury, F.G., Fractional Horsepower Electric Motors, I. Pitman, London, 1951.

Hicks, Tyler, Handbook on Fans, Power, Oct., 1951.

Electric Motors Machine Design, A Penton Publication, March 19, 1964.

Hopferwieser, Stephan E., Electric Motors and Applications, Brown, Boveri and Co., Baden, Switzerland.

Papers:

Luke, G.E., "The Cooling of Electric Machines," Trans. AIEE, Vol. 42, p 636.

Lyon, W.V., E. Wayne, and M.L. Henderson, "Heat Losses in DC Armature Conductors," Trans. AIEE, 1928.

Opal, L.G., "Limitations in Design of DC Adjustable Motors," Trans AIEE, Vol. 68, 1949, p. 1095.

Scott, David, "Unique Rolling-Rotor Motor," Popular Science, September, 1965.